A LONG-TERM PERFORMANCE PREDICTION METHOD FOR SOLAR DOMESTIC HOT WATER SYSTEMS

by

BLAKE VILELA MINNERLY

A thesis submitted in partial fulfillment of the
requirements for the degree of

Master of Science
(Mechanical Engineering)

at the

UNIVERSITY OF WISCONSIN-MADISON

1989

ABSTRACT

There are, at present, two main approaches to predicting the long-term performance of SDHW systems: short-term system performance tests and computer simulations. Computer simulation packages such as TRNSYS can give accurate performance predictions for any location having available weather data, but typically require between twenty to fifty system parameters to accurately describe the system's behavior. Extensive testing of system sub-components is required to determine the values of many of these parameters.

A short-term performance test conducted on the entire system, such as the ASHRAE-95, does not require sub-component testing. The performance measured by such a test, however, is representative only for the particular set of operating conditions employed during that test. The installed performance of the system in a given location may be quite different.

This thesis presents a long-term performance prediction method which combines these two approaches, thereby avoiding the limitations of either approach individually. The results of the ASHRAE-95 test are used to determine the parameters required to predict long-term system performance using TRNSYS.

This goal is achieved through the definition of an idealized SDHW system type, referred to as a simplified active system (SAS). This idealized system is defined such that it's hypothetical thermal behavior can be fully simulated using TRNSYS with only four parameter values: collector area, tank volume, and collector gain and loss

coefficients.

The simplified active system is used in the following fashion. The actual SDHW system whose long-term performance is desired is subjected to the ASHRAE-95 test, resulting in a measured value of performance. Logically, there must exist a simplified active system having the same collector area and tank volume as the actual system, with some unknown combination of collector gain and loss coefficients, such that it would theoretically yield the same test performance as the actual system. A simplified active system having these characteristics is referred to as 'equivalent' to the actual SDHW system.

It is shown that the test performance of the actual system can be used to develop a function relating the collector gain and loss coefficients of the equivalent simplified active system (ESAS). Any pair of gain and loss coefficients which satisfy this function, if used to simulate the ASHRAE-95 performance of the ESAS, will yield approximately the same performance as the actual system.

It is further shown that any of these pairs can be used to simulate the long term performance of the ESAS with nearly identical results, if two conditions are met. First, the average yearly mains temperature assumed during the simulation must be approximately equal to the average yearly ambient temperature of the location in question. Second, the total daily draw and hot water set temperature must be approximately equal to the values employed during the ASHRAE-95 test.

Extensive simulations indicate that the yearly performance of the ESAS and the actual system typically agree to within 3%, independent of location or system type. The experimental results of an ASHRAE-95 test and the monitored year-long outdoor performance of an actual system were also used to validate the accuracy of the prediction method. The simulated yearly performance of the ESAS, whose parameters

were determined from the results of the ASHRAE-95 test, agrees with the measured yearly performance of the actual system to within 1%.

ACKNOWLEDGEMENTS

The position of this particular section is somewhat misleading, as these words are in fact the last I will write in completing this thesis. I have just performed a rough calculation: it took about 700 hours to reach this point. But in spite of the hair loss and slow disintegration of my stomach lining those hours have cost me, or perhaps *because* of those things, I find myself reluctant to give it up to the library, where it will undoubtedly gather dust next to a 300 page treatise on the mating habits of tree slugs. Thus, to postpone the inevitable, I will now thank every person I ever met.

First, I'd like to thank Mrs. Herman, my third grade teacher, who said I'd never amount to anything. That may very well be true, but at least I wrote a thesis while I waited. I'd also like to thank Billy McKeever, for not telling his dad when we accidentally set his bean bag chair on fire. Thanks.

I can see this is getting excessive, so perhaps I'll thank some people who actually had something to do with this thesis. Open any page at random, and chances are that Sandy Klein's influence will somewhere be evident. He had the amazing and slightly annoying habit of often knowing the answer to a problem before it was even asked. Sandy, thank you for your numerous invaluable ideas and for only occasionally saying I told you so.

Jack Duffie and Bill Beckman were also very helpful, especially in damping the sudden mood swings a project like this inevitably creates. They were supportive when I was ready to toss the Macintosh out the window and recycle this thesis into generic toilet paper, and pushed me hard when I wanted to just coast. I owe them more than a

little peice of my sanity.

My dad is largely responsible for my interest in science (so you know who to blame). Through countless home experiments and improvised projects, he showed a small child that the essence of science is not money, industry, or even practical application. The essence of science is curiosity and play (and anyone who tells you otherwise works for the government). Thank you , Dad, for that gift among many others.

Without the support of my Mom and Grand Parents, both financially and emotionally, I would not writing this today. In fact, would probably be working the late shift at the seven-eleven, selling twinkies and microwave burritos and giving Mrs. Herman the satisfaction of watching her prediction come true. Thank you for saving me from a fate worse than death.

A special thanks must go to Manfred Wirsum, otherwise known as Dr. Fortran, for the zen-like computer wisdom he imparted to me whenever he wasn't too busy beating the IBMs with a baseball bat ("zis daam @#$%& zhing!). All my fellow students/slaves deserve thanks for making my time here much more than a job: Tim, Mark, Diane, Doug, Harald, Manni, Frank: Mien luftkisen boat ist uberfuted mit alle.

As one parting word to any future students, who may be reading this thesis (HAH!) in preparation for there own descention into research hell; there will be times when you will go home, after the tenth 14 hour day in a row, with a personality somewhat like a cross between Ghengis Khan and a rabid pit bull. If you are very lucky, there will be someone waiting for you who will put up with your crap, listen to your endless complaining, and not whack you over the head when you leave the dishes for the 50th time. I dedicate this to you, Anna....I *am* very, very lucky.

TABLE OF CONTENTS

LIST OF FIGURES

LIST OF TABLES

NOMENCLATURE

A = slope of linear correlation (Eq. 2.9)

A_c = collector area [m^2]

A_t = surface area of storage tank [m^2]

B = y-intercept of linear correlation (Eq. 2.10)

b_0 = incidence angle modifier constant

C_p = specific heat [J/kg°C]

D_r = diameter of collector riser pipe [mm]

ΔE = change in internal energy [kJ]

f = solar fraction

$F_r(\tau\alpha)_n$ = collector gain coefficient

$F_r(\tau\alpha)_n'$ = gain term of collector parameter pair that satifies Eq. 2.29

F_rU_l = collector loss coefficient [W/m^2°C]

F_rU_l' = loss term of collector parameter pair that satifies Eq. 2.29 [W/m^2°C]

G_{max} = peak radiation of triangular approximation [W/m^2]

G_t = instantaneous radiation incident on collector surface [W/m^2]

G_{tc} = instantaneous critical level of radiation on collector surface [W/m^2]

H_t = total daily radiation on a tilted surface [kJ/m^2]

$H_{t,on}$ = total incident radiation during pump operation [kJ/m^2]

$K_{\tau\alpha}$ = incident angle modifier

$\dot{m}_d$ = mass flow rate of hot water draw [kg/s]

M_d = mass of total daily draw [kg]

M_f = fluid mass within storage tank [kg]

n = number of data points

N_r = number of collector riser pipes per panel

Q_{load} = total hot water load [kJ]

Q_{solar} = total delivered solar energy [kJ]

T_a = ambient temperature [°C]

T_d = draw temperature [°C]

T_{env} = temperature of storage tank environment [°C]

T_i = collector inlet temperature [°C]

Δt_{on} = total time of pump operation [sec]

T_s = hot water set temperature [°C]

T_t = tank temperature [°C]

Δt_{tot} = integration period [sec]

U_t = tank loss coefficient [$W/m^2°C$]

V_t = tank volume [liters]

CHAPTER 1
Introduction

1.1 OBJECTIVE

Solar domestic hot water (SDHW) systems are simple, inexpensive devices which collect and store solar radiation for the purpose of supplementing a conventional domestic hot water system. Although all SDHW systems have two major components in common, a collector and a storage tank, these components can be found in a wide variety of system configurations. The vast majority of these configurations fit in one of three categories: integral collector storage (ICS) systems, forced circulation (active) systems, or thermosyphon systems. A description of these categories is given in sections 1.3-5.

Unlike conventional hot water systems, SDHW system performance is dependent on local climatic conditions, such as solar radiation and ambient temperature. As a result, the performance of a given SDHW system may vary widely from one location to another.

The ability to predict SDHW performance is desirable for several reasons. Performance prediction is an essential step in the development of a SDHW rating method, analogous to the methods already in existence for conventional water heating systems. Such rating methods would have a beneficial effect on the SDHW industry, by encouraging the construction of quality systems and increasing the public's faith in the technology. The development of such a rating method is the primary motivation

behind the undertaking of this project. In addition, performance prediction can be used to size systems for a particular application, provide customers with information on potential cost savings, and determine the suitability of an existing system for a particular location.

There are at present two main approaches to predicting SDHW system performance, each of which has a number of limitations. The first approach is to subject the system to some form of short-term test, similar to the tests conducted on conventional system. Many tests of this type have been proposed [1], and one in particular, the ASHRAE-95 [2], has become an accepted standard in the United States. A description of this test is given in section 1.2. The performance measured by these tests, however, is only representative of the system's performance under a specific set of test conditions. The system's installed performance may be quite different, due to the variability of climatic conditions.

The second approach is to simulate the operation of the system using either a detailed computer simulation package such as TRNSYS [3] or a performance correlation such as F-Chart [4]. TRNSYS is a collection of general mathematical models of various system components such as collectors, pumps, heat exchangers and storage tanks, whose parameters can be altered to describe a particular system. These models can be linked together in various configurations and subjected to forcing functions such as load demand and local hourly weather data. F-Chart is a semi-empirical correlation which predicts performance based on various system parameters and monthly average weather data. Both of these prediction techniques are described in more detail in subsequent sections.

Although these methods provide the actual installed system performance in

various location, the system parameters necessary to use these methods are often unknowns unless many additional tests are performed on individual components. F-Chart correlation has the added limitation of applying only to certain system types.

The goal of this project is to develop a SDHW prediction method which links the two approaches, thereby overcoming the limitations of either approach individually. This will be achieved by using the results of a short-term test (the ASHRAE-95) to derive the parameters necessary for long-term performance prediction using a detailed model (TRNSYS). In this manner, site-specific performance prediction can be provided without the extensive testing of individual components. It is desired that such a method be applicable to all major system types and locations with comparable accuracy.

1.2 THE ASHRAE-95/SRCC SHORT-TERM TEST

The ASHRAE-95 is an indoor, repeatable system test which attempts to recreate the climatic conditions and use patterns of a 'typical' water heating day. The test methodology is fixed, but the test conditions are specified by a rating agency, the most common of which is the Solar Rating and Certification Committee (SRCC) [5].

Incident solar radiation is simulated through the use of movable high intensity lamps. The daily irradiation, load, and incidence angle profiles specified by the SRCC are shown in table 1.1. The set temperature of delivered hot water is specified as 50 °C, and the ambient air and mains water temperatures are kept constant at 22 C.

The test procedure is as follows. The system is installed under the test apparatus according to manufacturer's instructions regarding set points, physical configuration,

and any other system settings which effect system operation. The system is then subjected to the previously described conditions. The solar energy delivered during the test day is measured by one of two methods. If the system has an auxiliary heater, the electrical energy supplied to that heater is subtracted from the load to determine the delivered solar energy. If the system has no auxiliary heater, the energy content of the delivered hot water is integrated over the test day by monitoring the water temperature and flow rate at ten minute intervals.. The test procedure is repeated for a number of identical days until the delivered solar energy changes from the value of the previous day by less than 3%. The solar fraction of the final test day, defined as the ratio of the delivered solar energy to the load, is presented as the system's test performance.

An alternative procedure is sometimes employed if the collector gain and loss coefficients have been previously determined experimentally. The gain coefficient is used to estimate the energy absorbed by the collector for a given level of irradiation, as described by Fanney and Thomas [19]. An electrical in-line heater can then be used to provide an equal amount of energy, replacing the high-intensity lamps as an energy source.

Although this test result is to some degree a measure of system performance, it by no means represents the installed performance a consumer can expect, as that performance will vary with local weather conditions. It is also inadvisable to compare systems on the basis of ASHRAE-95 test performance alone, as the relative merit of one system over another is also dependent to some extent on location. For these reasons, the ASHRAE-95 test is clearly not a true performance prediction method in itself.

Table 1.1

SRCC irradiation, incidence angle and draw profile during ASHRAE-95 test

Time	Irradiation.(W/m2)	Incidence Angle	Draw(Kg/hr)
8-9	1134	60	125
9-10	1692	45	0
10-11	2052	30	0
11-12	2376	15	0
12-1	2520	0	125
1-2	2376	15	0
2-3	2052	30	0
3-4	1692	45	0
4-5	1134	60	125

1.3 INTEGRAL COLLECTOR STORAGE (ICS) SYSTEMS

Of the three major SDHW system types, ICS systems are the simplest and least expensive. The name arises from the fact that he collector and storage tank of ICS systems are integrated into one unit, which serves as a simple preheater, mounted in series with the conventional water heater. Because there is no need to circulate water between the collector and tank, ICS systems have no pump or pump controller. The entire storage volume is continually exposed to the ambient environment. Under some conditions, the unit may actually cool the mains water and thereby increase the hot

water load. For this reason, ICS system performance is typically poorer than that of constrained systems, which shut off circulation to the collector when the system begins to loose energy. Their low cost and simplicity, however, has made them quite popular in spite of this fact. A schematic of an ICS system is shown in figure 1.1

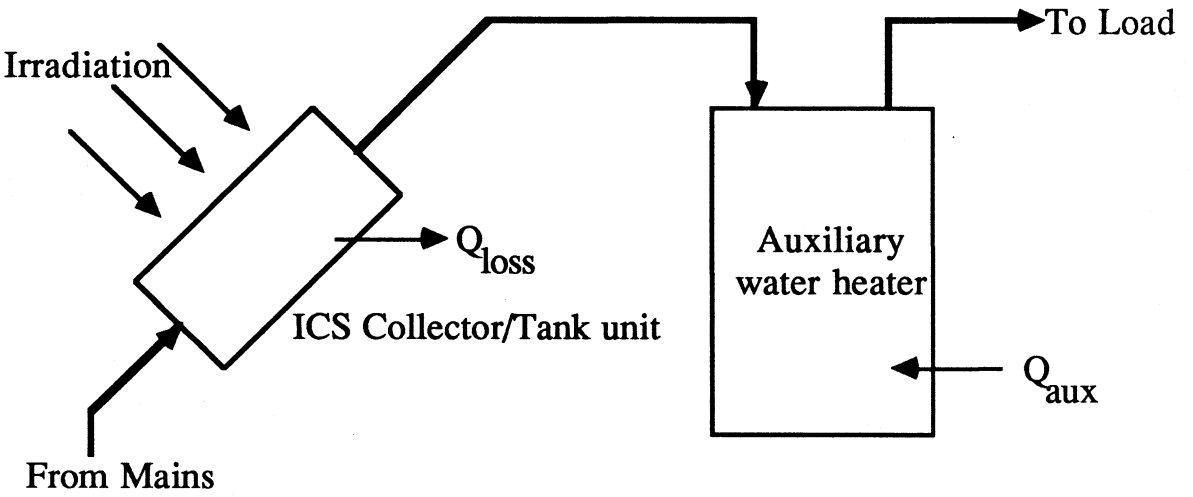

Figure 1.1 Schematic of Integral Storage Collector (ICS) system

A computer model of the ICS unit was developed by Zollner [6] for use with the TRNSYS simulation program. It a general model which can accommodate a variety of ICS geometries, but this generality makes the analytic calculation of the gain and loss parameters within the model impractical. As a result, these parameters must be determined experimentally. Stratification of the storage is modelled by dividing the unit into a variable number of isothermal nodes. An energy balance is solved numerically for each node at every time step during the simulation. The number of nodes necessary to correctly model the level of stratification in a given system is typically unknown.

This model can be linked with existing TRNSYS component models for equipment such as relief valves, pipes, and auxiliary heaters to simulate the operation of a complete ICS system. The simulated transient behavior and long-term performance of such a system were compared by Zollner to experimental data taken by DSET Labs [7] and Fowlks Engineering [8]. In both cases, the simulations exhibited very good agreement with the data.[6]

Zollner used this model to develop and validate a simple design method, which uses ASHRAE-95 results and a tank cool-down test to estimate the unit's loss and gain parameters. These parameters are substituted into a monthly energy balance, along with local average monthly weather data, to estimate the monthly solar fraction. The energy balance employed is valid only for well-mixed (non-stratified) systems, and an empirical correlation was developed to account for the effect of stratification. One parameter of this correlation is the number of tank nodes, which is not easily determined from a short-term test and must therefore be assumed. It was found, however, that the predicted performance is insensitive to the number of nodes selected.

The accuracy of this method was studied in a series of experiments conducted by Fanney and Klein [9] at NBS. The performance of several identical ICS systems was measured during outdoor yearly operation. It was found that Zollner's method was able to use the system's ASHRAE-95 performance (previously determined by the Florida Solar Energy Center [10]) to predict the measured monthly and yearly performance with very high accuracy.

Zollner's method is a viable means of converting ASHRAE-95 test results directly into long term performance predictions for ICS systems, although the method cannot be applied to other system types. The performance prediction of ICS systems is therefore

not included in the scope of this work.

1.4 FORCED CIRCULATION (ACTIVE) SYSTEMS

Active systems, unlike ICS systems, have separate collector and tank components connected by a pipe loop. Circulation through this loop is 'forced' by a pump, which controlled such that circulation only occurs when there is a net energy gain from the collector. The storage tank is typically located indoors and, as a result, active systems experiences lower losses to the environment than ICS systems. In addition, those losses, when they occur, serve to reduce the residential heating load. A schematic of a typical one-tank active system is shown in figure 1.2

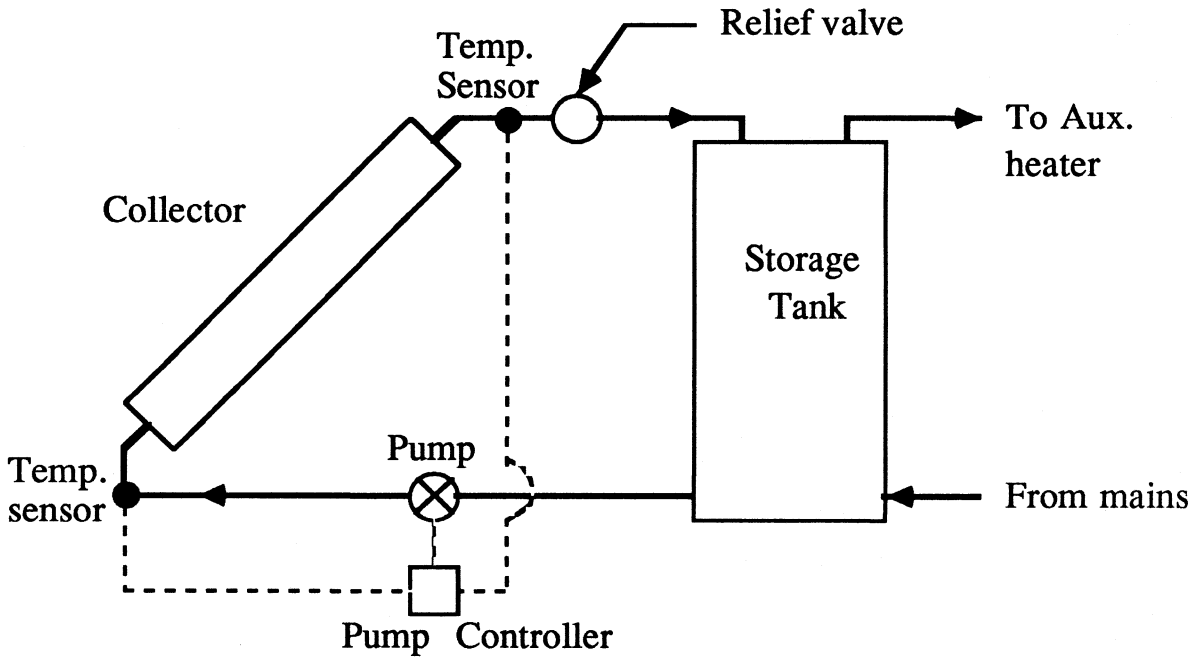

Figure 1.2 Active system schematic.

1.4.1 Active System Modelling with TRNSYS

TRNSYS is capable of linking existing models of various components, such as collectors, storage tanks, pumps and controllers, to simulate the behavior of most active systems. A number of physical parameters such as collector area and tank volume, as well as thermal parameters such as heat exchanger efficiencies and heat loss coefficients, must be known in order to use these models.

Many of these parameters are not intuitively obvious from the physical configuration of the system. The collector loss and gain coefficients, for example, must be determined experimentally, as with the ICS model developed by Zollner. If the effect of tank stratification is to be modelled, an appropriate number of thermal nodes must be estimated. The loss coefficients of the tank and connecting pipes are also typically unknown and additional tests must be performed to determine their values. The amount of testing required to determine the values of all these parameters can become prohibitively expensive and time consuming.

1.4.2 F-Chart

Klein [4] developed a correlation for well-mixed active systems, between monthly performance and two dimensionless system parameters. This correlation is the basis of a computer performance prediction method called F-Chart. The accuracy of this correlation was investigated in studies by Duffie and Mitchell [11] and Fanney and Klein [10], and was found to be within approximately 5%, for the range of system parameters and types for which it was developed. The performance predictions of F-Chart were also compared to those of TRNSYS in studies by Pearson [12].and Copsey [13]. The two were found to agree closely. F-Chart requires most of the same

physical and thermal parameters as TRNSYS. Its main advantage over TRNSYS is its computational simplicity. It has the added limitation, however, of being directly applicable only to well-mixed systems.

1.5 THERMOSYPHON SYSTEMS

Thermosyphon systems are similar in configuration to active systems, with the exception that circulation through the collector loop is achieved through the fluid buoyancy forces, resulting from temperature gradients in the storage tank and collector. This buoyant force is utilized by placing the collector outlet at a lower level than the tank outlet that supplies fluid to the collector, producing a difference in fluid density.that drives the circulation A check valve prevents reverse flow if the temperature gradient becomes negative, constraining the system much as a pump controller constrains the active systems. Thermosyphon systems typically operate at much lower collector flow rates.than active systems and as a result exhibit a higher degree of stratification. The performance of thermosyphon systems is therefore somewhat higher than active systems, all else being equal. A schematic of a typical thermosyphon system is shown in figure 1.3.

The TRNSYS component library contains a model of a thermosyphon collector-tank sub-unit which can be linked with other component models to simulate a thermosyphon system. This model combines the calculations performed by the collector and storage tank models used to simulate active systems, with fluid buoyancy calculations to determine the collector flow rate.

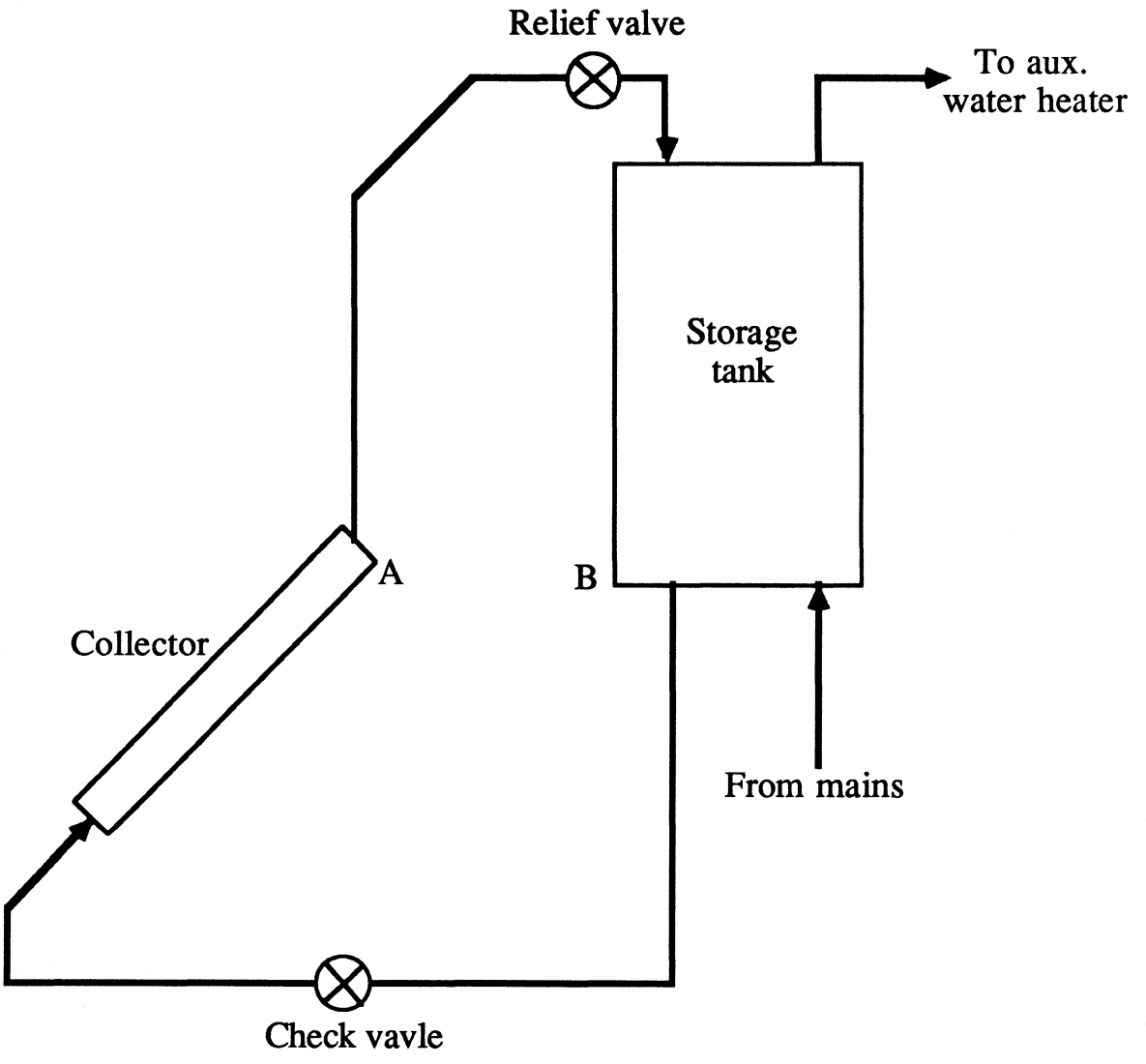

Figure 1.3 Thermosyphon system schematic. Circulation is driven by density differential between points A and B. Check valve prevents reverse flow.

The parameters required by this model are essentially the same as those required by the active system model, with the addition of several parameters describing vertical distance between the collector and tank, number of riser pipes per collector panel, and physical characteristics used to calculate the flow rate.

A comparison between TRNSYS simulations and measurements taken at the National Bureau of Standards was conducted by Morrison and Braun [14]. They found that the annual performance predicted by the TRNSYS model agreed very closely with the experimental data.

1.7 ORGANIZATION AND TERMINOLOGY

The prediction method described in this work can be divided into two main concepts, each of which is covered in a separate chapter. The first concept involves the definition of an idealized generic system type which will be referred to as a Simplified Active System (SAS). This idealized system is defined such that the only parameters required to simulate its operation with TRNSYS are the collector area, tank volume and the collector gain and loss coefficients.

The simplified active system is used in the following fashion. The actual SDHW system whose long-term performance is desired is subjected to the ASHRAE-95 test, resulting in a measured value of performance. Logically, there must exist a simplified active system having the same collector area and tank volume as the actual system, and a combination of collector gain and loss coefficients such that it would theoretically yield the same test performance as the actual system. A simplified active system having these characteristics is referred to as 'equivalent' to the actual SDHW system. It is

shown in Chapter 2 that the combination of collector gain and loss coefficients which meets the definition of the ESAS can be determined from the performance of the actual SDHW system.

The second, more crucial concept is that long term performance of an actual SDHW system is approximately equal to the simulated performance of it's ESAS, independent of location. It is therefore possible to test an actual SDHW system, solve for the collector gain and loss coefficients of it's ESAS. The simulated yearly performance of the ESAS can be expressed as a close approximation of the yearly performance of the actual system. This concept is developed in Chapter 3.

Ideally, experimental data consisting of the ASHRAE-95 test and long-term performance of various systems in various locations would be used to validate this prediction method. Such data, however, is virtually non-existent. TRNSYS models of various actual systems can be used to simulate both ASHRAE-95 test and long term performance in place of this data. Such models of actual systems will be referred to as 'complex' systems, by virtue of their increased complexity in comparison with the SAS. Simulations of this type are the primary means of validating the prediction method presented in this thesis. A limited amount of experimental data were also used for validation purposes. The results of this validation are presented at the end of Chapter 3.

CHAPTER 2
Simplified Active Systems and the ASHRAE-95

The number of parameters required to fully describe the behavior of an actual SDHW system using TRNSYS is on the order of 10 to 50. Many of these parameters may be unknown and it would be impossible to estimate the values of all these parameters from ASHRAE-95 test results alone.

It is possible, however, to define a simplified active system (SAS), for which the only unknown parameters are the collector gain and loss parameters. It is shown in this chapter that a function relating the gain and loss coefficients of the equivalent simplified active system (ESAS) can be derived solely from the ASHRAE-95 solar fraction, collector area and tank volume of the actual SDHW system.

Although the actual values of the collector gain and loss parameters cannot be determined explicitly from this function alone, it is shown that any parameter pair which satisfies this function, if used to simulate the ASHRAE-95 performance of the ESAS, will produce approximately the same performance as the actual system.

As a result, it is possible to test an actual SDHW system, and use it's measured performance to derive the collector parameter pairs of the ESAS that would yield that same test performance. In doing so, the entire thermal behavior of the actual system is effectively lumped into the collector gain and loss coefficients of the equivalent SAS. system. The crucial advantage of this ESAS is that it's long-term performance can be simulated using TRNSYS or F-Chart, as all it's system parameters are known.

2.1 DEFINITION OF THE SIMPLIFIED ACTIVE SYSTEM (SAS)

The SAS is defined to be a one tank active system of the configuration shown in Figure 1.4. The characteristic components and behavior of this system are defined as follows:

1) Stratification

The SAS is defined to be well-mixed, i.e. the storage tank is considered to be at uniform temperature at any instant in time. As a result, the system's behavior can be fully described by a single instantaneous energy balance.

2) Pipe Losses

Pipe losses in the SAS are considered negligible. Thus both the collector inlet temperature, T_i, and the draw temperature, T_d, are equal to the isothermal tank temperature, T_t, at any instant in time.

3) Incidence Angle Modification

The collector efficiency of the SAS is assumed to be independent of the angle of incident radiation. The transmittance-absorbtance product, $(\tau\alpha)$, is therefore constant, and equal to the transmittance-absorptance at normal incidence, $(\tau\alpha)_n$.

4) Tank Losses

The tank loss coefficient, U_t, of the SAS is assumed to be equal to 1.51 $W/m^2°C$. This is the value assumed in the development of the F-Chart correlation.

5) Controller Operation

The controller of the SAS is assumed to be perfect, meaning the pump is activated whenever the collector outlet temperature is infinitesimally higher than the inlet temperature. When modelling the SAS controller in TRNSYS, a one degree dead band is employed to prevent instability.

6) Collector Configuration

The SAS collector is defined as consisting of a single panel, regardless of the total area. Modification of the collector parameters to account for the effect of parallel or series-mounted panels is therefore unnecessary.

7) Collector Loop

The working fluid in the collector loop of the SAS is water. No heat exchanger is used. No modification of collector parameters is necessary to account for heat exchanger efficiency.

Given these simplifications, there are only four variable parameters which affect the performance of the SAS. They are

1. collector area, A_c (m^2)
2. tank volume, V_t (m^3)
3. collector gain coefficient, $F_r(\tau\alpha)_n$ (dimensionless)
4. collector loss coefficient, F_rU_l ($W/m^2°C$)

Of these four parameters, only two, the collector gain and loss coefficients, are unknown. If the values of these parameters are determined, the system's long-term performance can be predicted using TRNSYS or F-Chart.

2.2 SAS DAILY ENERGY BALANCE

An instantaneous energy balance on the tank of the SAS at any instant in time can be expressed as:

$$M_f C_p \frac{dT_t}{dt} = A_c [F_r(\tau\alpha)_n G_t - F_r U_l(T_i - T_a)]^+ - U_t A_t(T_t - T_{env}) - \dot{m}_d C_p(T_d - T_m) \qquad (2.1)$$

where

M_f	= fluid mass within the tank [kg]
C_p	= fluid specific heat [J/kg°C]
$\frac{dT_t}{dt}$	= rate of change of storage tank temperature with respect to time
G_t	= instantaneous radiation incident on collector surface [W/m^2]
T_a	= ambient temperature [°C]
T_{env}	= temperature of storage tank environment [°C]
$\dot{m}_d$	= mass flow rate out of storage tank to load [kg/s]

The superscripted addition sign shown in equation 2.1 signifies that the net collector gain is constrained to positive values by the operation of the pump controller.

Eq. 2.1 can be integrated over the last 24 hour period of the ASHRAE-95 test, to produce the daily energy balance shown below:

$$\Delta E = A_c\left[F_r(\tau\alpha)_n H_{t,on} - F_r U_l(\overline{T}_i - T_a)\Delta t_{on}\right] - U_t A_t(\overline{T}_t - T_{env})\,\Delta t_{tot} - M_d C_p(\overline{T}_d - T_m) \quad (2.2)$$

where,

ΔE	= total change in internal energy of tank fluid during test day[kJ]
$H_{t,on}$	= total incident radiation during pump operation [kJ]
$\overline{T}_i$	= integrated-average collector inlet temperature during period of pump operation [°C]
Δt_{on}	= total time of pump operation during integration period [sec]
$\overline{T}_t$	= integrated-average tank temperature during entire test day [°C]
Δt_{tot}	= integration period [86,400 sec]
M_d	= mass of total daily draw [kg]
$\overline{T}_d$	= integrated-average draw temperature during periods of draw [°C]

Several of the variables and parameters in Eq. 2.2 can be eliminated. On last day of the ASHRAE-95 test, the system has reached a periodic steady-state, so that the total change in internal energy over this period is negligible (i.e. $\Delta E \approx 0$). In addition, during the ASHRAE-95 test, the collector and tank are both exposed to the same 'environment'. Hence the tank environment temperature, T_{env}, is equal to the ambient temperature, T_a. Some parameters, which represent the conditions of the ASHRAE-95, such as set temperature, mains temperature and total draw mass, are known

constants. Others are known physical parameters of the system, such as collector area and tank volume. There remain, however, seven unknowns in Eq. 2.2. They are: the time of pump operation, Δt_{on}; the incident radiation during that time, $H_{t,on}$; the three average system temperatures: $\overline{T}_d$, $\overline{T}_t$, and $\overline{T}_i$; and the collector gain and loss coefficients: $F_r(\tau\alpha)_n$ and F_rU_l

If the first five of these unknowns are determined, Eq. 2.2 effectively becomes a functional relationship between the two collector parameters. The following two sections will describe the methods used to determine these five unknowns.

2.3 DERIVING AVERAGE SAS SYSTEM TEMPERATURES

The collector inlet temperature, T_i, and the draw temperature, T_d, are both equal to the tank temperature, T_t, at any given instant, as the SAS tank is fully mixed with no pipe losses. This equality, however, does not necessarily extend to the integrated-average values of these temperatures used in Eq. 2.2, as they are averaged over different integration periods. There may, in fact, be significant differences between the average values in systems with a low level of storage volume per unit collector area, V_t/A_c. The effect of V_t/A_c on this difference can be explained by the dynamics of tank temperature during the ASHRAE-95 test. Consider figures 2.1a and 2.1b, which show tank temperature as a function of time produced by TRNSYS simulations of the final ASHRAE-95 test day for two SAS's: one system with a low value of V_t/A_c = 30 l/m^2 (Fig. 2.1a), and the other with a more moderate value of 100 l/m^2(Fig. 2.1b).

The collector gain and loss terms shown in Eq. 2.2 are integrated over the period of pump operation, as it is only during this period that the collector gains or losses energy. As a result, the value of $\overline{T}_i$ used in the collector loss term is averaged over the time of pump operation, Δt_{on}, shown in Figures 2.1a and b.

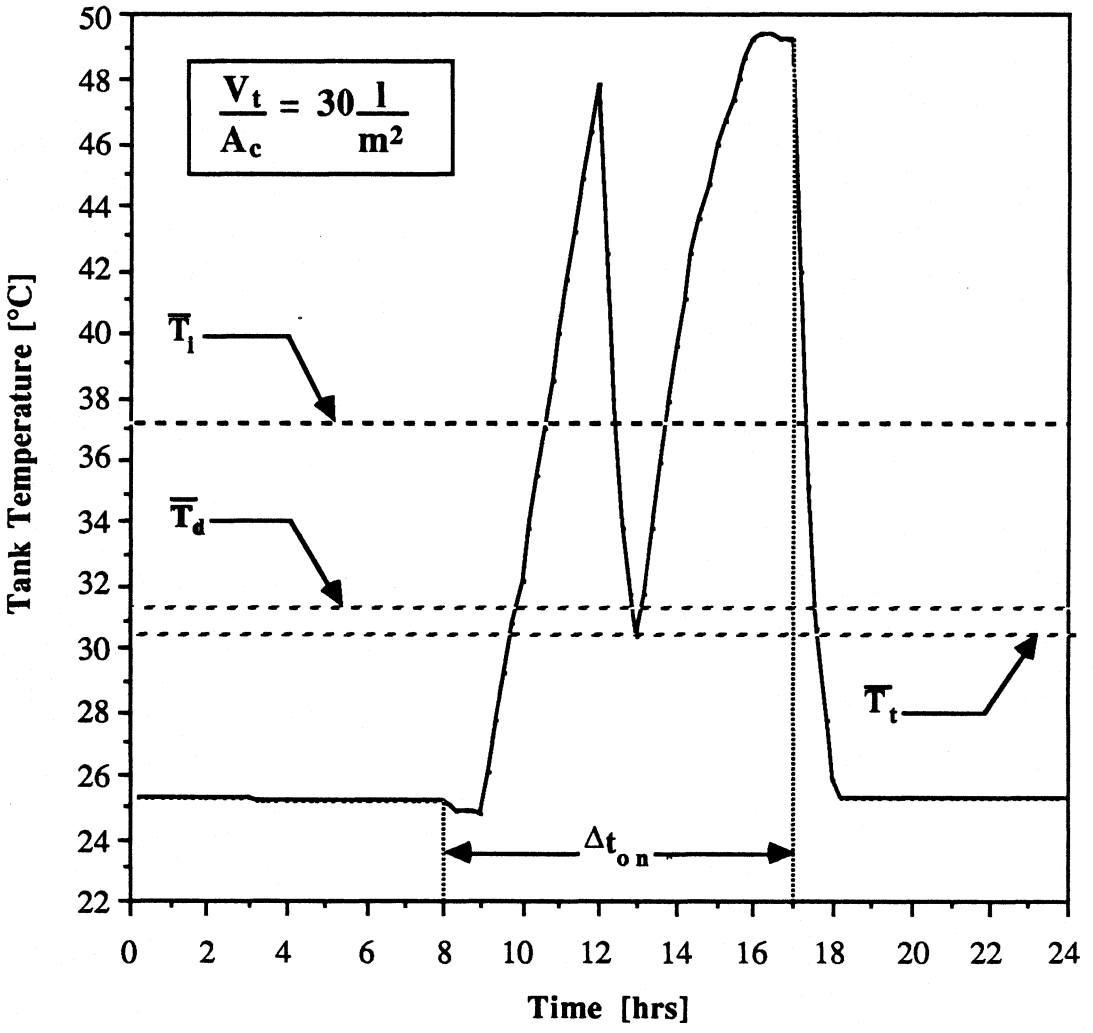

Figure 2.1a Tank temperature as a function of time during the final day of the ASHRAE-95 test, for a system with low storage volume per unit area.

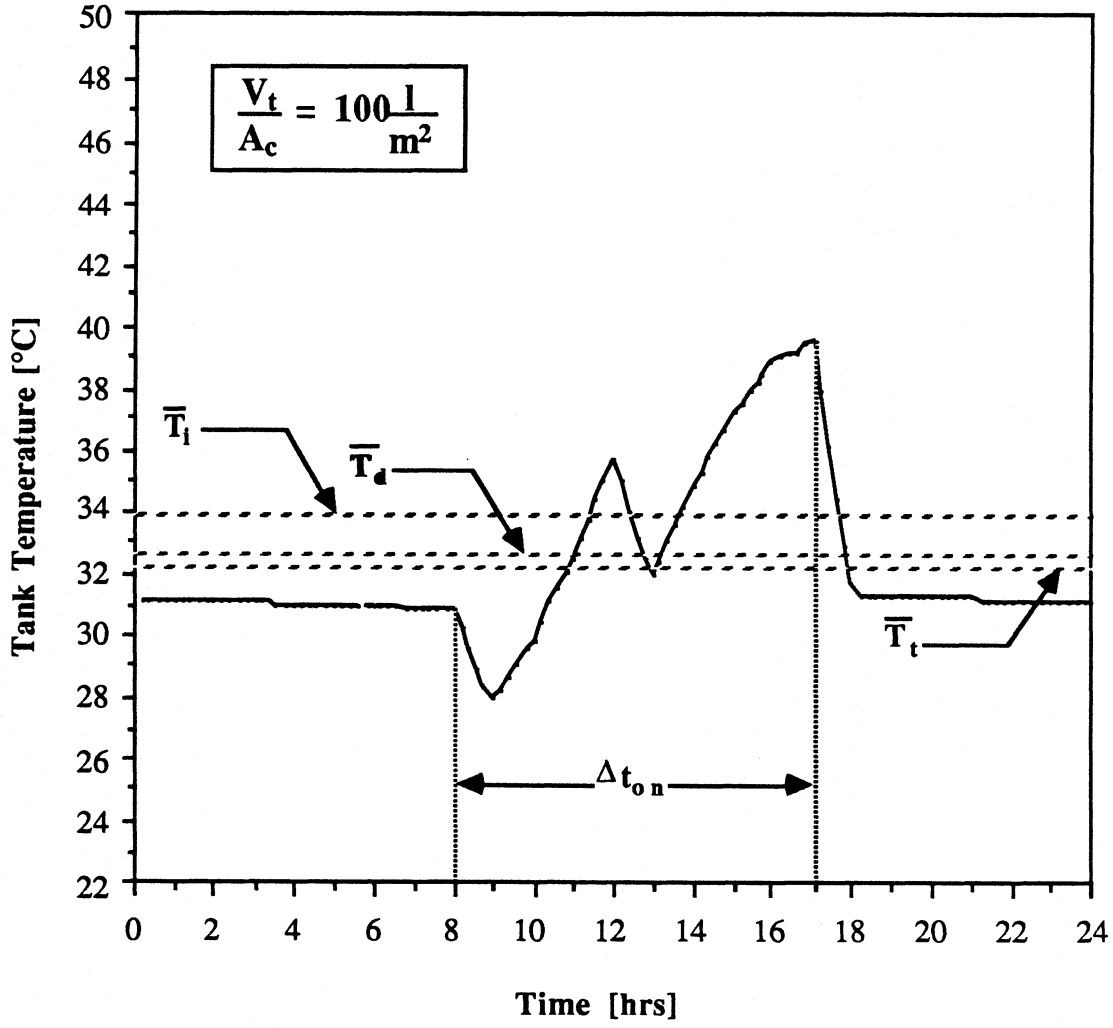

Figure 2.1b SAS tank temperature as a function of time for a system with moderate storage volume per unit collector area.

In contrast, the value of $\overline{T}_t$ used in the tank loss term is averaged over the entire test day, as tank losses occur continuously. Because the two are averaged over different periods of the test day, $\overline{T}_i$ is not necessarily equal to $\overline{T}_t$, even though their instantaneous values are identical.

In Figure 2.1a, the difference between these temperatures is quite marked (~7 °C), due to the fact that a low value of V_t/A_c , the increase in tank temperature during the period of irradiation (i.e. Δt_{on}) is quite pronounced, due to the relatively low degree of thermal inertia. At the more moderate value of V_t/A_c shown in Figure 2.1b, the difference is considerably smaller (~ 1.5 °C).

An analogous explanation applies to the difference between $\overline{T}_t$ and $\overline{T}_d$. The value of $\overline{T}_d$ used in the draw term of Eq. 2.2 must be averaged over the draw periods prescribed by the SRCC. The figures suggest, however, that this difference is close to negligible (<1 °C), even at low values of V_t/A_c.

2.3.1 Average Draw Temperature

The average draw temperature can be related to *f*, the fraction of the load met by solar energy, through the following expression:

$$f = \frac{Q_{solar}}{Q_{load}} \tag{2.3}$$

where

$$Q_{solar} = \int \dot{m} C_p (T_d - T_m) dt = M_d C_p (\overline{T}_d - T_m) \tag{2.4}$$

and

$$Q_{load} = M_d C_p (T_s - T_m) \tag{2.6}$$

where

T_s = hot water set temperature

combining Eqs 2.3-6 and solving,

$$f = \frac{\overline{T}_d - T_m}{T_s - T_m} \tag{2.7}$$

Eq. 2.4, however, implicitly assumes that the draw temperature never exceeds the set temperature during the draw period. To investigate the potential error this assumption may introduce to Eq. 2.7, TRNSYS simulations of the ASHRAE-95 test were performed for SAS having three different values of V_t/A_c. The solar fraction on the final day of these simulations is compared to the right-hand side of Eq. 2.7 in Figure 2.2

Eq. 2.7 appears to provide an accurate means of estimating the average draw temperature until a critical solar fraction is reached, at which point increasing error is exhibited. The value of this critical solar fraction appears to increase with the level of storage per unit collector area.

This error, and it's dependence on V_t/A_c, can also be explained in terms of the tank temperature dynamics. The instantaneous draw temperature increases during the period of collector operation, as shown in figures 2.1a and b.

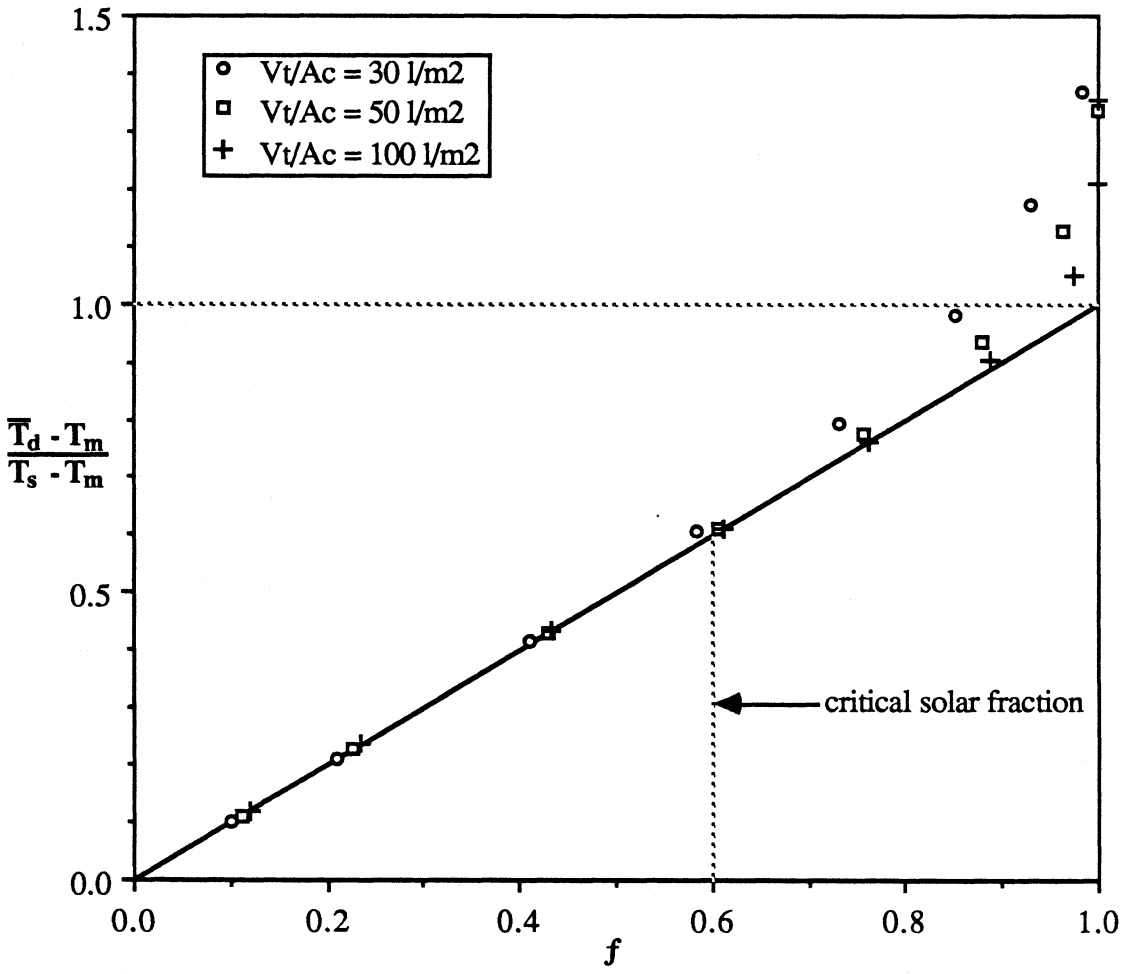

Figure 2.2 SAS solar fraction vs. dimensionless average draw temperature during ASHRAE-95 final test day. Eq. 2.7 appears valid under $f = 0.6$ for all values of Vt/Ac above 30 l/m2.

At a critical value of solar fraction, the draw temperature increases above the set temperature during some period of the the draw. The water drawn at this point has excess energy, by virtue of its excessive temperature, which does not contribute to the load. That is, the same performance would result if the draw temperature during this period were reduced to the set temperature. The integration performed in Eq. 2.4, however, does not make this distinction, and will therefore over estimate Q_{solar}. As a result, Eq. 2.7 will under predict the average draw temperature if solar fractions above the critical level are used.

Systems with low levels of storage will have greater fluctuations in tank temperature and will therefore exceed the set temperature at lower solar fractions. Specifically, at a value of V_t/A_C = 30 l/m2, the critical solar fraction would appear from figure 2.2 to be approximately 0.6. It is concluded that Eq. 2.7 can be used to determine the average draw temperature during the ASHRAE-95 test of any SAS for which Vt/Ac ≥ 30 l/m2, if the solar fraction yielded by that test is below 0.6. A means of ensuring that solar fractions during the ASHRAE-95 test remain below 0.6 is discussed in section 2.6

2.3.2 Average Tank Temperature

If the draw during the ASHRAE-95 test were continuous, the average tank temperature would be exactly equal to the average draw temperature, and could therefore be determined from Eq. 2.7. Although the draw during the ASHRAE-95 test is not continuous, a study of ICS systems performed by Zollner [6] indicates that draw profile has little effect on performance, as long as the profile is roughly symmetric about solar noon. As the SRCC profile satisfies this condition, it is logical to assume

that average draw temperature during the ASHRAE-95 test would be the nearly same as if a continuous draw was used. This would imply that the average draw temperature is approximately equal to the average tank temperature during the ASHRAE-95 test, as seen in Figures 2.1a and b. A comparison of average tank temperature and average draw temperature during the ASHRAE-95 test is shown in Fig. 2.3, for the same range of systems shown in Fig. 2.2. As the figure indicates, the assumption that $\overline{T}_d = \overline{T}_t$ introduces little error for the range of systems simulated. The RMS error, defined as

$$RMS = \left[\frac{1}{n}\Sigma(\overline{T}_d - \overline{T}_t)^2\right]^{0.5}$$

where n is the total number of simulations performed, is 0.77 °C. Tank losses from the SAS during the ASHRAE-95 test are quite small; on the order of 5% of the delivered solar energy. Hence, an error of 0.77 °C in the tank temperature will introduce negligible error to the daily energy balance (Eq. 2.2).

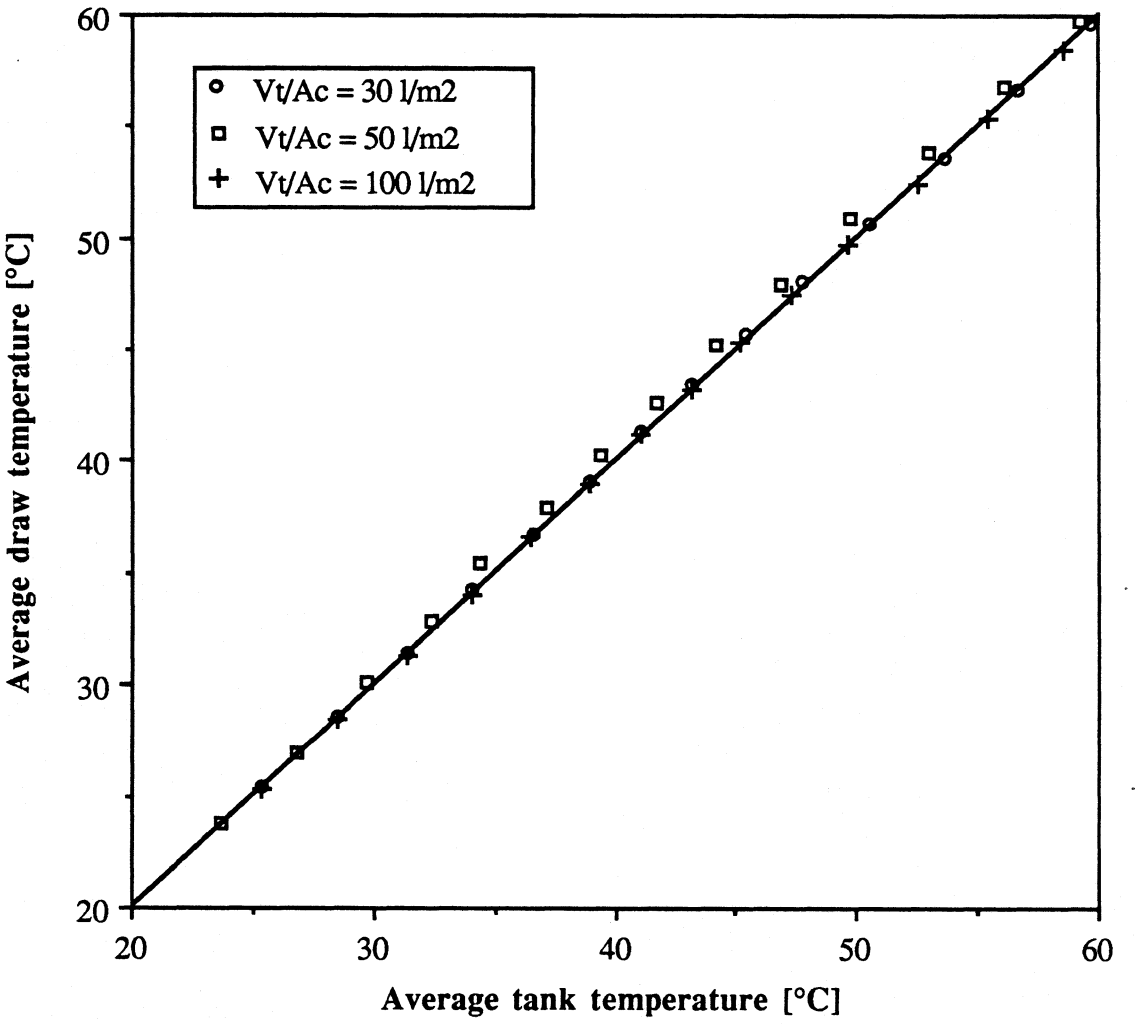

Figure 2.3 SAS Average tank temperature vs average draw temperature during ASHRAE-95 final test day.

2.3.3 Average Collector Inlet Temperature

Figure 2.4, which shows a comparison of average collector inlet temperature and average draw temperature based on the same set of simulations, indicates that the assumption $\overline{T}_i = \overline{T}_d$ would introduce significant error to the daily energy balance. At low values of V_t/A_c, the average collector inlet temperature can be up to 10 °C higher than the average draw temperature. The assumption could therefore result in a significant underprediction of the losses from the collector.

Fig. 2.4 suggests that a linear correlation of the type

$$\frac{\overline{T}_i - T_m}{T_s - T_m} = A\left[\frac{\overline{T}_d - T_m}{T_s - T_m}\right] + B \qquad (2.8)$$

could be employed to accurately fit the data, where the slope A, and the y-intercept, B, are both functions of the total incident radiation per unit volume, $A_C H_t/V_t$. A plot of such a correlation, using the data from figure 2.4, is shown in Fig. 2.5, where

$$A = 1.0 - 8.753 \times 10^{-4}\left(\frac{A_c H_t}{V_t}\right) + 5.28 \times 10^{-7}\left(\frac{A_c H_t}{V_t}\right)^2 \qquad (2.9)$$

$$B = 6.72 \times 10^{-4}\left(\frac{A_c H_t}{V_t}\right) + 1.04 \times 10^{-7}\left(\frac{A_c H_t}{V_t}\right)^2 \qquad (2.10)$$

with area in m^2, volume in liters and H_t in kJ.

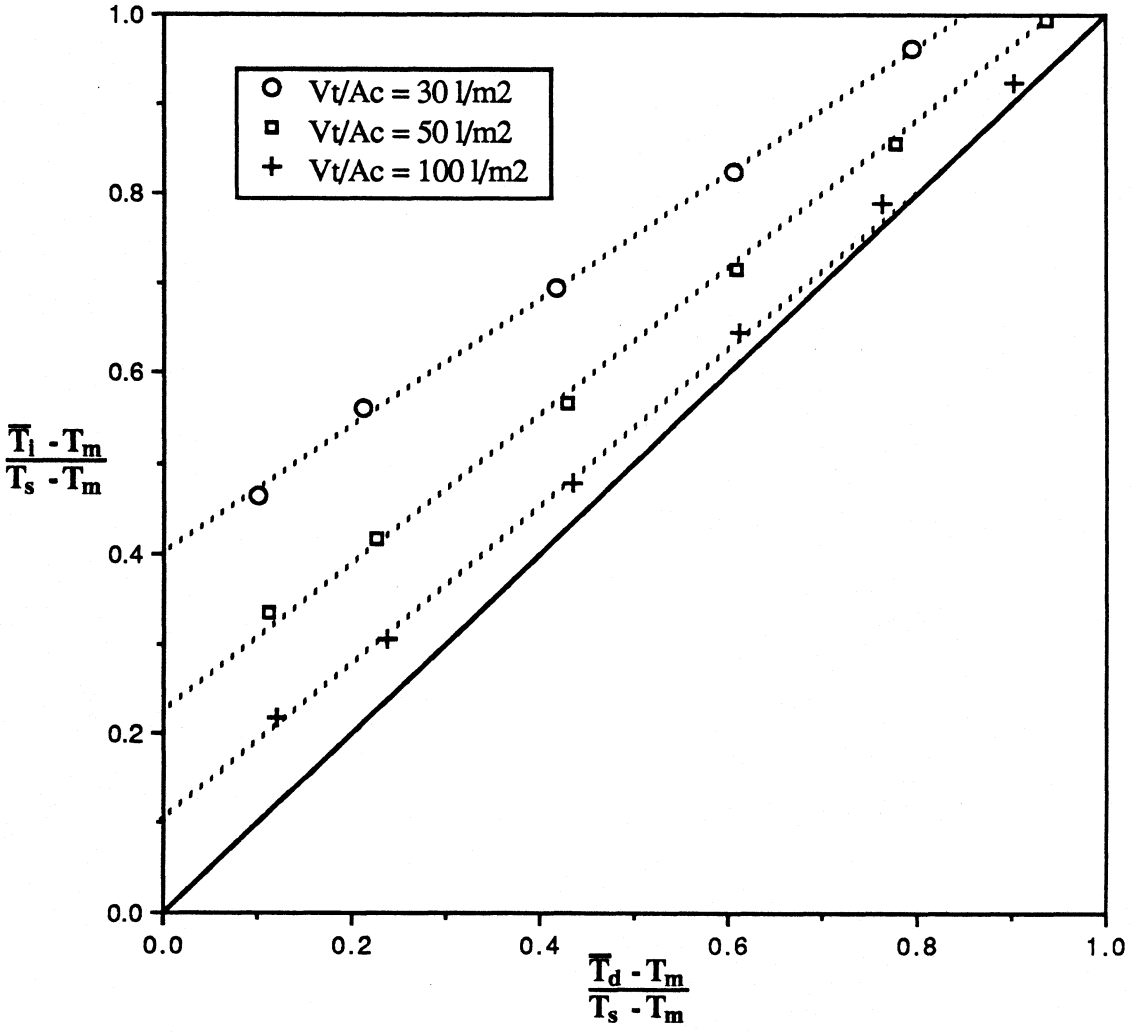

Figure 2.4 SAS dimentionless average collector inlet temperature vs. dimentionless average draw temperature during ASHRAE-95 final test day. The data can be closely fit by the linear approximations shown as dotted lines.

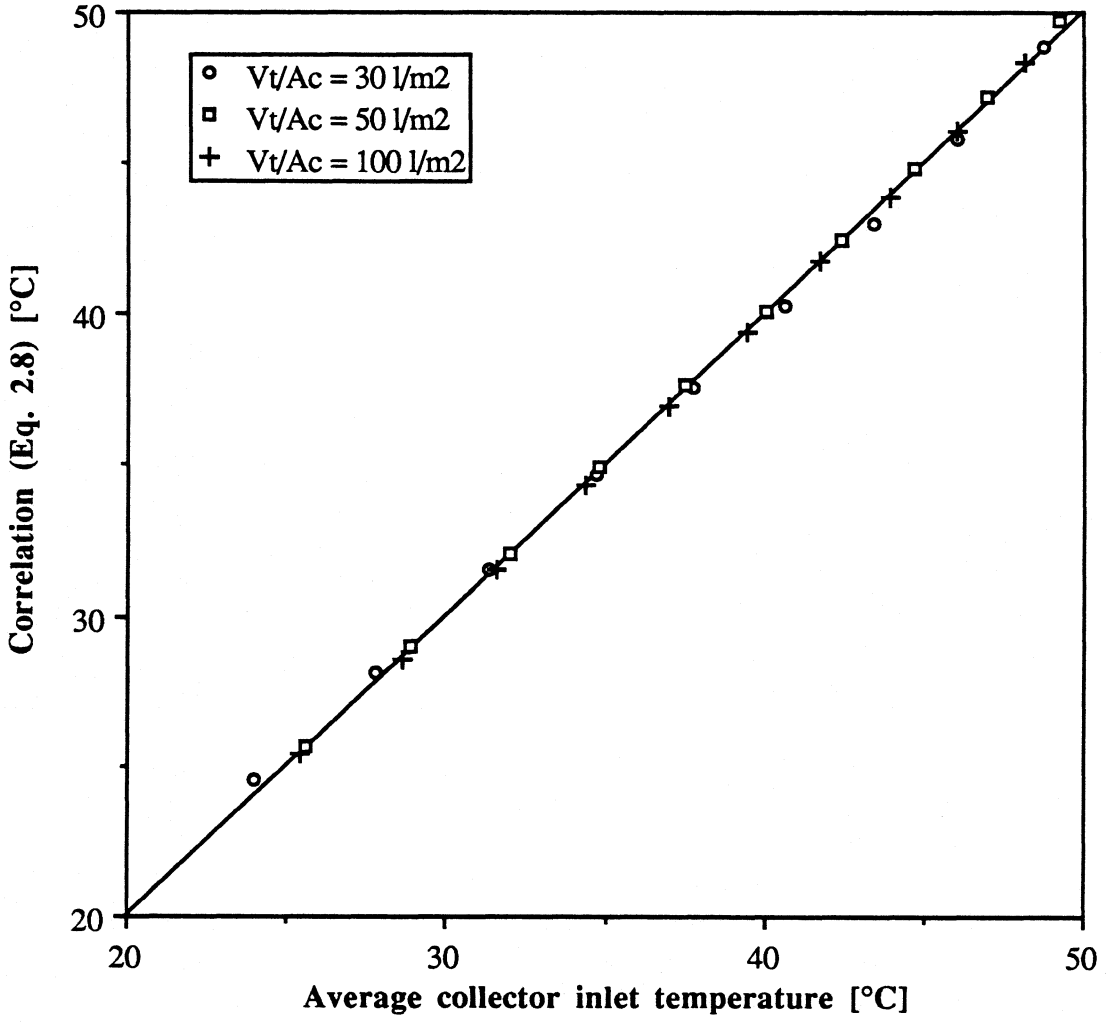

Figure 2.5 SAS average collector inlet temperature vs. correlation shown in Eq 2.8. The RMS error of the correlation is 0.97%

For certain combinations of high solar fraction and high storage volume per unit area, this correlation may predict values of average inlet temperature that are lower than the average draw temperature. Such predictions are clearly erroneous. In systems with these combinations, the average collector inlet and draw temperatures are nearly identical. As a result, the value predicted by the correlation and the draw temperature predicted by Eq. 2.7 should be compared, and the greater of the two used as the collector inlet temperature. With this modification, the RMS error of the correlation shown in Fig. 2.5 is 0.0096, where the RMS error is defined as

$$RMS = \left[\frac{1}{n}\Sigma\left(\frac{\overline{T}_{i,corr} - \overline{T}_i}{T_s - T_m}\right)^2\right]^{0.5}$$

The average draw temperature used in this correlation is derived from Eq. 2.7, which was shown to be consistently accurate only below a critical solar fraction of 0.6. The correlation, therefore, inherits the same limitation. Given these restrictions, it is concluded that the correlation can be used to solve for average collector inlet temperature with negligible error.

In summation, the simulation results presented in this section have established the validity of the following three statements concerning SAS thermal behavior during the final day of the ASHRAE-95 test:

1. $\overline{T}_d = f\,(T_s - T_m) + T_m \quad (\text{for } f<0.6)$ (2.11)

2. $\overline{T}_d = \overline{T}_t$ (2.12)

3. $\overline{T}_i = \max\left[\{(T_s - T_m)(Af + B) + T_m\}\,,\ \overline{T}_d\right]$ (2.13)

2.4 ELIMINATING $H_{t,on}$ AND Δt_{on}

The total incident radiant energy on the SAS collector surface during pump operation, $H_{t,on}$, and the time of pump operation, Δt_{on}, could be measured during the ASHRAE-95 test by monitoring the pump. The goal of this project, however, is to develop the ability to test thermosyphon systems (among others) and use the test results to derive the parameters of the SAS that would exhibit the same test performance. As thermosyphon systems have no pump to monitor, and, hence, $H_{t,on}$ and Δt_{on} cannot be measured, a means of calculating or eliminating these two variables must be developed.

2.4.1 Utilizability

One method of eliminating these variables is to apply the concept of utilizability developed by Hottel and Whillier [15] and later refined by Liu and Jordan [16] and Klein [17]. Utilizability is based on the definition of a critical level of incident radiation, G_{tc}, at which the rate of useful energy gain from the collector, q_u, is exactly zero. This critical radiation level can be determined by setting the Hottel-Whillier equation [17] equal to zero.

$$q_u = 0 = A_c\left[F_r(\tau\alpha)_n G_{tc} - F_r U_l (T_i - T_a)\right]^+ \qquad (2.16)$$

Thus,

$$G_{tc} = \frac{F_r U_l (T_i - T_a)}{F_r(\tau\alpha)_n} \qquad (2.17)$$

With this definition of critical radiation level, the rate of useful energy gain can be expressed as:

$$q_u = A_c\left[F_r(\tau\alpha)_n(G_t - G_{tc})^+\right] \tag{2.18}$$

The superscripted plus signs in Eqs. 2.16 and 2.18 indicate that the useful energy gain is constrained to positive values by the pump controller. Integrating Eq. 2.18 over the final ASHRAE-95 test day yields:

$$Q_u = A_c\left[F_r(\tau\alpha)_n\int (G_t - G_{tc})^+dt\right] \tag{2.19}$$

Eq. 2.19 represents the total daily solar energy delivered to the tank, and is equivalent to the difference between the collector gain and loss terms in Eq. 2.2. Eq. 2.19 can be simplified by defining the integrated average critical radiation level as:

$$\overline{G}_{tc} = \frac{F_rU_l(\overline{T}_i - T_a)}{F_r(\tau\alpha)_n} \tag{2.20}$$

The daily utilizable fraction [15,16,17], ϕ, is defined as the fraction of the total daily incident radiation, H_t, that is above the average critical radiation level. Thus, the utilizable fraction can be expressed as:

$$\phi = \frac{(\overline{G}_t - \overline{G}_{tc})^+\Delta t}{H_t} \tag{2.21}$$

Substituting ϕ into Eq. 2.19 yields:

$$Q_u = A_c F_r (\tau\alpha)_n \phi H_t \qquad (2.22)$$

If this expression for the total daily useful energy gain is substituted for the collector loss and gain terms in the integrated daily energy balance, Eq. 2.2, the following expression results:

$$\Delta E = A_c F_r (\tau\alpha)_n \phi H_t - U_t A_t (\overline{T}_t - T_{env}) \Delta t_{tot} - M_d C_p (\overline{T}_d - T_m) \qquad (2.23)$$

Utilizability has therefore succeeded in eliminating the variables $H_{t,on}$ and Δt_{on}, but has added another unknown, ϕ.

2.4.2 An Expression for ϕ During ASHRAE-95

The incident radiation profile specified by the SRCC for the ASHRAE-95 test is shown in Fig. 2.6. The shaded region represents the total incident radiation above the average critical level; i.e , the total utilizable radiation. The daily utilizable fraction, ϕ, is the ratio of this utilizable radiation to the total incident radiation, H_t. Graphically, therefore, this ratio can be represented by the area of the shaded region divided by the total area under the profile.

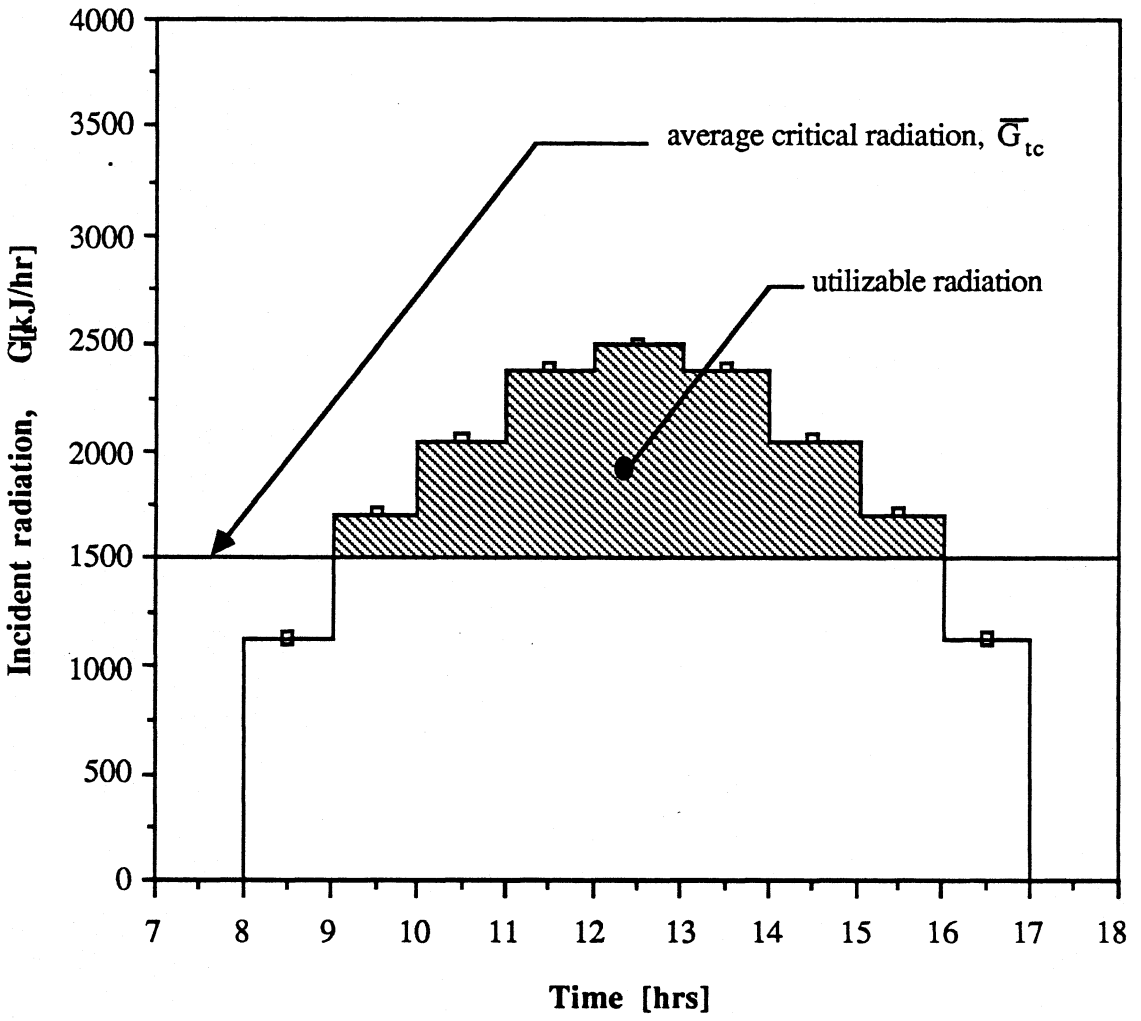

Figure 2.6 SRCC radiation profile, incident radiation vs. time. Shaded region above average critical radiation level represents total daily utilizable energy.

During final ASHRAE-95 test day, ΔE equals approximately zero, and Eq. 2.23 can be solved for ϕ, yielding:

$$\phi = \frac{U_t A_t(\overline{T}_t - T_{env})\,\Delta t_{tot} + M_d C_p(\overline{T}_d - T_m)}{A_c F_r(\tau\alpha)_n H_t} \qquad (2.24)$$

If $F_r(\tau\alpha)_n$ is known, Eq 2.24 and the radiation profile shown in Fig. 2.6 can be used to solve for F_rU_l in the following manner. The given value of $F_r(\tau\alpha)_n$ is used in Eq. 2.24 to solve for the corresponding value of ϕ. The critical radiation level which yields this utilizable fraction can be calculated by numerical integration of the SRCC profile shown in Fig 2.6. The integration is performed iteratively, employing successive substitution or Newton's method, until the utilizable energy (i.e. the radiation above G_{tc}) is equal to ϕH_t. This value of critical radiation can then be used to derive F_rU_l by solving Eq.2.20, yielding:

$$F_rU_l = \frac{\overline{G}_{tc} F_r(\tau\alpha)_n}{(\overline{T}_i - T_a)} \qquad (2.25)$$

The need for iterative numerical integration can be eliminated, by approximating the SRCC radiation profile with a triangular profile that provides the same total daily radiation, as shown in Fig. 2.7. It will be subsequently established that this assumption does not significantly alter the estimated performance of the system.

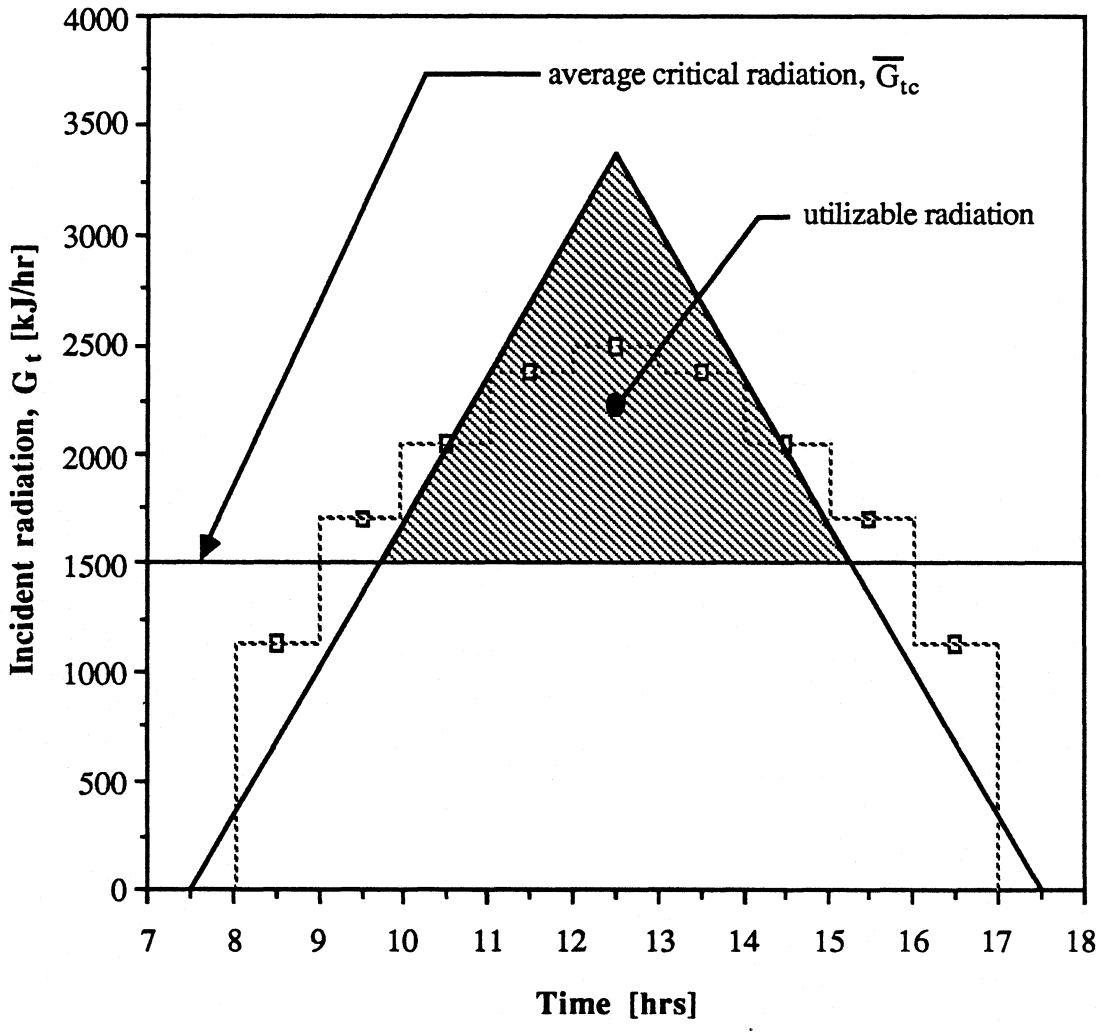

Figure 2.7 Triangular approximation of SRCC radiation profile. Total daily radiation under triangle is identical to SRCC total (17,022 kJ/m2).

For the special case of a triangular profile, the relationship between the utilizable fraction and the critical radiation level simplifies to:

$$\phi = 1 - 2\frac{\overline{G}_{tc}}{G_{max}} + \left(\frac{\overline{G}_{tc}}{G_{max}}\right)^2 \tag{2.26}$$

where G_{max} is the peak irradiation of the triangular profile (3404 kJ/hr). Substituting this expression into Eq. 2.24 yields:

$$1 - 2\frac{\overline{G}_{tc}}{G_{max}} + \left(\frac{\overline{G}_{tc}}{G_{max}}\right)^2 = \frac{U_t A_t(\overline{T}_t - T_{env})\,\Delta t_{tot} + M_d C_p(\overline{T}_d - T_m)}{A_c F_r(\tau\alpha)_n H_t} \tag{2.27}$$

Solving the quadratic equation for $\overline{G}_{tc}$,

$$\overline{G}_{tc} = G_{max}\left(1 - \sqrt{\frac{U_t A_t(\overline{T}_t - T_{env})\,\Delta t_{tot} + M_d C_p(\overline{T}_d - T_m)}{A_c F_r(\tau\alpha)_n H_t}}\right) \tag{2.28}$$

Thus,

$$F_r U_l = \frac{F_r(\tau\alpha)_n G_{max}}{(\overline{T}_i - T_a)}\left(1 - \sqrt{\frac{U_t A_t(\overline{T}_t - T_{env})\,\Delta t_{tot} + M_d C_p(\overline{T}_d - T_m)}{A_c F_r(\tau\alpha)_n H_t}}\right) \tag{2.29}$$

For a given SAS, this expression constitutes an explicit functional relationship between the collector parameters F_rU_l and $F_r(\tau\alpha)_n$. If F_rU_l were known, for example, Eq. 2.29 could be used to calculate $F_r(\tau\alpha)_n$.

The accuracy of Eq. 2.29 was tested in the following manner. TRNSYS

simulations of the ASHRAE-95 test were conducted on four SAS's. The parameters of these four systems, shown in table 2.1, represent a typical range of system sizes and collector parameters.

Table 2.1
Range of Parameters Simulated in Fig. 2.8

	A_c [m^2]	V_t/A_c [l/m^2]	F_rU_l [$W/m^2°C$]
System A	2	30	2.0
System B	1	100	2.0
System C:	2	150	4.0
System D	4	150	8.0

For each of these systems, simulations were conducted with eleven different values of $F_r(\tau\alpha)_n$, ranging from 0.4 to 0.9. The solar fractions from these simulations were used in Eqs 2.11-15 to calculate the average draw, tank and collector inlet temperatures. These three temperatures, and the actual value of F_rU_l used in the simulations, were input into Eq.2.29 to to attempt to predict the value of $F_r(\tau\alpha)_n$. The predicted values are compared to the actual values used in the simulations of each system in tables 2.2-5 and Fig. 2.8.

Table 2.2

System A: predicted values of $F_r(\tau\alpha)_n$ from Eq. 2.29 compared to actual values used in TRNSYS simulations.

$F_r(\tau\alpha)_n$ TRNSYS	f_{TRNSYS}	$F_r(\tau\alpha)_n$ Eq. 2.29
0.400	0.263	0.416
0.450	0.296	0.463
0.500	0.329	0.509
0.550	0.362	0.556
0.600	0.395	0.602
0.650	0.428	0.648
0.700	0.460	0.694
0.750	0.493	0.739
0.800	0.525	0.785
0.850	0.557	0.830
0.900	0.589	0.875

Table 2.3

System B: predicted values of $F_r(\tau\alpha)_n$ from Eq. 2.29 compared to actual values used in TRNSYS simulations.

$F_r(\tau\alpha)_n$ TRNSYS	f_{TRNSYS}	$F_r(\tau\alpha)_n$ Eq. 2.29
0.400	0.140	0.403
0.450	0.158	0.452
0.500	0.176	0.502
0.550	0.194	0.551
0.600	0.212	0.601
0.650	0.229	0.649
0.700	0.247	0.698
0.750	0.264	0.747
0.800	0.282	0.795
0.850	0.299	0.844
0.900	0.317	0.893

Table 2.4

System C: predicted values of $F_r(\tau\alpha)_n$ from Eq. 2.29 compared to actual values used in TRNSYS simulations.

$F_r(\tau\alpha)_n$ TRNSYS	f_{TRNSYS}	$F_r(\tau\alpha)_n$ Eq. 2.29
0.40	0.249	0.411
0.45	0.280	0.461
0.50	0.312	0.510
0.55	0.343	0.559
0.60	0.374	0.609
0.65	0.405	0.658
0.70	0.436	0.707
0.75	0.467	0.757
0.80	0.498	0.806
0.85	0.530	0.856
0.90	0.561	0.905

Table 2.5
System D: predicted values of $F_r(\tau\alpha)_n$ from Eq. 2.29 compared to actual values used in TRNSYS simulations.

$F_r(\tau\alpha)_n$ TRNSYS	f_{TRNSYS}	$F_r(\tau\alpha)_n$ Eq. 2.29
0.425	0.370	0.436
0.475	0.413	0.483
0.525	0.457	0.531
0.575	0.500	0.579
0.625	0.544	0.627
0.675	0.588	0.674
0.725	0.631	0.722
0.775	0.675	0.770
0.825	0.718	0.818
0.875	0.762	0.865
0.925	0.805	0.913

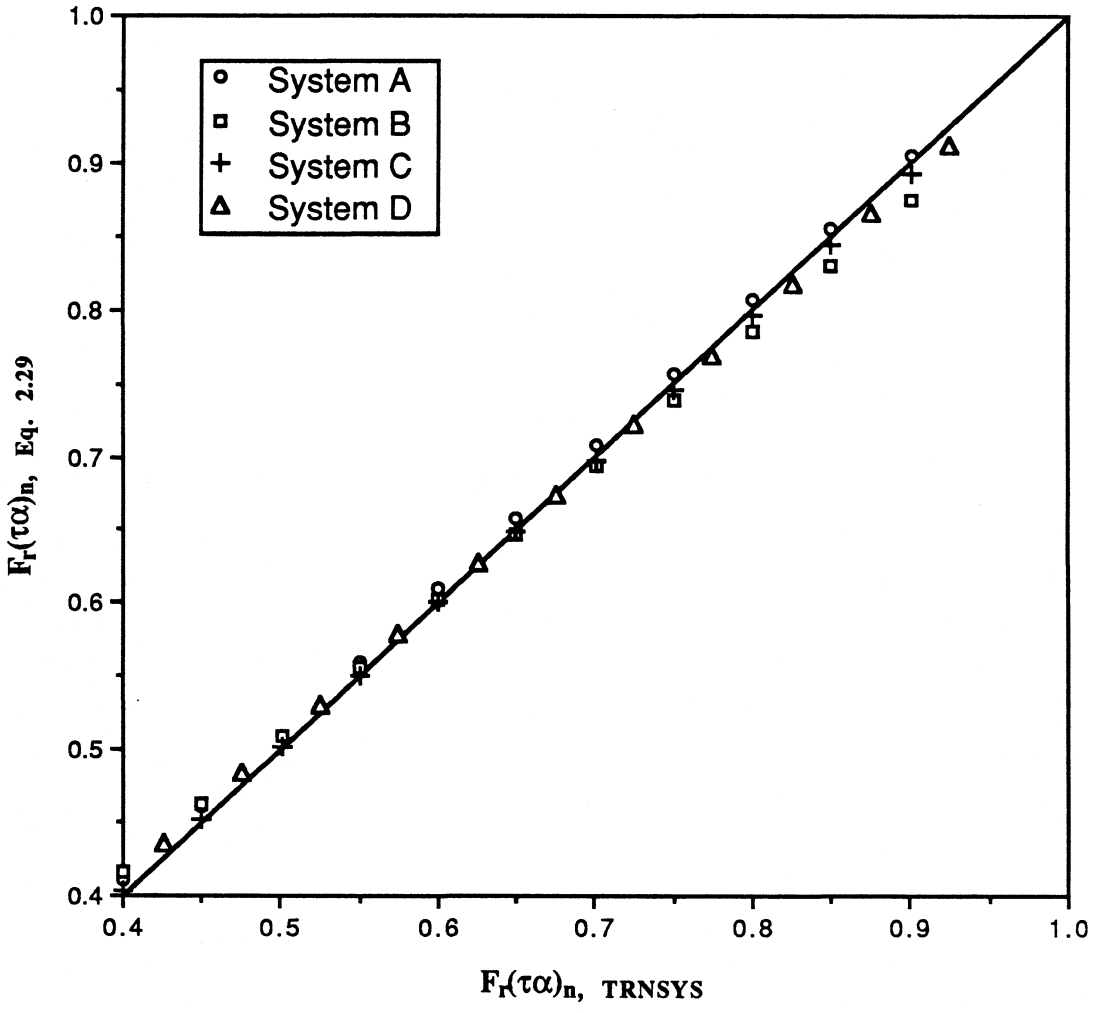

Figure 2.8 Value of $F_r(\tau\alpha)_n$ predicted by Eq 2.29 vs. actual value used in TRNSYS simulations of ASHARE-95 test

The RMS error of Eq. 2.29, defined as,

$$RMS = \left[\frac{1}{n}\Sigma\left(\frac{F_r(\tau\alpha)_{n,TRNSYS} - F_r(\tau\alpha)_{n,\ Eq.\ 2.29}}{F_r(\tau\alpha)_{n,TRNSYS}}\right)^2\right]^{0.5}$$

is 0.015. It is therefore concluded that Eq. 2.29 is capable of accurately predicting the value of $F_r(\tau\alpha)_n$, if given the value of F_rU_l. This result further verifies that the triangular radiation profile used to develop Eq 2.29 introduces negligible error to the values of the derived collector parameters.

2.5 SAS Performance Sensitivity

Eq. 2.29 is capable of predicting the value of one collector parameter if provided with the value of the other. Both collector parameters of the SAS, however, are unknown, and further information regarding the relationship between these parameters is therefore required.

Eq. 2.29, which represents a functional relationship between the collector parameters of the SAS, was derived from a daily energy balance on the last day of the ASHRAE-95. When a value of F_rU_l is input to this function, the resulting value of $F_r(\tau\alpha)_n$ by definition satisfies this daily energy balance. If a different value, F_rU_l', is substituted, a corresponding value, $F_r(\tau\alpha)_n'$, is produced by Eq. 2.29, such that the daily energy balance remains satisfied. For a given SAS, therefore, Eq 2.29 defines a family of parameter pairs, $(F_r(\tau\alpha)_n', F_rU_l')$, all of which satisfy the daily energy balance. A prime will be used to denote that a parameter is one member of a pair which satisfies Eq. 2.29. This line of reasoning suggests that SAS performance should be

insensitive to the particular pair selected, as all the pairs satisfy the daily energy balance.

This hypothesis was tested in the following manner. Simulations of the ASHRAE-95 test were performed for systems Systems A through D with $F_r(\tau\alpha)_n$ = 0.7. The solar fractions provided by these simulations were used to estimate the average draw, tank, and collector inlet temperatures of each system. These values of temperature were input to Eq. 2.29 to determine the collector parameter function corresponding to each system. Each of these functions defines a family of collector parameter pairs, ($F_r(\tau\alpha)_n'$, F_rU_l'), which satisfy the daily energy balance of that particular system. Table 2.6 shows seven members from each of the parameter pair families corresponding to systems A through D. Fig. 2.9 shows a plot of $F_r(\tau\alpha)_n'$ vs. F_rU_l' for the families corresponding to systems A and B.

Table 2.6
Families of collector parameter pairs which satisfy Eq. 2.29,
for systems A through D.

	$F_r(\tau\alpha)_n'$			
F_rU_l'	A	B	C	D
2.0	0.694	0.698	0.655	0.503
3.0	0.734	0.717	0.681	0.538
4.0	0.773	0.736	0.707	0.571
5.0	0.811	0.754	0.733	0.604
6.0	0.849	0.772	0.759	0.636
7.0	0.886	0.790	0.784	0.667
8.0	0.922	0.808	0.808	0.698

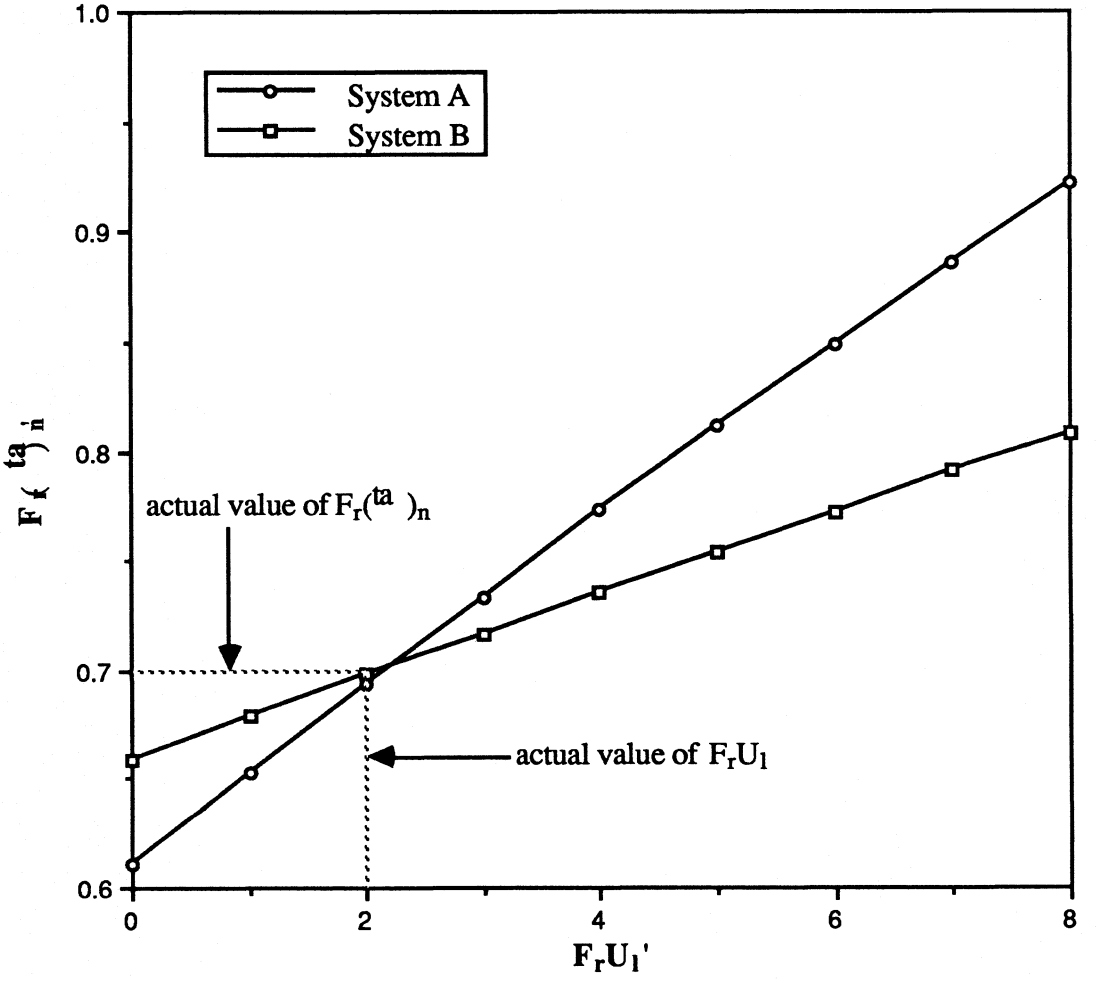

Figure 2.9 F_rU_l' as a function of $F_r(\tau\alpha)_n'$ from Eq. 2.29 The dotted lines represent the actual collector parameters of systems A and B.

Note that systems A and B have the same actual collector parameters (F_rU_l=2 W/m^2°C, $F_r(\tau\alpha)_n$=0.7). As a result, the two lines shown in Figure 2.9 should intersect approximately at the point (2, 0.7), given the established accuracy of Eq. 2.29. The slopes of these lines, however, should differ substantially, as system B, having only half the area of System A, operates at a lower average collector temperature, and is therefore less sensitive to to the value of F_rU_l'. Hence, a small change in $F_r(\tau\alpha)_n'$ must be balanced by a large change in F_rU_l', resulting in a lower slope. Fig. 2.9 confirms both of these expectations.

Each member of the parameter pair families shown in tables 2.6 and 2.7 were used to simulate the ASHRAE-95 performance of the corresponding system. The resulting solar fractions are plotted verses the value of F_rU_l' that corresponds to the parameter pair used in the simulation. The results, shown in Fig. 2.10, indicate that the simulated ASHRAE-95 performance of a given SAS is almost totally independent of the parameter pair selected. Any parameter pair which satisfies the collector parameter function of a given SAS can be used to simulate the system's ASHRAE-95 performance with nearly identical results.

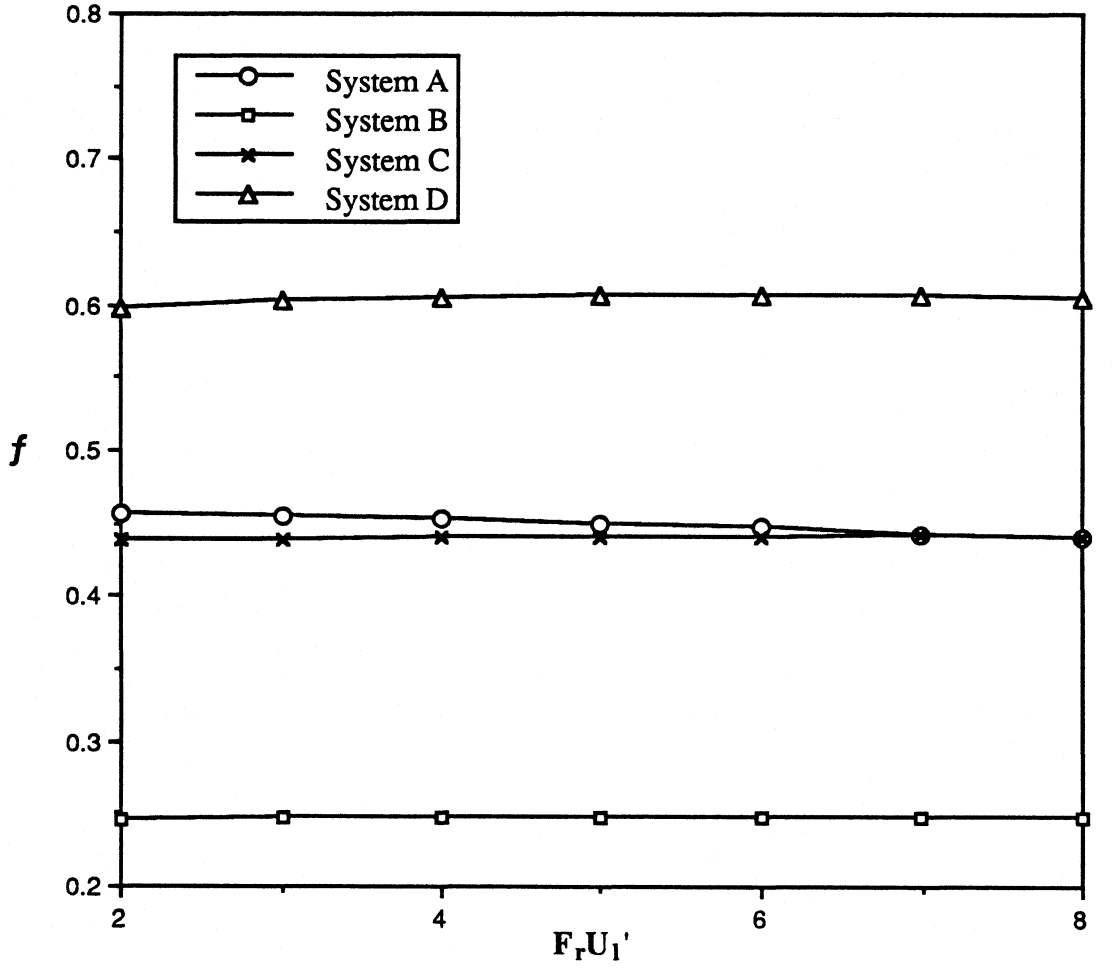

Figure 2.10 ASHRAE-95 solar fraction vs. choice of FrUl'. For each value of FrUl', a corresponding value of $F_r(\tau\alpha)_n'$ was derived using Eq. 2.29

2.6 EFFECT OF RADIATION PROFILE

The derived relationship between solar fraction and average draw temperature shown in Eq. 2.7 can be considered consistently accurate only if the solar fraction is below a critical value of 0.6. As Eq. 2.29 is based in part on this relationship, it inherits the same limitation. The question of what to do with large systems which yield solar fractions above 0.6 naturally arises.

It was shown in section 2.5.2, that a triangular radiation profile can be substituted for the SRCC profile without significantly effecting the system's behavior. This insensitivity to radiation profile suggests a possible answer to the previous question. Namely, it may be possible to adjust the SRCC profile, such that the solar fraction of the system being tested remains below 0.6. A reasonable rule of thumb to accomplish this task is to set the total incident daily radiation (i.e. $A_C H_t$) roughly equal to the total daily load (44,995 kJ). To determine what error, if any, such adjustment would cause, the procedure used to derive the parameter pairs shown in Fig. 2.9 was repeated in identical fashion, with the exception that the ASHRAE-95 simulations of systems A through D were performed with two alternate radiation profiles. These profiles, labelled 1 and 2 in figure 2.11, were created by multiplying the SRCC profile by 0.5 and 1.5, respectively.

The triangular approximation, substituted for for the SRCC profile in the development of Eq. 2.29, must be adjusted to fit the alternate profiles. This is effectively achieved by changing the value of G_{max}, the peak radiation of the triangular approximation, such that the total area under triangle remains equal to the total daily radiation of the profile used in the ASHRAE-95.

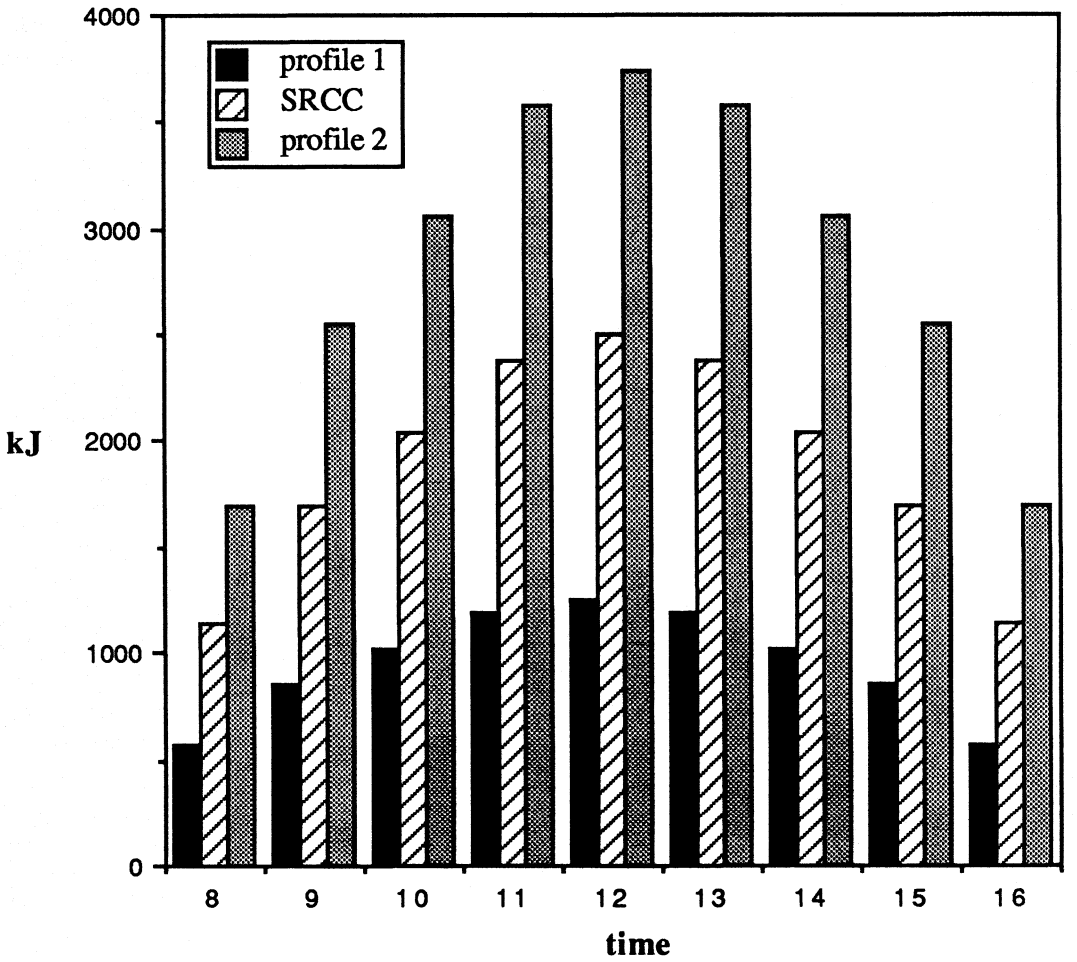

Figure 2.11 The SRCC radiation profile, compared with alternative profiles 1 and 2.

Thus,

$$G_{max,1} = 0.5\, G_{max,srcc} = 1702.2 \text{ kJ/m}^2$$

$$G_{max,2} = 1.5\, G_{max,srcc} = 5106.6 \text{ kJ/m}^2$$

where,

$G_{max,1}$ = peak radiation of triangular approx. of profile 1
$G_{max,2}$ = peak radiation of triangular approx. of profile 2
$G_{max,srcc}$ = peak radiation of triangular approx. of SRCC profile

The value of H_t used in the correlation for average collector inlet temperature must be equal to the adjusted value used during the test

Tables 2.7-10 compare the values of $F_r(\tau\alpha)_n'$ derived using profiles 1 and 2, to those derived using the SRCC profile. The values of $F_r(\tau\alpha)_n'$ derived from Eq 2.29 appear almost totally insensitive to the radiation profile used in the ASHRAE-95 test, if the appropriate corrections are made in G_{max} and H_t. The greatest difference, for example, between the values derived using profile 1 instead of the SRCC profile (a 50% reduction in H_t) is 1.42%. The SRCC profile may therefore be adjusted, if necessary, such that H_tA_C= 45,000 kJ, thus avoiding the introduction of significant error through the use of Eq 2.7. Such an adjustment, as evidenced by tables 2.7-10, does not introduce significant error to Eq. 2.29, and would result in moderate solar fractions (0.3-0.6) for the vast majority of SDHW systems tested.

Table 2.7
Comparison of Collector parameter pairs, derived from
ASHRAE-95 simulation results of system A, using three different radiation profiles

	$F_r(\tau\alpha)_n'$		
F_rU_l'	profile 1	SRCC	profile 2
0.0	0.6093	0.6106	0.6037
1.0	0.6537	0.6528	0.6458
2.0	0.6967	0.6938	0.6866
3.0	0.7386	0.7338	0.7263
4.0	0.7795	0.7728	0.7652
5.0	0.8196	0.8111	0.8032
6.0	0.859	0.8486	0.8406
7.0	0.8977	0.8856	0.8774
8.0	0.9358	0.9221	0.9137

Table 2.8
Comparison of Collector parameter pairs, derived from
ASHRAE-95 simulation results of system B, using three different radiation profiles

	$F_r(\tau\alpha)_n'$		
F_rU_l'	profile 1	SRCC	profile 2
0.0	0.6530	0.6592	0.6587
1.0	0.6732	0.6787	0.6775
2.0	0.6930	0.6979	0.6960
3.0	0.7127	0.7168	0.7142
4.0	0.7320	0.7355	0.7323
5.0	0.7511	0.7540	0.7501
6.0	0.7700	0.7723	0.7678
7.0	0.7888	0.7904	0.7853
8.0	0.8073	0.8084	0.8026

Table 2.9
Comparison of Collector parameter pairs, derived from
ASHRAE-95 simulation results of system C, using three different radiation profiles

	$F_r(\tau\alpha)_n'$		
F_rU_l'	profile 1	SRCC	profile 2
0	0.5992	0.5996	0.5999
1	0.628	0.6273	0.6267
2	0.6562	0.6545	0.6529
3	0.6838	0.6811	0.6786
4	0.7109	0.7073	0.7039
5	0.7377	0.7331	0.7288
6	0.764	0.7585	0.7533
7	0.7899	0.7836	0.7776
8	0.8156	0.8083	0.8015

Table 2.10
Comparison of Collector parameter pairs, derived from
ASHRAE-95 simulation results of system D, using three different radiation profiles

	$F_r(\tau\alpha)_n'$		
F_rU_l'	profile 1	SRCC	profile 2
0.0	0.4312	0.4315	0.4265
1.0	0.4693	0.4681	0.4615
2.0	0.5060	0.5034	0.4953
3.0	0.5416	0.5377	0.5281
4.0	0.5763	0.5711	0.5601
5.0	0.6102	0.6038	0.5914
6.0	0.6434	0.6359	0.6221
7.0	0.6761	0.6673	0.6523
8.0	0.7082	0.6983	0.6820

2.7 SUMMARY

An idealized system type, referred to as a simplified active system (SAS), was defined. It was shown that for this idealized system type, a function relating the collector parameters $F_r(\tau\alpha)_n$ and F_rU_l can be developed if hypothetical values of ASHRAE-95 solar fraction, collector area and tank volume are input to Eq. 2.29. Any pair of collector parameters which satisfy this function, if used to simulate the system's ASHRAE-95 performance, will produce approximately the same solar fraction originally used to develop the function. The accuracy of this function decreases above a critical value of solar fraction, but the SRCC radiation profile can be reduced to insure solar fraction is below this value.

If, instead of hypothetical values, the collector area, tank volume and ASHRAE-95 performance of an actual system are input to Eq. 2.29, the resulting function defines the parameter pair family of the equivalent SAS; that is, the SAS having the same collector area and tank volume, which exhibits simulated ASHRAE-95 performance approximately equal to the test performance of the actual system. The crucial advantage of this equivalent SAS is that it's long-term performance can be predicted using TRNSYS or F-Chart, while the performance of the actual system often cannot, as many of the actual system parameters are unknown.

CHAPTER 3
ESAS and Long Term Performance

It was established in Chapter 2 that the collector parameters of an equivalent simplified active system (ESAS) can be derived from the ASHRAE-95 test performance of an actual SDHW system. The simulated ASHRAE-95 performance of this ESAS will, by definition, be nearly identical to the ASHRAE-95 performance of the actual system. This chapter will establish that the simulated yearly performance of the ESAS can be used to closely approximate the yearly performance of the actual system, independent of location.

3.1 SENSITIVITY OF LONG-TERM PERFORMANCE

It was shown in section 2.5 that the ASHRAE-95 performance of the SAS is insensitive to change in F_rU_l, due to a compensating change in $F_r(\tau\alpha)_n$, as calculated by Eq. 2.29. For a given SAS, any collector parameter pair, (F_rU_l', $F_r(\tau\alpha)_n'$), that satisfies Eq. 2.29 can be used to simulate the ASHRAE-95 performance of that SAS with nearly identical results. It must be shown that any of these pairs will also yield nearly identical simulated yearly performance, independent of location, if simulations of the SAS are to be used to estimate the yearly performance of actual systems

The operating conditions experienced by the SAS during long-term outdoor installation differ substantially from the conditions experienced during the ASHRAE-95

test. The total daily draw, draw profile, and hot water set temperature of a particular residence may vary substantially from the values specified by the SRCC. The daily radiation profile, ambient temperature, and mains temperature will also vary from the ASHRAE-95 conditions, both from hour to hour and from location to location. As the family of parameter pairs for a particular SAS is determined under ASHRAE-95 test conditions, these variations may affect the sensitivity of SAS performance to the particular pair selected for use during simulation.

The effects of variation in draw profile and set temperature are not considered in the scope of this project. The draw profile of a particular residence is typically unknown, rules of thumb, based on family size, number of bathrooms, etc. are usually employed to estimate the hot water demand. As this project is concerned primarily with the development of a rating method, rather than the ability to size a system for a particular residence, a typical draw profile and set temperature are selected. The SRCC profile and set temperature used during the ASHRAE-95 are assumed to be 'typical' for a residential application, and are used for all long-term simulations.

Although the actual radiation profile during installed operation varies substantially from the profile used during the ASHRAE-95, it is not likely that this variation will affect the insensitivity of SAS performance to the choice of parameter pairs. It was shown in section 2.6 that the radiation profile used during the ASHRAE-95 test has negligible effect on the values of the parameter pairs produced by Eq. 2.29. Any of the the parameter pairs derived using one radiation profile, can therefore be used to accurately simulate the ASHRAE-95 performance using another profile. As the insensitivity of simulated SAS ASHRAE-95 performance is unaffected by variation in radiation profile, it seems likely that the same will be true of simulated yearly SAS

performance. This suspicion will be tested later in the development of this section.

It can be shown, however, that a variation in mains temperature or ambient temperature will significantly affect the insensitivity of SAS ASHRAE-95 performance to the parameter pair selected for simulation. The following procedure was used to demonstrate this fact. Recall that four typical SAS's, systems A through D, were defined in section 2.5. The parameters of these systems are shown in table 3.1 The ASHRAE-95 performance of system C was simulated, and the corresponding parameter pair family was determined using Eq. 2.29. Four different parameter pairs from this family, shown in table 3.2, were used to simulate the ASHRAE-95 performance of system C, at three different values of mains temperature. The first value was 22 °C; the original value of mains temperature used during the derivation of the parameter pair family. The second and third values were 12 °C and 28 °C respectively. All other ASHRAE-95 test conditions, including ambient temperature, were kept at their original values.

The results, shown in fig. 3.1a, indicate that the sensitivity of ASHRAE-95 performance to the parameter pair used in the simulation is significantly increased when the mains temperature is changed. When the simulations are performed using the original value of mains temperature, the two parameter pairs corresponding to the values $F_RU_l'=2.0$ and $F_RU_l'=8.0$ produce virtually identical simulated solar fraction. If these same two parameter pairs are used to simulate ASHRAE-95 performance at a mains temperature of 12 °C , the change in solar fractions is approximately 5%. At a mains temperature of 28 °C, the change is also approximately 5%, but opposite in sign.

Table 3.1
actual parameters of systems A through D

	A_c [m^2]	V_t/A_c [l/m^2]	F_rU_l [$W/m^2°C$]	$F_r(\tau\alpha)_n$
System A	2	30	2.0	0.7
System B	1	100	2.0	0.7
System C:	2	150	4.0	0.7
System D	4	150	8.0	0.7

Table 3.2
Parameter pairs of system C determined from simulated
ASHRAE-95 performance and Eq. 2.29

$\underline{F_rU_l}'$	$\underline{F_r(\tau\alpha)_n}'$
2.0	0.655
4.0	0.707
6.0	0.759
8.0	0.808

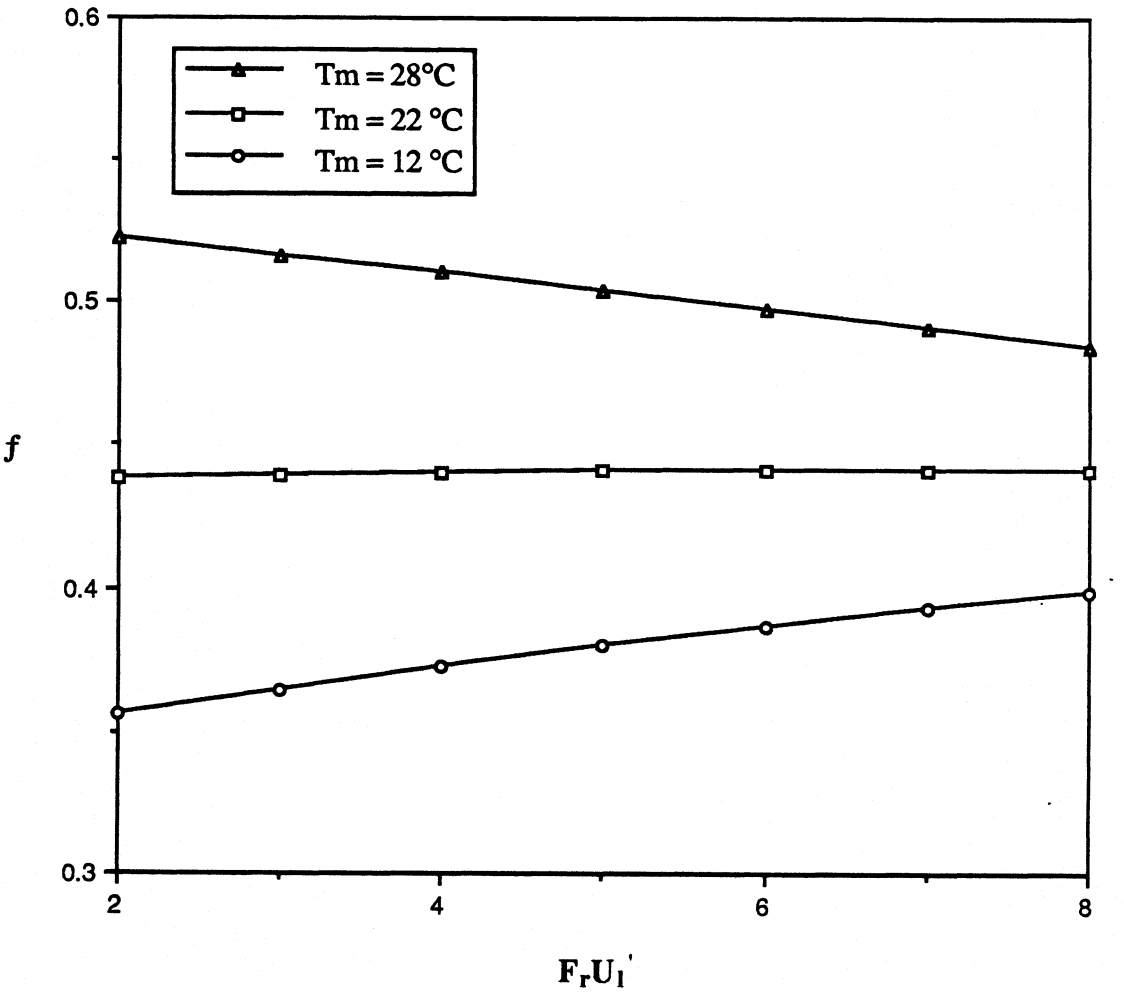

Figure 3.1a ASHRAE-95 solar fraction for three values of mains temperature vs. choice of parameter pair $\left(F_rU_l', F_r(\tau\alpha)_n'\right)$; System C

These results suggest that different members of the parameter pair family of a given SAS will produce different simulated yearly solar fractions, if the mains temperature used during the simulation differs from the value used during the ASHRAE-95 test. Considering the variability of mains temperature from location to location, this limitation would seriously detract from the usefulness of the ESAS prediction method.

An identical procedure was used to investigate the effect of variation in ambient temperature. In this case, the mains temperature was kept at its original value of 22 °C, and the simulations were performed for three values of ambient temperature: 12, 22, and 28 °C. The effect of this variation, shown in Fig. 3.1b, is similar to the effect of variation in mains temperature shown in Fig. 3.1a, with one crucial difference. The change in simulated solar fraction between the parameter pairs corresponding to F_rU_l'=2.0 and F_rU_l'=8.0 is positive when ambient temperature is increased from its original value and negative when decreased from its original value. The change in solar fraction between these parameters is *negative* when mains temperature is increased, and positive when decreased. Thus, the changes in the sensitivity of SAS ASHRAE-95 performance, caused by changes in mains and ambient temperature, are approximately equal in magnitude but opposite in sign.

These results suggest that variation in either mains or ambient temperatures will not affect the insensitivity of SAS performance to the selection of parameter pairs, if the two temperatures are varied concurrently, such that T_m=T_a. To verify this claim, the ASHRAE-95 simulations of system C, conducted in creating Figs. 3.1a and b, were repeated, varying ambient and mains temperature concurrently. The results are shown in Fig. 3.2.

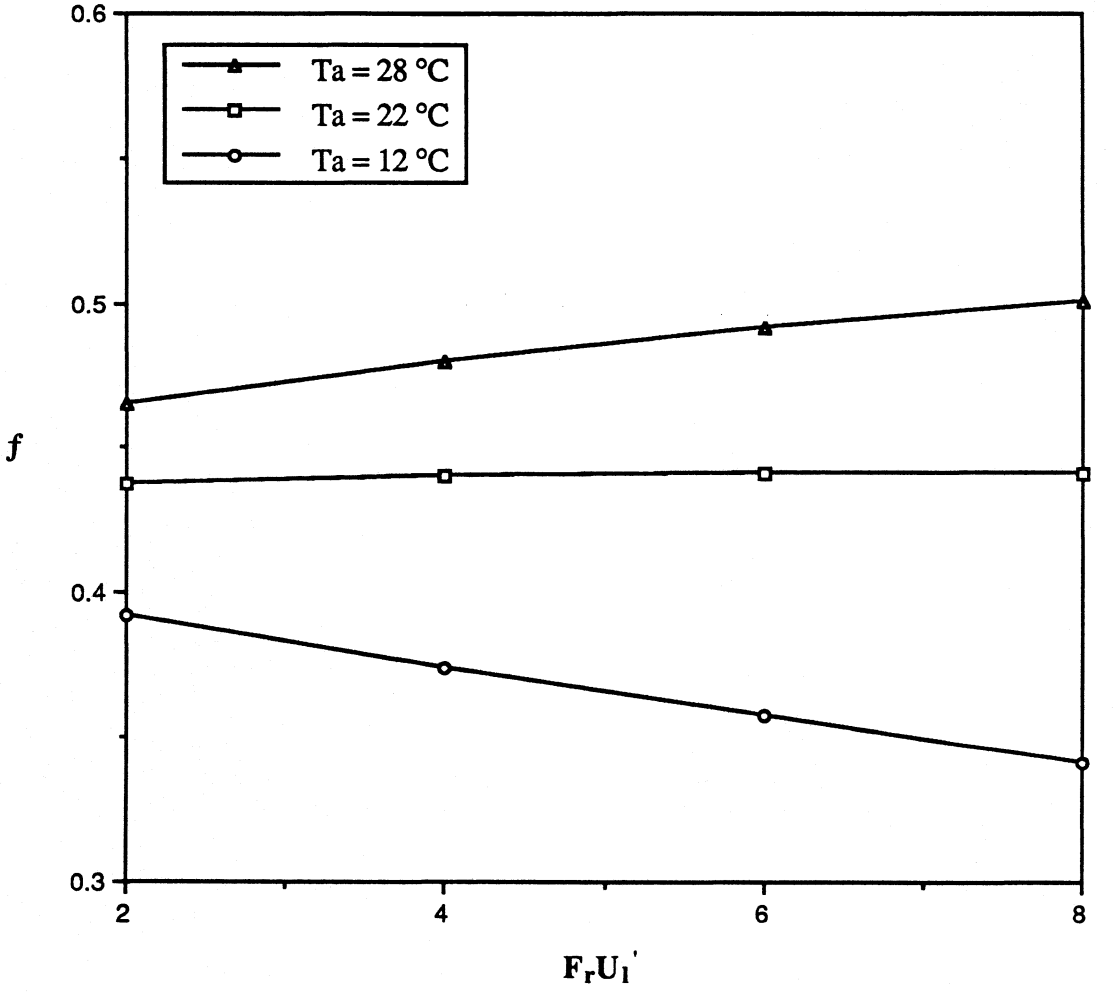

Figure 3.1b ASHRAE-95 solar fraction for three values of ambient temperature vs. choice of parameter pair $(F_rU_l', F_r(\tau\alpha)_n')$; System C

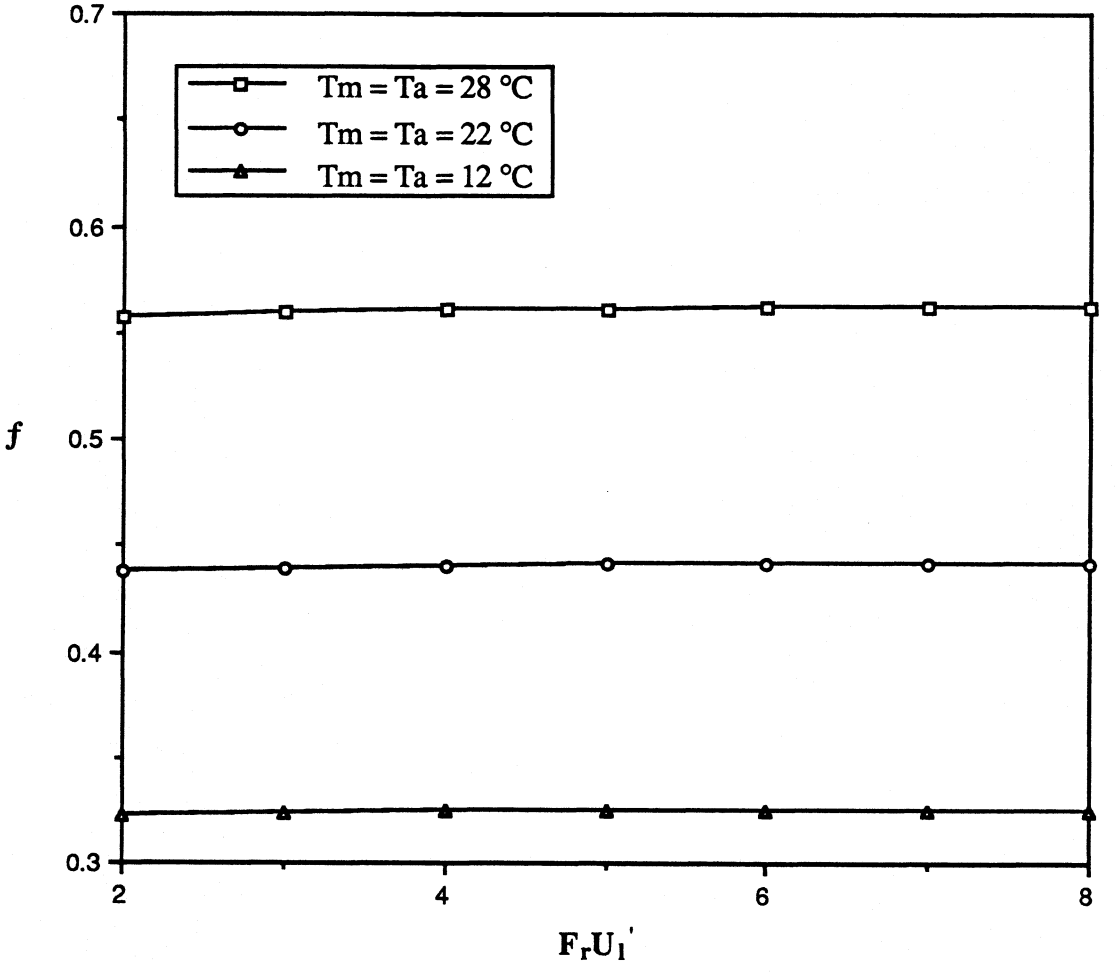

Figure 3.2 Simulated ASHRAE-95 solar fraction for system C verses choice of parameter pair $\left(F_rU_l', F_r(\tau\alpha)_n'\right)$ for three values of Tm = Ta.

When the constraint $T_m = T_a$ is imposed, all of the parameter pairs result in essentially the same simulated ASHRAE-95 performance, at all three values of ambient and mains temperature. An explanation for this phenomenon can be provided by the SAS integrated daily energy balance, Eq. 2.2.

$$\Delta E = A_c\left[F_r(\tau\alpha)_n H_{t,on} - F_r U_l(\overline{T}_i - T_a)\Delta t_{on}\right] - U_t A_t(\overline{T}_t - T_{env})\,\Delta t_{tot} - M_d C_p(\overline{T}_d - T_m) \quad (2.2)$$

On the last test day of the ASHRAE-95, $\Delta E \approx 0$, $T_{env}=T_a=T_m$, and $\overline{T}_d=\overline{T}_t$. With these simplifications, Eq. 2.2 can be rearranged, yielding:

$$F_r(\tau\alpha)_n\left[\frac{H_{t,on}}{(\overline{T}_d - T_m)}\right] - F_r U_l\left[\frac{(\overline{T}_i - T_a)}{(\overline{T}_d - T_m)}\,\Delta t_{on}\right] = \frac{U_t A_t \Delta t_{tot} + M_d C_p}{A_c} \qquad (3.1)$$

For a given SAS, the right-hand side of Eq 3.1 is a constant, while the quantities in the square brackets are determined by the three operating conditions, T_m, T_a and H_t. Eq 3.1 therefore defines a family of $Fr(ta)n'/F_rU_l'$ pairs which satisfy the energy balance of a particular SAS at a particular set of ASHRAE-95 conditions. If a change in one of these conditions results in a change in the bracketed quantities, a different family of pairs would be defined. Thus, the insensitivity of performance exhibited by a given family is affected by a change in an operating condition, only if that change alters the bracketed quantities.

Consider the effect of changing mains temperature, independent of ambient temperature, on the bracketed quantities. When the mains temperature is raised, the draw temperature is increased by some unknown amount. The average collector inlet

temperature, therefore, increases by a roughly equal amount. If the ambient temperature remains the same, the average temperature difference, $\overline{T}_i - T_a$, experienced by the collector increases, resulting in higher collector losses. The useful energy delivered to the tank is therefore reduced which in turn reduces the quantity, $\overline{T}_d - T_m$. The bracketed quantities are therefore changed by variation in mains temperature independent of ambient temperature.

Consider now the effect of raising mains temperature with the constraint, $T_m=T_a$. Again , the draw temperature and collector inlet temperature are increased by an unknown, but roughly equal amount. If the average draw temperature is increased as a result of this change, such that the quantity $\overline{T}_d - T_m$ decreases from its original value, then the quantity $\overline{T}_i - T_a$ also decreases by an equal amount. This in turn decreases the average temperature difference across the collector, reducing collector losses and increasing the useful energy delivered to the tank. This serves to drive the quantity $\overline{T}_d - T_m$ back towards it's original value. By the same logic, if quantity $\overline{T}_d - T_m$ *increases*, the collector losses increase, which in turn *decreases* the useful energy and $\overline{T}_d - T_m$, again driving it towards it's original value. Thus, the dynamics of the SAS are such that when $T_m=T_a$, the quantity $\overline{T}_d - T_m$ is independent of mains temperature. As ambient temperature is equal to mains temperature, the quantity $\overline{T}_i - T_a$, is also driven to its original value, and is therefore independent of mains temperature.

To verify these statements, ASHRAE-95 simulations of systems A through D were conducted at ten different values of mains temperature, ranging from 12 °C to 32 °C. The ambient temperature was set equal to the mains temperature for each of these simulations. The quantities $\overline{T}_d - T_m$ and $\frac{(\overline{T}_i - T_a)}{(\overline{T}_d - T_m)}$ provided by these simulations are plotted against the corresponding values of mains and ambient temperature in Figs 3.3

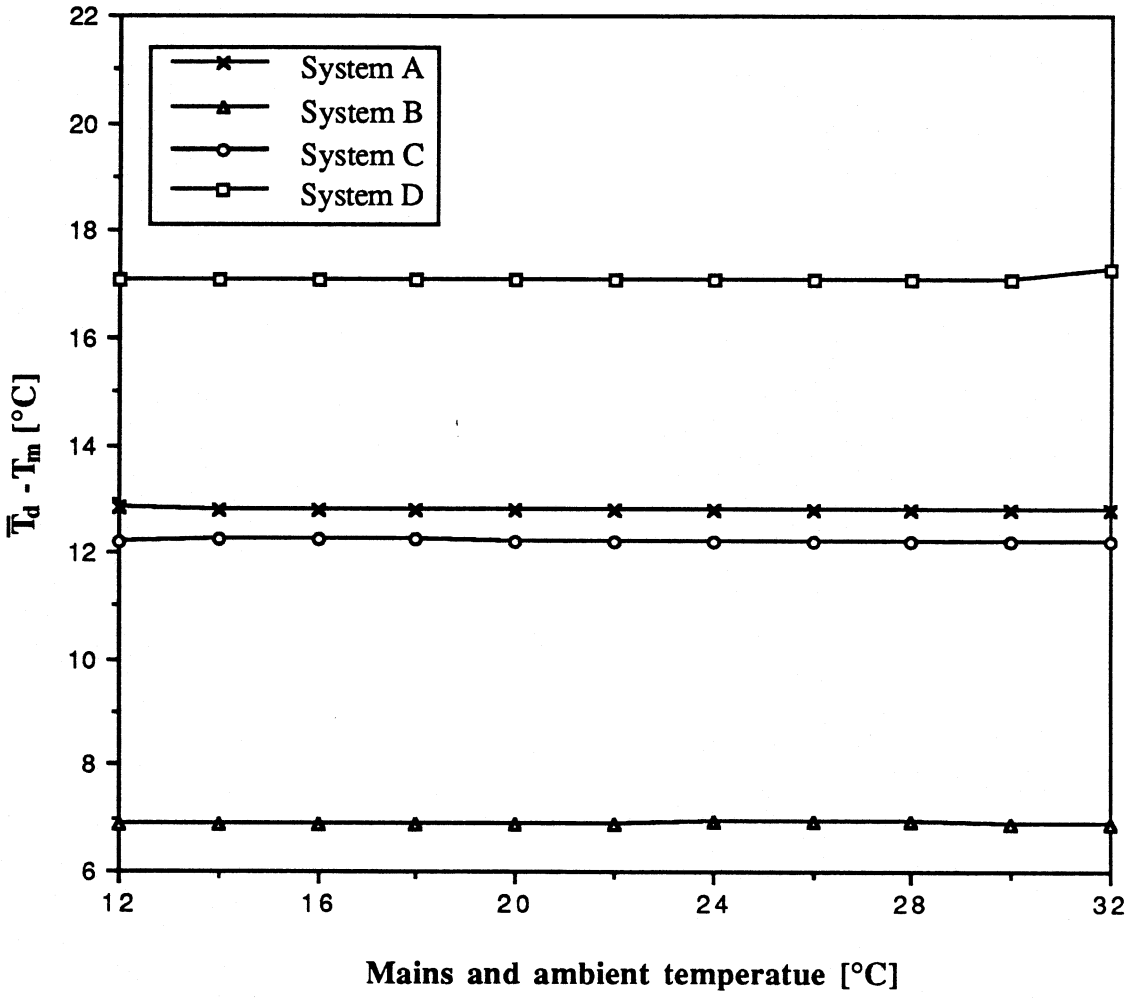

Figure 3.3 $\overline{T}_d - T_m$ verses mains and ambient temperature with the condition $T_a = T_m$. From ASHRAE-95 simulations of systems A-D.

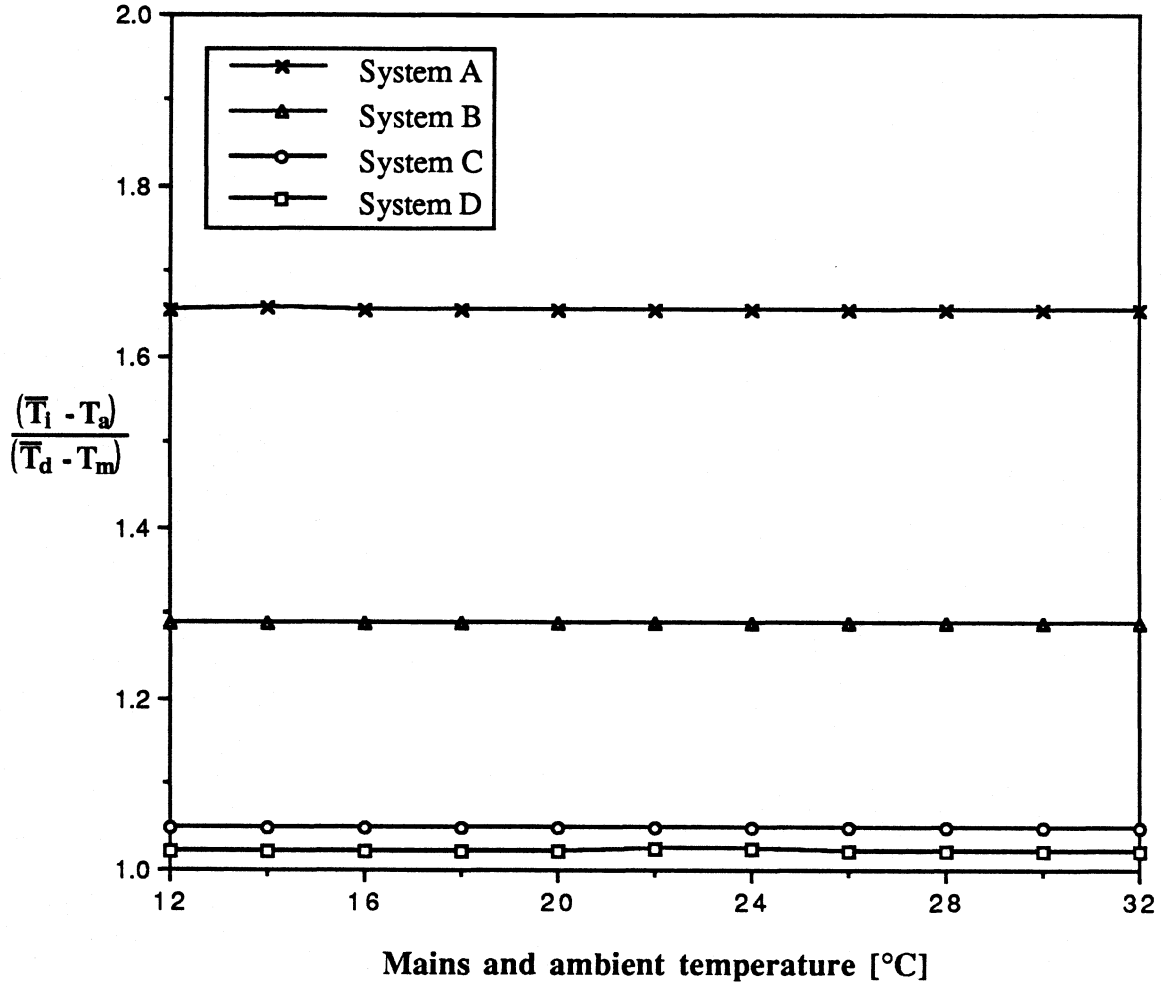

Figure 3.4 The quantity $\frac{(\overline{T}_i - T_a)}{(\overline{T}_d - T_m)}$ verses mains temperature with the condition $T_a = T_m$; from ASHRAE-95 simulations of systems A-D.

and 3.4. The figures indicate that both quantities are independent of mains temperature for all four systems, if the ambient and mains temperatures are equal.

By an analogous argument, the variables $H_{t,on}$ and t_{on} are also independent of mains or ambient temperature when $T_m=T_a$. Recall that both of these variables are fixed for a given value of critical radiation level, $\overline{G}_{tc}$, where:

$$\overline{G}_{tc} = \frac{F_r U_l(\overline{T}_i - T_a)}{F_r(\tau\alpha)_n} \qquad (3.2)$$

If the quantity $\overline{T}_d - T_m$ was increased by a change in mains temperature, the quantity $\overline{T}_i - T_a$ would also increase by a roughly equal amount. This would in turn increase the critical radiation level, according to Eq. 3.2. An increase in $\overline{G}_{tc}$, however, would decrease the utilizable energy and thus decrease the quantity $\overline{T}_i - T_a$. In this manner, $\overline{T}_i - T_a$ and G_{tc} maintain their original values, independent of changes in mains temperature, as long as $T_a=T_m$.

As $H_{t,on}$, t_{on}, $\overline{T}_d - T_m$ and $\overline{T}_i - T_a$ are all independent of mains temperature if $T_a=T_m$, the bracketed quantities in Eq 3.1 remain unchanged. The insensitivity of SAS ASHRAE-95 performance to the parameter pair selected is therefore unaffected by variation in mains temperature and ambient temperature, as long as the two temperatures are equal.

It is seems likely that the same result will occur during long term installed operation, for the following reasons. The daily energy balance shown in Eq. 2.2 can be converted to a yearly energy balance that applies to long-term installed operation, by changing the period of integration. During long-term installed operation, however, both the mains temperature and the ambient temperature vary over time. It is therefore necessary to replace the constant values of these temperatures shown in Eq 2.2 with the

integrated yearly average values.

The nature of variation in mains temperature over time depends on the source of the mains water in a given location. If the source is deep ground water, the mains temperature will remain essentially constant. If the source is surface water, the mains temperature will follow the variation in ambient temperature by a constant lag time, but at a lower amplitude. These two extremes are shown in figure 3.5. In both cases, the average yearly mains temperature is approximately equal to the average yearly ambient temperature. The yearly load will be approximately the same for either mains water source, at a given set temperature and total daily draw. It is therefore assumed, when simulating yearly installed operation, that the mains water source is ground water, and the mains temperature is set equal to the average yearly ambient temperature of the location in question. As the mains temperature and yearly average ambient temperature are equal, the yearly performance of the SAS should exhibit the same insensitivity to the choice of parameter pairs observed during simulations of the ASHRAE-95.

To test this hypothesis, the parameter pairs derived from ASHRAE-95 simulations of systems A through D were used to simulate the yearly operation of those systems in five locations: Madison, New York, Nashville, Albuquerque, and Miami. The simulations were performed using Typical Mean Year (TMY) weather data, with the mains temperature set equal to the average yearly ambient temperature for the location in question. The daily draw profile and set temperature used during the simulations were the same as those specified by the SRCC for the ASHRAE-95 test. Figures 3.6 to 3.10 show the results of these simulations. The RMS difference between the yearly solar fraction produced by the parameter pairs corresponding to F_RU_l'=2.0 W/m2 and F_RU_l=8.0 W/m2 is 1.6%.

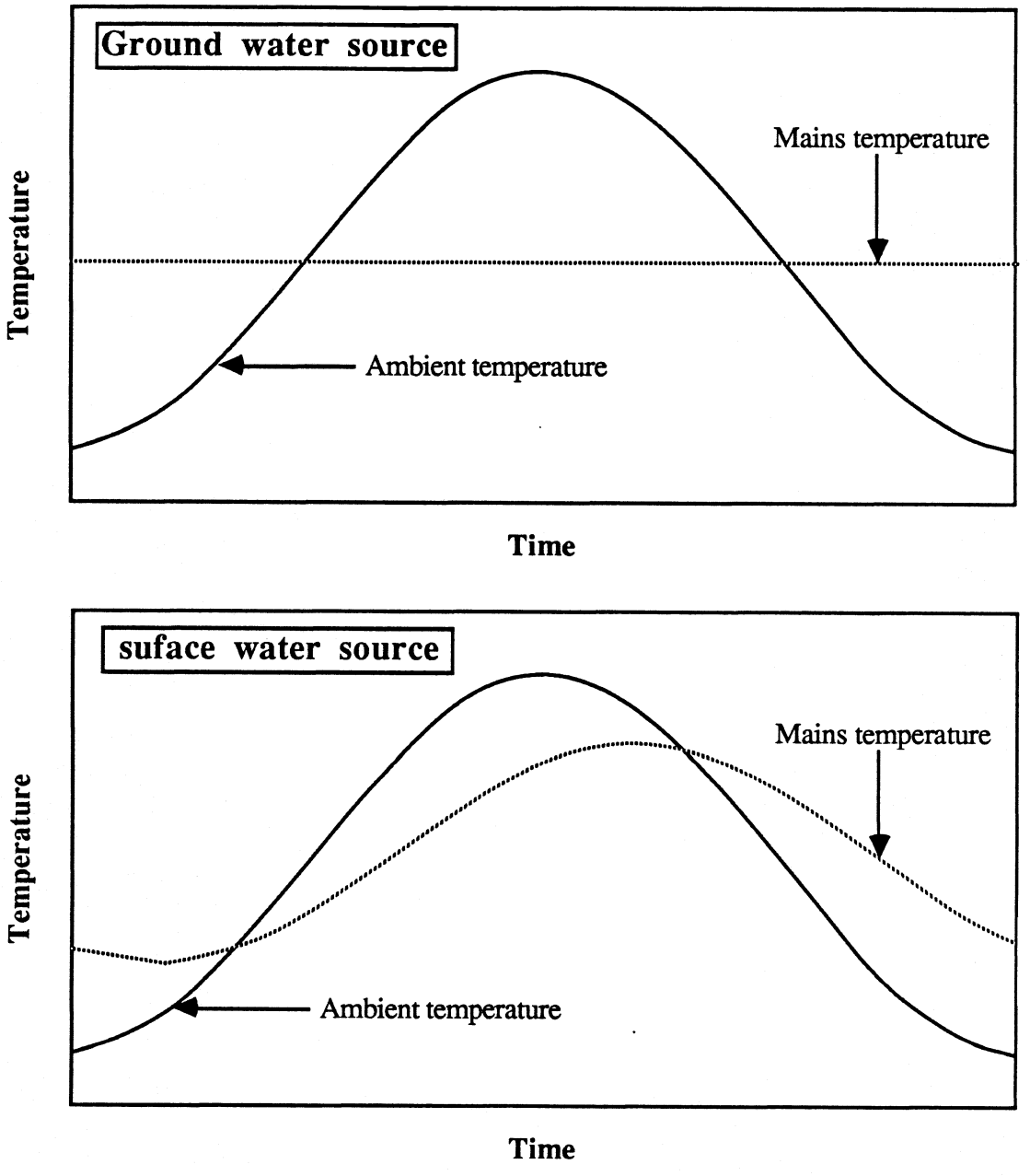

Figure 3.5 typical profiles of mains temperature and ambient temperature for ground water and surface water sources.

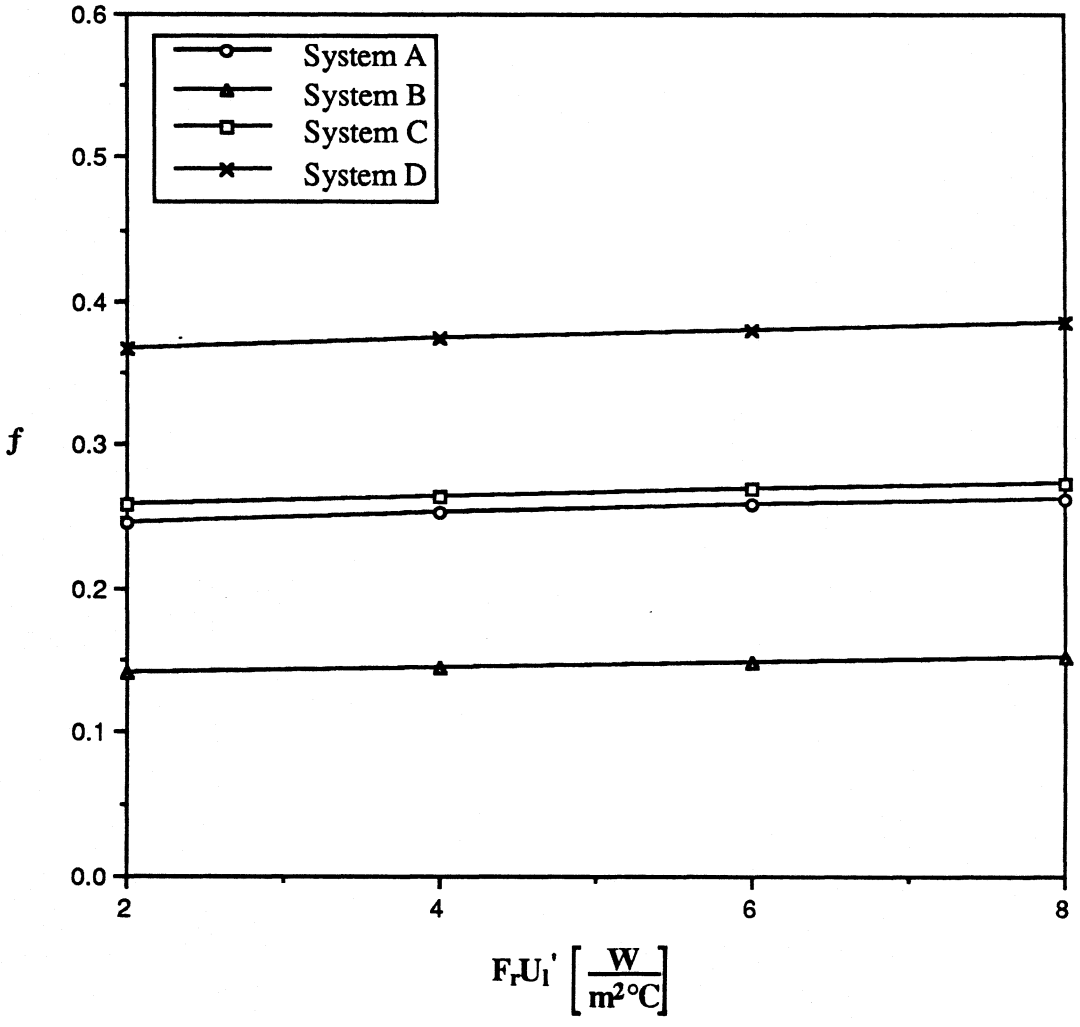

Figure 3.6 Simulated yearly solar fraction verses choice of parmeter pair $(F_rU_l', F_r(\tau\alpha)_n')$ with mains temperature equal to average yearly ambient temperature; Madison.

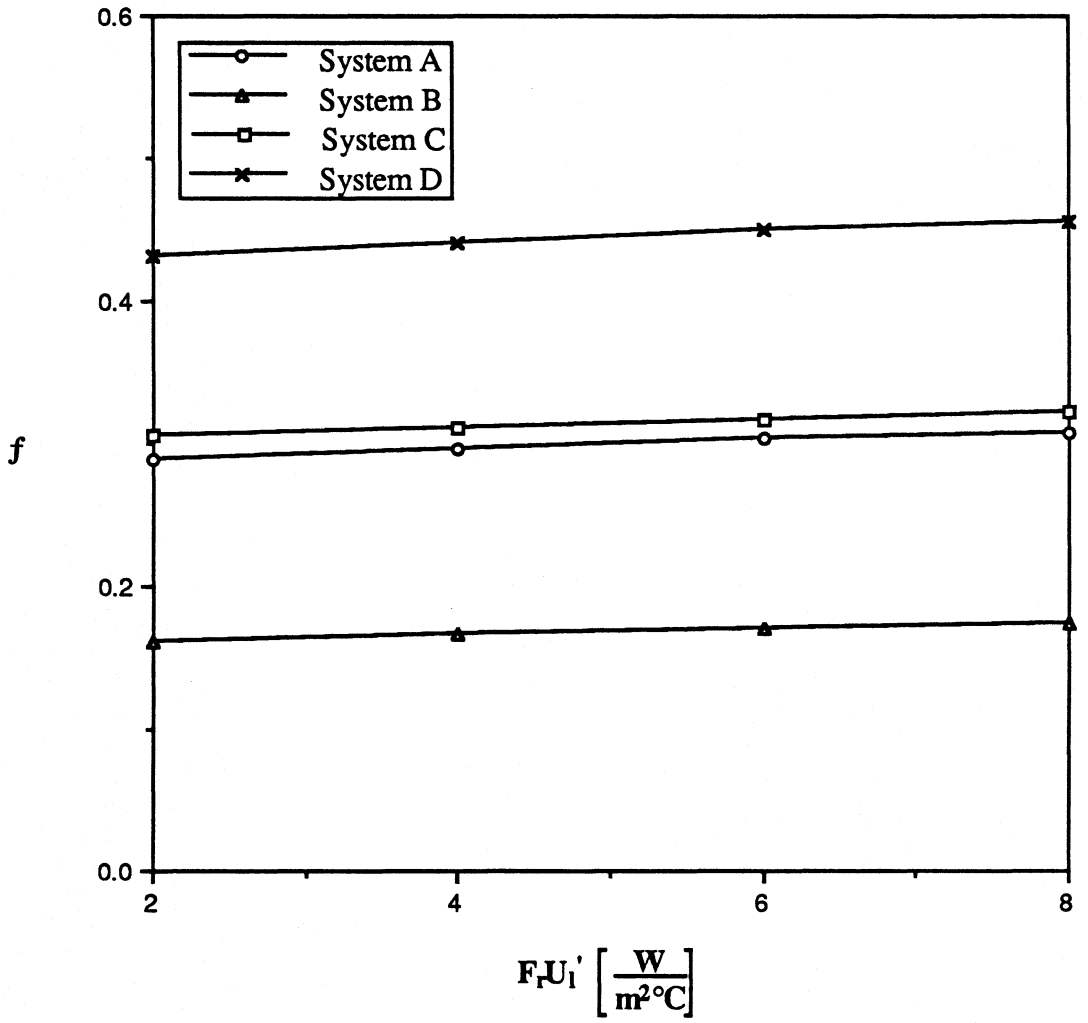

Figure 3.7 Simulated yearly solar fraction verses choice of parmeter pair $(F_rU_l', F_r(\tau\alpha)_n')$ with mains temperature equal to average yearly ambient temperature; Nashville.

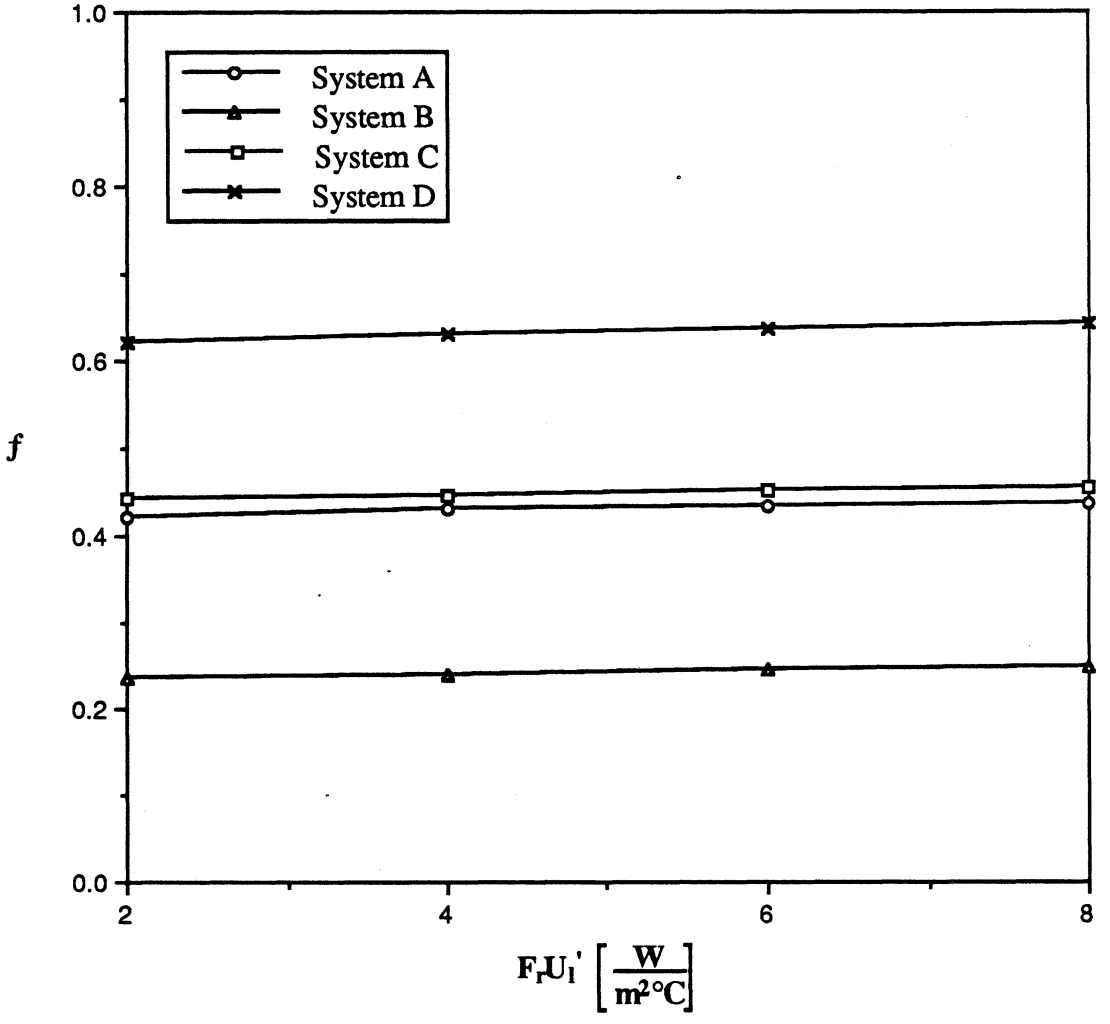

Figure 3.8 Simulated yearly solar fraction verses choice of parmeter pair $(F_rU_l', F_r(\tau\alpha)_n)$ with mains temperature equal to average yearly ambient temperature; Albuquerque.

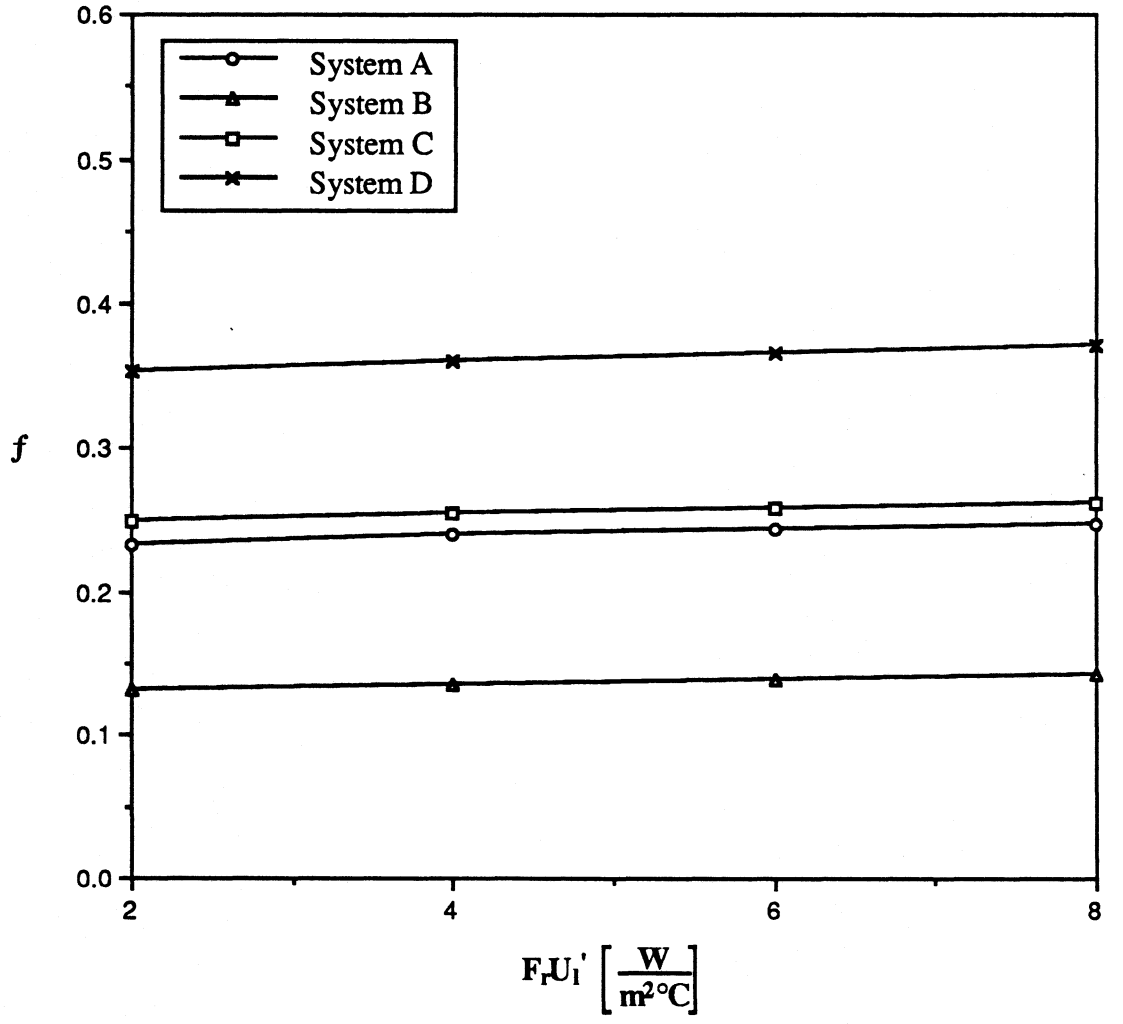

Figure 3.9 Simulated yearly solar fraction verses FrUl' with mains temperature equal to average yearly ambient temperature; New York.

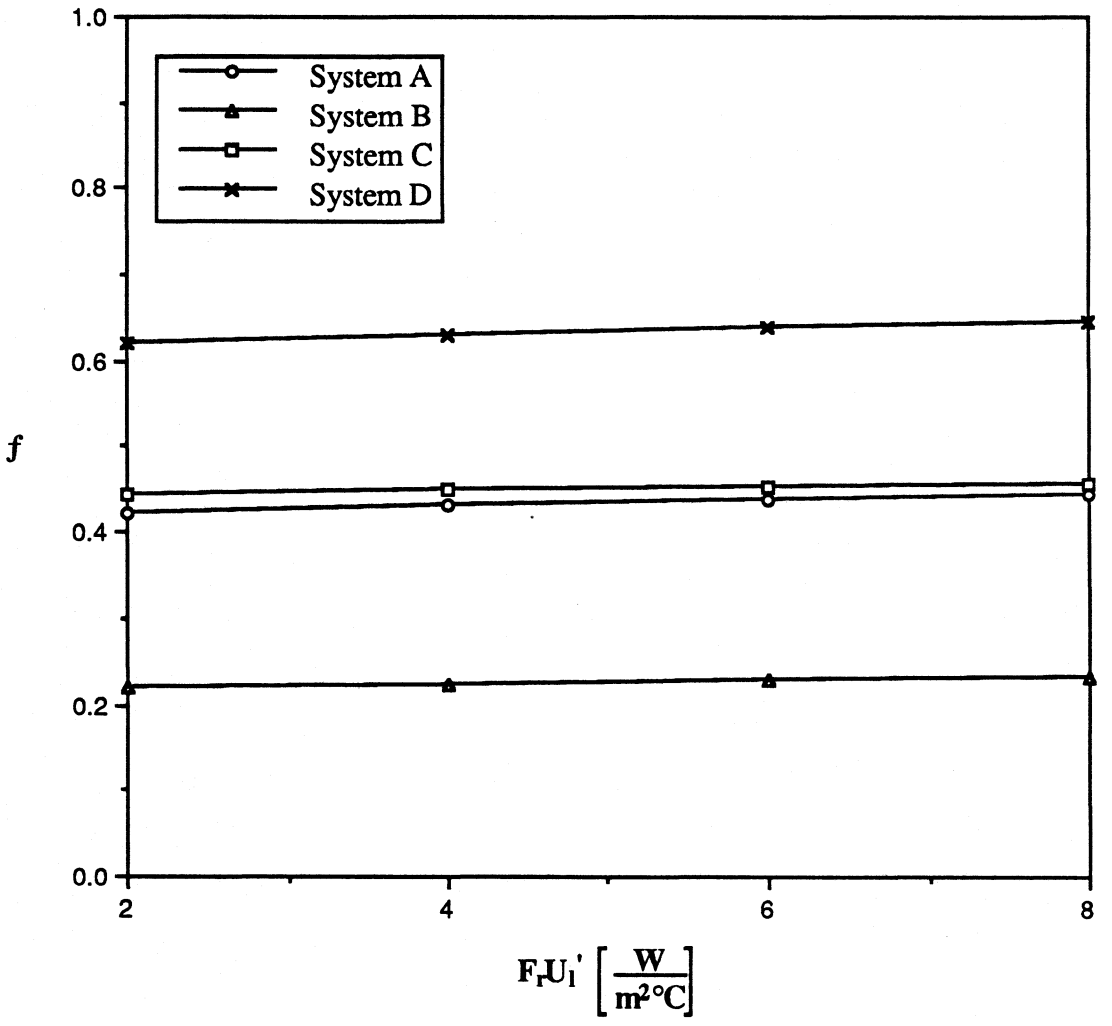

Figure 3.10 Simulated yearly solar fraction verses choice of parmeter pair $[F_rU_l', F_r(\tau\alpha)_n]$ with mains temperature equal to average yearly ambient temperature; Miami.

It is concluded that any of the parameter pairs derived for a given SAS at ASHRAE-95 test conditions, can be used to simulate the yearly performance of that SAS with nearly identical results, independent of location.

3.2 ESAS VERSES COMPLEX SYSTEM PERFORMANCE

This section compares the simulated performance of a variety of complex systems to the simulated performance of their equivalent simplified active systems, in five locations. The procedure used to perform all these comparisons is as follows: A simulated ASHRAE-95 test of the complex system is conducted using the appropriate detailed TRNSYS models. The total daily radiation used during this simulation is adjusted, when necessary, in the manner described in section 2.6. The resulting solar fraction is used to determine the collector parameter function (Eq. 2.29) of the equivalent simplified active system, as described in chapter 2. As all the parameter pairs which satisfy this function yield essentially the same simulated yearly performance for that SAS, a moderate value of F_rU_l'=5.0 W/m^2, is selected for all yearly ESAS simulations.

This value of F_rU_l', and the corresponding value of $F_r(\tau\alpha)_n'$ which satisfies Eq. 2.29, are used to simulate the yearly operation of the ESAS in the five locations shown in Figs. 3.6-10. The yearly operation of the complex system is simulated for the same locations, and the resulting values of performance are compared in sections 3.2.1 to 3.2.3.

The following statements apply to all yearly simulations whose results are presented in this section. TMY data are used to provide hourly values of ambient

temperature and total radiation on a horizontal surface, for each location. The collector slope in each location is set equal to the latitude of that location. Erb's correlation [18] and geometrical calculations of sun position are used to determine the radiation incident on the collector surface at this slope, during each time step. The mains temperature for a given location is constant, and is set equal to the local yearly-average ambient temperature. The load profile and set temperature are those specified by the SRCC.

3.2.1 Incidence Angle Dependence and Tank losses

The collector efficiency of the SAS, by definition, is independent of the angle of incident radiation. In reality, the absorbtance and reflectance of all collectors have some dependence on incidence angle. This dependence is typically determined experimentally, by a collector test such as the ASHRAE-93. A constant, b_0, can be determined from the results of such a test, which relates incidence angle to a correction factor, $K_{\tau\alpha}$, defined as:

$$K_{\tau\alpha} = \frac{(\tau\alpha)}{(\tau\alpha)_n} = 1 + b_0\left(\frac{1}{\cos\theta} - 1\right) \qquad (3.4)$$

where

$(\tau\alpha)$ = Transmittance-absorbtance product at angle θ

$(\tau\alpha)_n$ = Transmittance-absorbtance product at normal incidence

The collector models used in TRNSYS account for the effect of incidence angle on performance by using value of b_0 as a parameter, and multiplying the collector gain coefficient by $K_{\tau\alpha}$ during each time-step of a simulation. When simulating the

performance of the SAS, the parameter b_0 is set equal to zero.

The incidence angle dependence of an actual SDHW system is accounted for in the collector parameters of it ESAS in the following fashion. An actual system whose collector has a high value of b_0 will exhibit decreased efficiency during the morning and evening periods of the ASHRAE-95 test day. Such a system will yield a lower solar fraction during the ASHRAE-95 test than an otherwise identical system whose collector efficiency is independent of incidence angle. If this lower value of solar fraction is used to derive the parameters of the equivalent SAS, the value of $F_r(\tau\alpha)_n'$ will reflect this decreased efficiency, in satisfying the daily energy balance. As a result, the collector parameters of the ESAS contain what amounts to a built-in average correction factor for the incidence angle dependance of it's actual counterpart.

The tank loss coefficient of the SAS, 1.5 $W/m^2°C$, is also unrealistic. Actual SDHW systems typically have values many times larger, but the additional tank losses are accounted for in a similar manner. The ASHRAE-95 performance of a system with large tank losses will be lower than for a system with small losses. This difference will be reflected in the collector parameters of the corresponding ESAS. In essence, the entire thermal behavior of an actual system is lumped into the collector parameters of the ESAS.

As a result, it is reasonable to expect that the long term performance of actual SDHW systems having incident angle dependence and high tank losses can be approximated by the yearly performance of their equivalent simplified active systems. To investigate the accuracy of such an approximation, systems A through D were given incidence angle dependance, by setting b_0 to 0.2. The tank losses experienced by these systems were increased by raising the tank loss coefficient , from 1.5 to 6.0

$W/m^2°C$. With these modifications, systems A through D are no longer simplified active systems. They are computer models which represent a degree of complexity exhibited by actual systems. Such models will therefore be referred to as complex systems. The simulated yearly performance of the complex versions of systems A through D is compared to ESAS yearly performance in Fig. 3.11. The RMS error in the solar fractions predicted by the ESAS, defined as,

$$RMS = \left[\frac{1}{n}\Sigma(f_{complex} - f_{ESAS})^2\right]^{0.5}$$

is 0.014, which indicates that ESAS performance can be used to closely estimate the performance of the active, well-mixed systems, having incidence angle dependence and large tank losses.

3.2.2 Stratified Active Systems

Many actual SDHW systems, including active systems, will exhibit some degree of stratification. Due to the effect of fluid buoyancy, a vertical temperature gradient develops in the tank during operation, such that the bottom fluid is colder than the top fluid. Such a temperature gradient has a beneficial effect on performance, due to the decrease in collector inlet temperature. The collector of a stratified system experiences lower losses and can therefore deliver greater useful energy to the tank than if the same system were well-mixed.

Stratification is modelled in TRNSYS by dividing the tank into a number of isothermal nodes. During TRNSYS simulations, a separate energy balance is solved for each one of these nodes, at each time step. Refer to the TRNSYS manual [3], for a

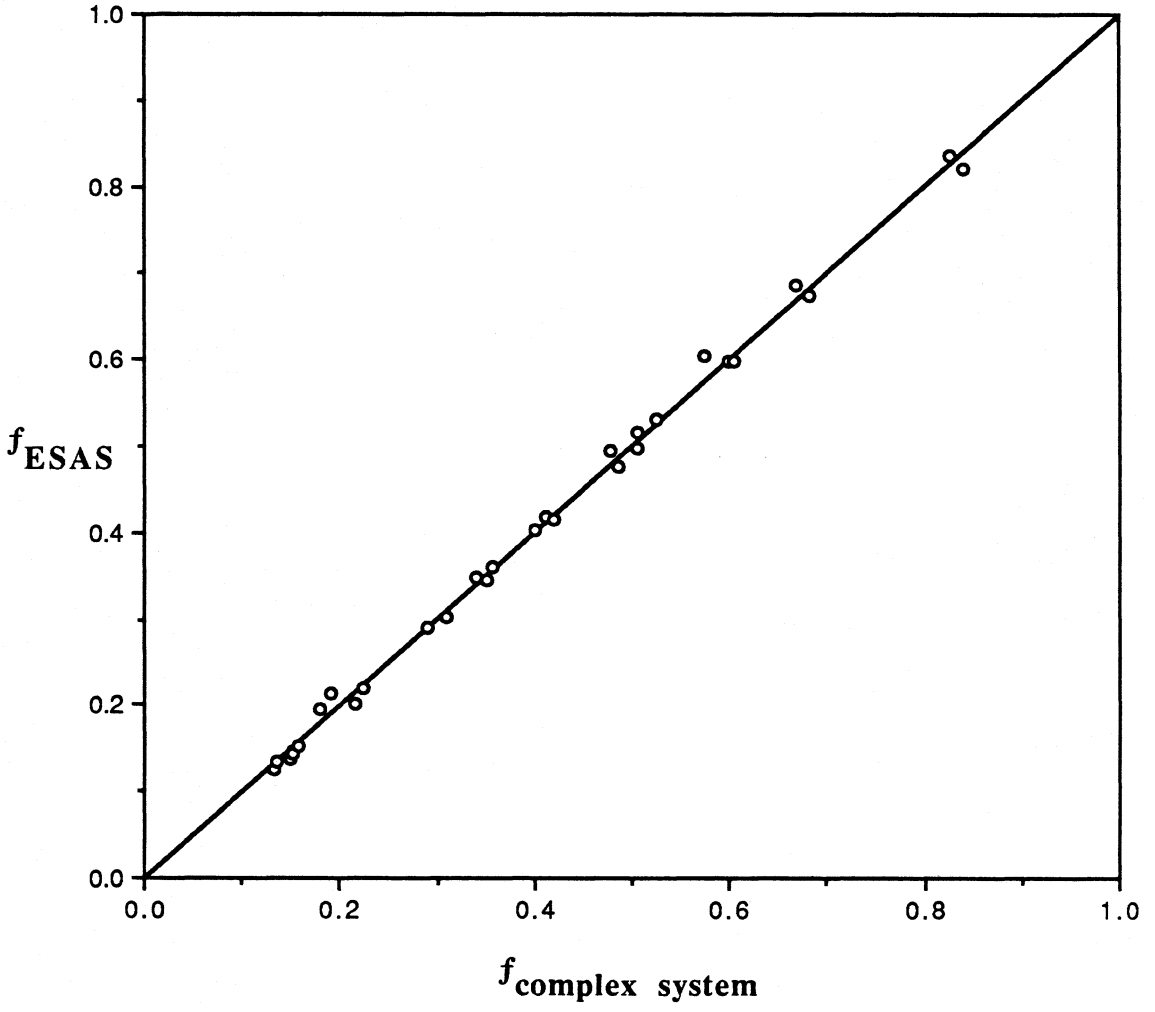

Figure 3.11 Simulated yearly performance of systems having incidence angle dependance and larger tank loss coefficients verses ESAS performance.

detailed discussion of stratified storage models.

The degree of stratification (i.e., the magnitude of the temperature gradient in the tank) is a strong function of the collector flow rate. At low values of collector flow rate, less mixing of the tank occurs, and stratification increases. Stratification is also enhanced by the use of a variable tank inlet. Such an inlet is vertically adjustable, and automatically moves to the level at which tank fluid is closest in temperature to the returning fluid from the collector.

The accuracy of estimating the yearly performance of stratified active systems using ESAS performance was investigated by introducing a high degree of stratification to the models of systems A through D. This was achieved by setting the collector flow rate of these systems equal to a low value of 25 l/hr, and dividing the tank into ten thermal nodes. A variable inlet was also introduced. The effect of these changes on the simulated ASHRAE-95 performance of systems A through D is shown in table 3.3.

Table 3.3
ASHRAE-95 solar fraction of systems A-D with one node tank verses solar fraction of same systems with 10 node tank, variable inlet and a collector flow rate of 25 l/hr

	A_c [m^2]	V_t/A_c [l/m^2]	F_rU_l [$W/m^2°C$]	f 1 node	f 10 nodes
System A	2	30	2.0	0.595	0.657
System B	1	100	2.0	0.637	0.684
System C:	2	150	4.0	0.564	0.685
System D	4	150	8.0	0.394	0.676

The introduction of stratification improves the performance of all four systems, but the effect is particularly dramatic for systems C and D. These systems have larger values of $F_T U_l$, and the reduction in collector inlet temperature due to stratification therefore causes a greater reduction in collector losses than for systems A and B.

The solar fractions shown in the far right hand column of table 3.3 and Eq. 2.29 were used to determine the parameters of the equivalent simplified active systems corresponding to the stratified versions of systems A through D. The simulated yearly solar fractions of these ESAS are compared to the simulated yearly solar fraction of the stratified systems in Fig. 3.12. The RMS error is 0.022, indicating that the ESAS can be used to accurately estimate the performance of stratified active systems, independent of location.

3.2.3 Thermosyphon Systems

Thermosyphon systems differ from active systems in that they rely on fluid buoyancy to drive the circulation of fluid between the collector and tank. The configuration of thermosyphon systems is such that the collector outlet is located below the level of the tank outlet that supplies fluid to the collector. When the the collector outlet temperature becomes greater than the collector inlet temperature, a difference in fluid density is created between the collector outlet and the tank outlet, which drives circulation. A check valve prevents circulation in the opposite direction, when the collector outlet is colder than the collector inlet. The operation thermosyphon systems is therefore controlled in a manner similar to active systems; both systems only circulate fluid when the useful gain from the collector is positive.

Four typical thermosyphon systems were modelled using TRNSYS to investigate

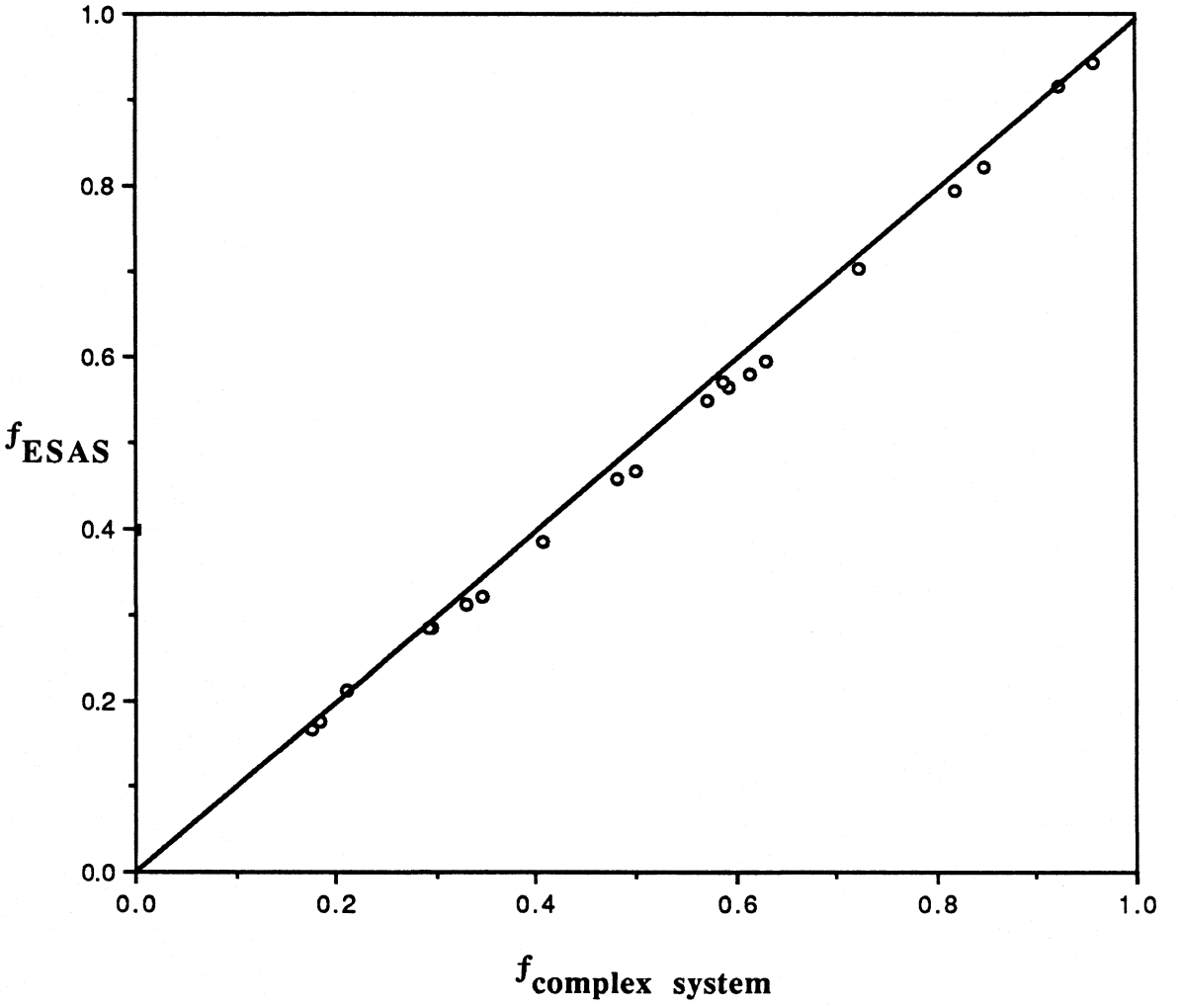

Figure 3.12 Simulated yearly performance of highly stratified active systems (10 node tank) verses ESAS performance.

the accuracy of estimating thermosyphon performance with ESAS performance. Refer to the TRNSYS manual [3] for a detailed discussion of the thermosyphon model. The parameters of these four systems, labelled E through H, are shown in table 3.4. The simulated yearly performance of these systems is compared to the performance of their equivalent simplified active systems in Fig. 3.13. The RMS error is 1.69%.

Table 3.4
Parameters of thermosyphon systems E through F

System		E	F	G	H
A_c	[m^2]	1	2	3	4
V_t/A_c	[l/m^2]	300	150	100	75
F_rU_l	[$W/m^2°C$]	2	4	6	8
$F_r(\tau\alpha)_n$		0.6	0.7	0.8	0.9
U_t	[$W/m^2°C$]	0	2	4	6
b_0		0.0	0.05	0.1	0.15
H_{ct}	[m]	0.0	1.0	2.0	3.0
N_r		20	15	10	5
D_r	[mm]	10	20	30	40
mode		1	2	1	1

Key: H_{ct} = vertical distance between collector outlet and tank outlet
N_r = number of riser tubes per collector panel
Dr = diameter of riser tubes
mode: 1 = fixed tank inlet 2 = variable tank inlet

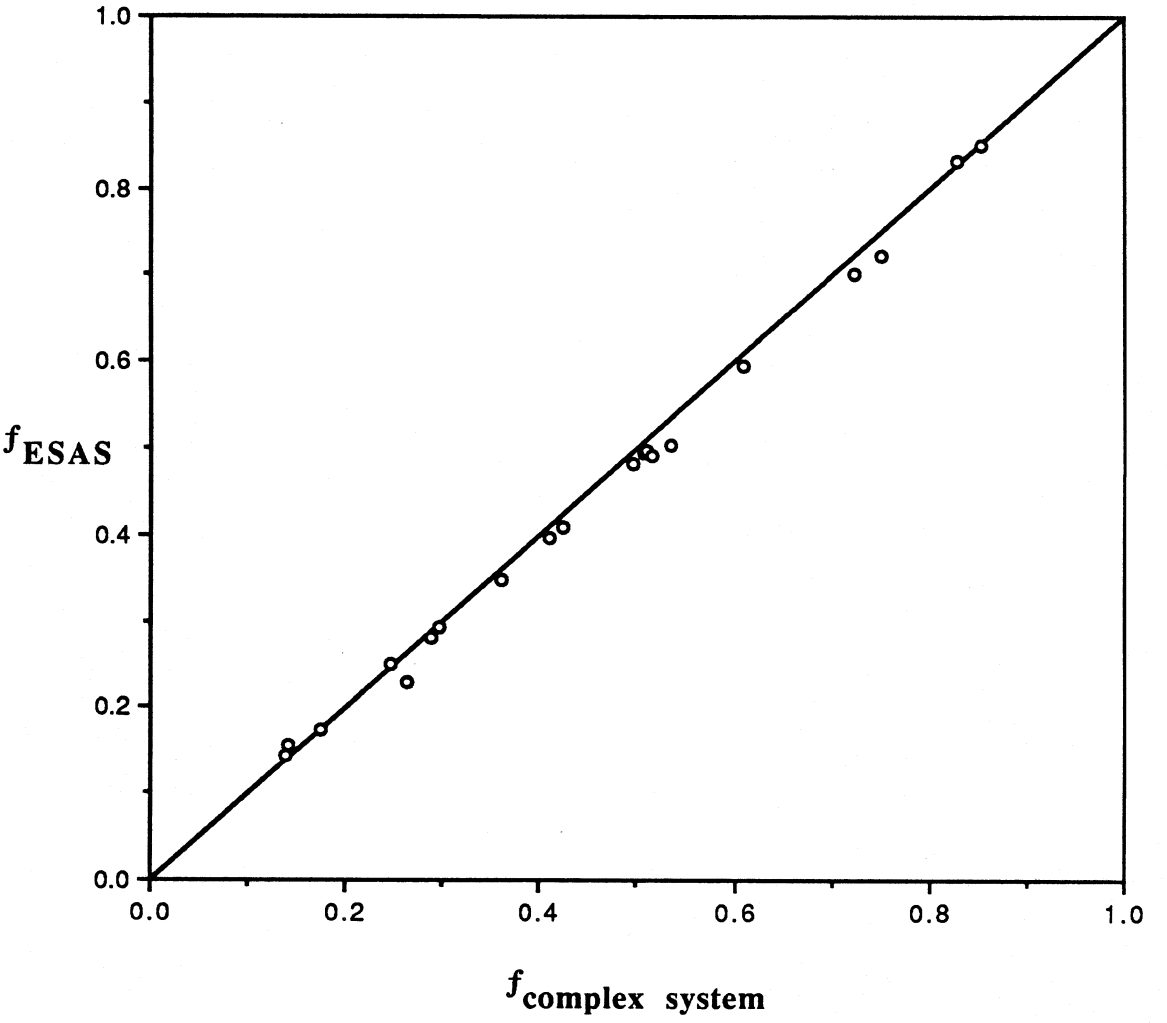

Figure 3.13 Simulated yearly performance of thermosyphon systems E-H verses ESAS performance.

3.3 EXPERIMENTAL VALIDATION

In 1979, Klein and Fanney monitored the outdoor yearly performance of six SDHW system at the National Bureau of Standards (NBS) in Washington D.C. [10]. One of these systems was also subjected to an ASHRAE-95 test at NBS [22], although the test conditions adopted by Fanney and Klein differ from those specified by the SRCC. In this section, the ASHRAE-95 test performance of this system, as measured by Fanney and Klein, is used to determine the parameters of the equivalent simplified active system, using the procedure described in Chapter 2. The simulated yearly performance of the ESAS is compared to the measured yearly performance of the actual system.

3.3.1 System Description

The system subjected to the ASHRAE-95 test by Klein and Fanney is a single-tank indirect (STI) active system with a wrap around heat-exchanger. Indirect, in this context, refers to the fact that the collector loop transfers heat to the storage tank indirectly, through the use of a heat exchanger. A schematic of the STI system is shown in Fig. 3.14. A description of the various components of this system are given below. A more detailed system description is given in [22].

1) Collector

The collector array of the STI system consists of three collector panels mounted in parallel. Each panel has a single glass cover with a net aperture area of 1.40 m^2, and is backed fiberglass insulation. Instantaneous efficiency tests of these collectors were conducted at NBS to estimate the values of the collector gain and loss coefficients and the incident angle modifier constant. Least squares fits of the resulting data yielded the following values:

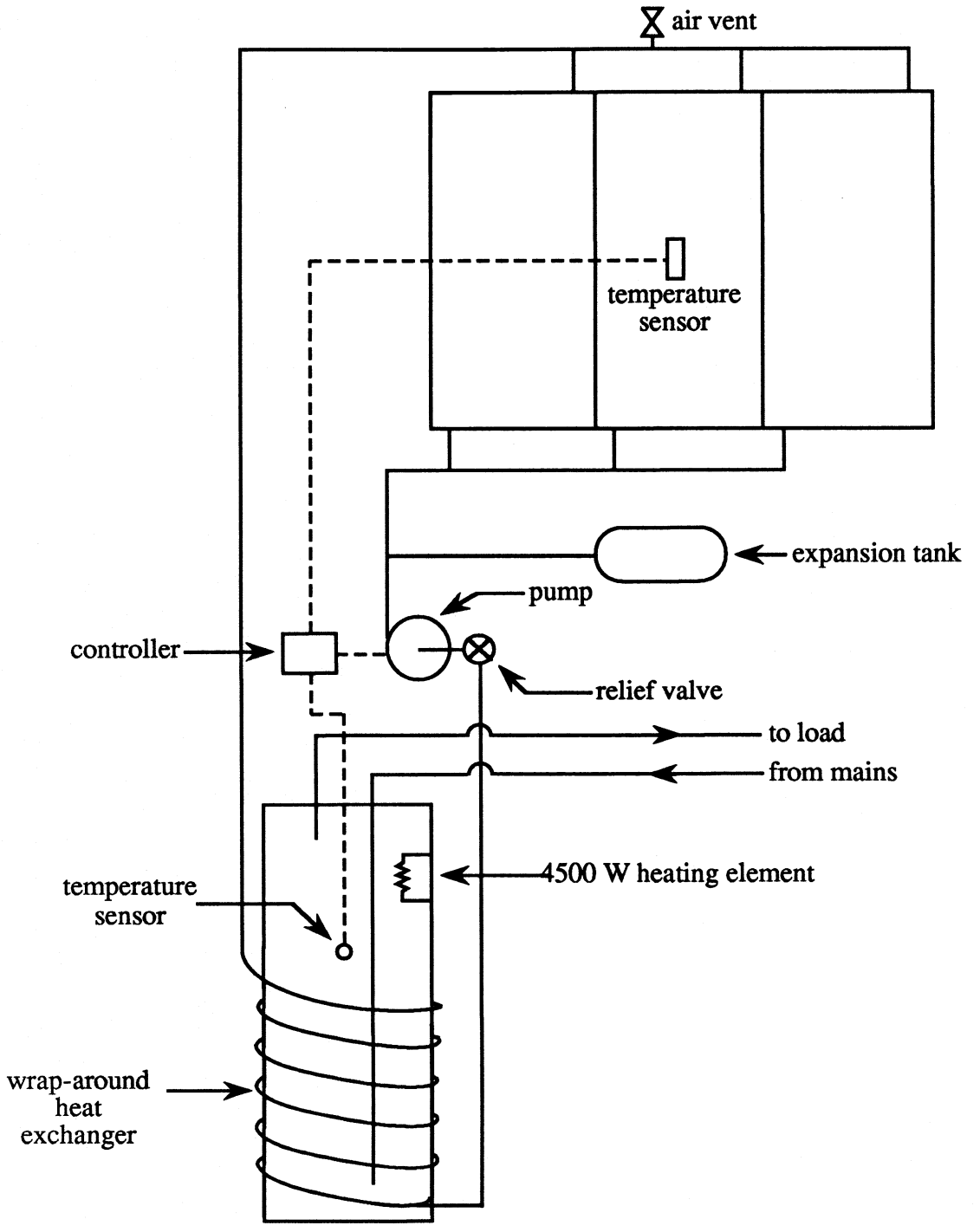

Figure 3.14 Schematic of single-tank indirect system tested at NBS

$F_r(\tau\alpha)_n$ = 0.805

F_rU_l = 4.73 W/m^2°C

b_0 = 0.10

2) Storage tank

The Solarstream tank of the STI system has a total storage volume of 310 liters and outside dimensions of 1.42 m in height and 0.71 m in diameter. It is surrounded by a 76 mm thick fiberglass blanket. An auxiliary 4500 W heating element is located in the upper section of the tank. When a thermocouple is located immediately above the element registers below 60 °C, the element is activated.

A 72 hour tank cool down test was performed at NBS to estimate the tank loss coefficient. The tank was initially charged with 70 °C water and allowed to cool for 72 hours, without insolation, or addition or withdrawal of water. Thermocouples inside and outside the tank were used to monitor the average tank and ambient temperatures over the cooling period. An exponential decay function was fit to the temperature data, resulting in an estimated tank loss coefficient of 3.02 W/°C.

The degree of stratification exhibited by the storage tank was investigated by installing thermocouples at 152 mm intervals along the tank's vertical axis. The tank temperature at these various positions was monitored during the ASHRAE-95 test conducted at NBS. The results indicate that the tank exhibited a high degree of stratification during the entire test day.

3) Heat exchanger

The STI system employes a wrap-around heat exchanger consisting of a two-walled metal jacket mechanically bonded to the tank surface. The working fluid which circulates through the heat exchanger and collector is a 40% by weight mixture of ethylene glycol and distilled water, having a specific heat of 3.60 kJ/kg°C and a specific

gravity of 1.042 at 40 °C. The heat exchanger effectiveness was determined experimentally to be approximately 0.24.

4) Pump and pump controller

The collector pump circulates the working fluid through the collector loop at a flow rate of 0.0833 l/s. A controller actuates the pump whenever a temperature sensor mounted on the absorber plate of the collector registers 10 °C higher than a similar sensor mounted on the tank surface. Circulation ceases if the temperature difference decreases to below 1.7°C.

3.3.2 The NBS ASHRAE-95 Test

The ASHRAE-95 test procedure performed by Klein and Fanney at NBS was similar to the alternative test procedure described in Section 1.2. As the collector gain and loss parameters had been previously determined, the high intensity lamps were replaced by an electrical in-line heater which provided an equivalent amount of absorbed energy, in accordance with the method described by Fanney and Thomas [19].

The set of conditions used during the NBS test differ in several respects from the conditions specified by the SRCC. The ambient temperature and incident radiation profiles adopted by Klein and Fanney are shown in table 3.5. The draw profile used was that specified by the RAND corporation [21], which is shown in table 3.6. The hot water delivery set temperature and mains water temperature during the test were 60 °C and 20 °C, respectively.

There are three significant differences between the SRCC test conditions and the conditions shown in tables 3.5 and 3.6. First, the ambient temperature specified by the SRCC remains constant over the entire test day, while the NBS test conditions specify an ambient temperature profile having variations of up to 12 °C. Second, the ambient and mains water temperatures are equal under SRCC test conditions, while the average

ambient temperature during the NBS test day (24 °C) is 4 °C higher than the mains temperature. Finally, the RAND draw profile used during the NBS test is somewhat evening weighted, while the SRCC draw is symmetric about solar noon.

Although the NBS radiation profile is also slightly different than that specified by the SRCC, the general shape and total radiation of the two profiles are roughly equivalent. As the accuracy of the ESAS prediction method is insensitive to the radiation profile used during the ASHRAE-95 test, the differences in the NBS radiation profile can be considered negligible.

Studies by Zollner [6] and Kummer [20] indicate that draw profile has negligible effect on performance, unless that profile is heavily weighted during the evening or morning periods. Although the RAND profile is evening weighted, the degree of weighting is small, and the draw is spread out over a relatively long period (six a.m. till midnight). It is therefore expected that the differences between the RAND and SRCC draw profiles will have negligible effect on the applicability of the ESAS prediction method to the NBS test.

The fact that the mains and average ambient temperatures are not equal during the NBS test day may have a more significant effect. It was shown that any parameter pair which satisfies the collector parameter function of a given SAS can be used to simulate the yearly performance of that SAS, if the mains temperature is equal to the yearly-average ambient temperature of the location in question. This result, however, was based on the fact that the mains and ambient temperatures are equal during the ASHRAE-95 test, under SRCC test conditions. The parameter pairs derived from the results of the NBS test may therefore produce different values of simulated yearly solar fraction, due to the difference between the mains and average ambient temperatures during the NBS test day.

Table 3.5
Radiation on a tilted surface and ambient temperature
during ASHRAE-95 test at NBS

Hour	G_t [kJ/m2]	T_a [°C]
6.5	439.2	16.1
7.0	669.6	16.4
7.5	910.8	17.0
8.0	1159.2	17.8
8.5	1404.0	18.8
9.0	1641.6	20.1
9.5	1857.6	21.2
10.0	2048.4	22.4
10.5	2206.8	23.3
11.0	2325.6	24.3
11.5	2397.6	25.3
12.0	2419.2	25.9
12.5	2397.6	26.6
13.0	2325.6	27.2
13.5	2206.8	27.9
14.0	2048.4	28.2
14.5	1857.6	28.5
15.0	1641.6	28.5
15.5	1404.0	28.5
16.0	1159.2	28.3
16.5	910.8	27.9
17.0	669.6	27.4
17.5	439.2	26.9
Total	18270	
Average		24.1

Table 3.6
RAND load profile used during ASHRAE-95 test of STI system at NBS

Hour	Liters
6	4.2
7	13.2
8	21.1
9	23.8
10	18.6
11	13.2
12	10.0
13	14.3
14	8.2
15	6.9
16	5.3
17	10.0
18	18.6
19	33.8
20	26.6
21	18.6
22	14.3
23	13.2
24	5.3
Total	279

3.3.3 Comparison of ESAS and Actual System Performance

During the period from Jan. 1979 to Jan 1980, Fanney monitored and recorded the outdoor performance of the STI system on a daily basis [10,22]. The hot water delivery temperature during this monitoring period was set to 60 °C, and was held roughly constant over the entire year. Hot water was drawn from the tank automatically, according to the RAND draw profile. Variations on the order of 5-10% in total daily draw, however, produced an average yearly daily value of 255 liters per day, due the limited accuracy of the automatic draw system.

Several hardware problems during the monitoring period resulted in the invalidation of a number of daily performance measurements. The monthly average values of system performance and climatic conditions reported by Fanney and Klein are therefore often based on a reduced number of daily values. The monthly average values of insolation, ambient temperature and mains temperature during the year-long monitoring period, and the number of valid daily measurements, N, on which those average values are based, are shown in table 3.7.

Table 3.7
Average monthly meteorological conditions during year-long outdoor performance monitoring of STI system at NBS

	N [days]	$\overline{H}$ [MJ/m^2]	$\overline{T}_a$ [°C]	$\overline{T}_m$ [°C]
JAN	27	5.77	0.0	8.2
FEB	23	10.29	0.0	9.6
MAR	24	12.33	6.1	10.4
APR	18	18.80	12.4	12.5
MAY	23	19.78	19.3	17.7
JUN	24	22.84	20.1	19.1
JUL	19	22.35	25.0	19.5
AUG	16	17.59	24.0	24.9
SEP	23	16.18	21.2	26.1
OCT	17	11.17	11.1	20.8
NOV	17	7.99	6.0	13.1
DEC	19	5.93	0.3	10.4
YEARLY AVERAGE			12.1	16.0

The collector parameters of the equivalent simplified active system were determined from the results of the NBS ASHRAE-95 test in the following manner. The amount of electrical energy supplied to the auxiliary heater of the STI system during the final test day was used to determine the solar fraction, through the following expression:

$$f = 1 - \frac{Q_{AUX}}{Q_{LOAD}} \tag{3.5}$$

The resulting value of solar fraction was 0.65.

This value of solar fraction, plus the collector area and tank volume of the actual STI system, were input to Eqs. 2.11-13 to determine the average tank, draw, and collector inlet temperatures of the equivalent simplified active system. These temperatures were in turn input to Eq. 2.29 to determine the collector parameter function of the ESAS. Several parameter pairs which satisfy that function are shown in table 3.8.

Table 3.8
Collector parameter pairs which satisfy Eq. 2.29,
from NBS ASHRAE-95 test of STI system

$F_R U_l'$	$F_R(\tau\alpha)_n'$
2.0	0.516
3.0	0.559
4.0	0.601
5.0	0.641
6.0	0.681
7.0	0.720
8.0	0.758

The parameter pair, (5.0, 0.641), was selected for use in simulating the yearly performance of the ESAS. In this case, TRNSYS could not by used to simulate the performance of the equivalent simplified active system, as the required hourly weather data was unavailable. F-Chart, which uses average monthly weather data of the type presented in Table 3.7, was used instead. The parameter values input to the F-Chart correlation are shown in Table 3.9.

The outdoor yearly performance of the ESAS, as calculated by F-Chart, is compared to the measured performance of the STI system in Table 3.10. Although the monthly performance of the ESAS differs from the monthly performance of the STI system by up to 7%, the yearly performances agree to 1%. Some of the difference in monthly performance may be due to the fact that a constant daily draw of 255 liters was assumed in the F-Chart calculation. Although this value represents the average daily draw from the STI system based on the entire year, the average monthly value may vary from month to month.

The other parameter pairs shown in table 3.8 were also used to calculate yearly performance with F-Chart, to investigate the sensitivity of ESAS performance to the choice of parameter pairs. The calculated yearly performance resulting from the selection of each pair is shown in Table 3.11. As was expected, there is some difference in the calculated solar fractions produced by the various parameter pairs. The parameter pair, 2.0, 0.516, produces a calculated solar fraction of 0.42, while the pair, 8.0, 0.758 produces a calculated solar fraction of 0.47.

Table 3.9
Parameter values used in F-Chart simulation of ESAS performance

Water Storage System		
City call no. (DC)	220	
Water volume / collector area	73.80	liters/m^2
Building UA (0 if only DHW)	0.00	W/C
Fuel (Elec,Gas,Oil,Other)	Elec.	
Efficiency of fuel usage	100.00	%
Domestic hot water (Yes,No)	Yes	
Daily hot water usage	255	liters
Water set temperature	60.0	°C
Environmental temperature	20.0	°C
UA of auxiliary storage tank	0.00	W/C
Pipe heat loss (Yes,No)	No	
Relative load heat exchanger size	1.00	
Collector-store heat exchanger (Yes,No)	No	
Flat Plate Collector		
Number of collector panels	1	
Collector panel area	4.20	m^2
FR*UL (Test slope)	5.000	W/m^2-°C
FR*TAU*ALPHA (Test intercept)	0.641	
Collector slope	39	degrees
Collector azimuth (South=0)	0	degrees
Incidence angle modifier calculation	Constant	
Inc angle modifier constant	0.000	
Collector flowrate/area	0.020	kg/sec-m^2
Collector fluid specific heat	4.19	kJ/kg-°C
Modify test values (Yes,No)	No	

Table 3.10
ESAS monthly average daily performance, as calculated by F-Chart,
verses measured STI system performance at NBS (Washington, D.C.)

		$\overline{H}_t$ [MJ/day]		$\overline{Q}_{load}$ [MJ/day]		$\overline{Q}_{aux}$ [MJ/day]		$\overline{f}$	
	N [days]	meas.	ESAS	meas.	ESAS	meas.	ESAS	meas.	ESAS
JAN	27	8.19	8.22	52.3	55.5	42.0	46.8	0.197	0.15
FEB	23	14.75	14.00	45.8	53.9	26.3	33.6	0.426	0.38
MAR	27	13.57	14.00	51.9	52.9	32.4	31.9	0.376	0.40
APR	18	19.09	19.30	52.1	50.7	20.8	20.3	0.601	0.60
MAY	24	16.78	18.20	46.5	45.2	19.3	17.7	0.584	0.61
JUN	22	18.00	20.20	44.0	43.7	16.0	14.0	0.636	0.68
JUL	19	18.41	20.10	43.1	43.2	14.6	12.6	0.661	0.71
AUG	16	16.18	17.10	34.6	37.4	15.8	14.8	0.545	0.61
SEP	23	18.34	18.10	37.1	36.3	13.0	13.3	0.649	0.64
OCT	22	14.91	14.40	45.6	41.9	26.2	23.5	0.426	0.44
NOV	30	11.75	12.00	52.6	50.0	33.2	34.0	0.369	0.32
DEC	25	9.76	9.20	50.8	52.9	37.4	42.9	0.264	0.19
				YEARLY TOTALS					
	276	4024	4129	12966	13124	7140	7391	**0.449**	**0.44**

Table 3.11
Yearly solar fraction of ESAS as calculated by F-Chart,
verses choice of parameter pair.

F_rU_l'	$F_r(\tau\alpha)_n'$	*f* (F-Chart)
2.0	0.516	0.42
3.0	0.559	0.42
4.0	0.601	0.43
5.0	0.641	0.44
6.0	0.681	0.45
7.0	0.720	0.46
8.0	0.758	0.47

This difference is a result of the fact that the mains temperature during the NBS ASHRAE-95 test was 4 °C lower than the average ambient temperature, but was 4 °C higher than the yearly average ambient temperature during outdoor operation. The bracketed quantities shown in Eq. 3.1 therefore have different values during outdoor operation than during the ASHRAE-95 test, resulting in an increase in the sensitivity of ESAS yearly performance to the choice of parameter pairs, as described in section 3.1. That sensitivity, however, is still fairly small. Note that no matter which parameter pair is selected, the resulting solar fraction is still within 3% of the actual yearly performance. It is therefore concluded that moderate deviations from the requirement that mains temperature equal average yearly ambient temperature will not introduce much error to the prediction method. If such deviation is unavoidable, the accuracy of the method can be maximized by selecting the parameter pair corresponding to the collector loss coefficient of the actual system. Although this coefficient may be unknown, a good estimate can often be determined from the insulation thickness and

number of glazings of the collector in question.

The close agreement between the simulated yearly performance of the ESAS and the measured performance of the actual system also indicates that the mains temperature need not be constant, as assumed in section 3.2, for the ESAS prediction method to be applicable. As long as the yearly average mains temperature is roughly equal to the yearly average ambient temperature (i.e. within 4 °C), variation in mains temperature does not appear to detract from the accuracy of the ESAS prediction method.

3.4 SUMMARY

Any parameter pair, (F_rU_l', $F_r(\tau\alpha)_n'$),derived for a particular SAS using Eq. 2.29 under ASHRAE-95 test conditions can be used to simulate that SAS's long term performance with nearly identical results, if the following conditions are met:

1) The load profile and set temperature specified by the SRCC for the ASHRAE-95 test are used to simulate long term performance.

2) The mains temperature used when simulating SAS performance, in a given location, is set equal to the average-yearly ambient temperature for that location.

The thermal behavior of actual SDHW systems, such as stratification of storage, incidence angle dependence, tank losses and thermosyphon circulation can be lumped into the collector parameter pair of the corresponding ESAS. The yearly performance of actual systems can therefore be accurately estimated by the yearly performance of their equivalent simplified active systems, independent of location.

Experimental validation, using the measured ASHRAE-95 and outdoor performance of an actual system, supports this conclusion. The measured yearly performance of the STI system studied by Fanney and Klein, and the simulated yearly

performance of its equivalent simplified active system agreed to within 3%. This agreement further suggests that moderate differences between average yearly mains and average yearly ambient temperature (on the order of 4 °C) does not introduce significant inaccuracy to the prediction method.

CHAPTER 4
Conclusions

4.1 Method Summary

A SDHW prediction method has been developed which uses the ASHRAE-95 test performance of an actual SDHW system to derive the parameters of an equivalent simplified active system, having the same collector area and tank volume. The yearly performance of the equivalent simplified active system can be simulated using TRNSYS, and presented as a close estimate of the performance of the actual system.

The procedure used in applying this method is as follows. The actual SDHW system is subjected to the ASHRAE-95 test under the conditions specified by the SRCC. The total radiation of the SRCC is reduced, if necessary, such that the product of the collector area and the total incident radiation is less than or equal to the daily load. That is,

$$H_t A_c \leq 44{,}000 \text{ kJ}$$

This results in ASHRAE-95 solar fractions below 0.6 for the majority of SDHW systems.

This solar fraction is input to Eqs. 2.11 to 2.13 to calculate the average draw, tank and collector inlet temperatures of the equivalent simplified active system. The values of these three temperatures are used in Eq. 2.29 to create a functional relationship between the collector parameters of the ESAS. For the sake of

consistency, it is recommended that a value of F_rU_l'=5 W/m^2°C be assumed for all TRNSYS simulations. The corresponding value of $F_r(\tau\alpha)_n'$ can be determined by explicitly solving Eq. 2.29. The listing of a FORTRAN 77 code which calculates this parameter pair, based collector area, tank volume and ASHRAE-95 performance, is presented in Appendix A.

This parameter pair is then used in TRNSYS to simulate the yearly performance of the ESAS in the desired location. A sample TRNSYS deck which can be used for this purpose is listed in Appendix B. The mains water temperature used during this simulation must be set equal to the average-yearly ambient temperature of the location being simulated The load profile and set temperature must be those specified by the SRCC.

Complex TRNSYS models of actual systems, including thermosyphon systems, and systems exhibiting stratification and incidence angle dependence, were used to determine the accuracy of this method. The simulated ASHRAE-95 performance of these complex systems was used to determine the parameters of the corresponding ESAS. The simulated yearly performance of the complex and equivalent simplified systems was compared in five locations, and was found to agree to within approximately 2% for all system types and locations.

Experimental validation, using data provided by NBS, confirmed this accuracy. The ESAS prediction method was able to predict the measured yearly performance of the STI system studied by Fanney and Klein to within 1%. This result further indicated that a moderate difference between yearly average mains temperature and yearly average ambient temperature (i.e. < 5 °C) will not significantly detract from the accuracy of the prediction method. If performance predictions are desired for locations in which a

moderate difference between average yearly mains and ambient temperature exists, the accuracy of the prediction can be maximized by selecting the parameter pair, (F_rU_l', $F_r(\tau\alpha)_n'$), which corresponds to an estimate of the actual collector loss coefficient.

4.2 Future Work

Although a broad range of system sizes and types were considered in this work, the accuracy of the ESAS prediction method needs to be investigated for a number of additional system types. In particular, the applicability of the method to systems having the following characteristics should be investigated.

1) drain-back collectors
2) concentrating collectors
3) phase-change storage
4) large controller dead-bands

The ESAS prediction method is not, at present, capable of determining the effect of changes in actual system parameters on yearly performance. If, for example, a stratified system was tested at a certain flow rate, but it's yearly performance at a higher flow rate was desired, the system would have to be retested at that higher flow rate. Given the expense of retesting, the usefulness of the ESAS as a design tool is limited. Future work in this area should include determining the effect of component substitution on system performance. How, for example, can the method account for the effect of replacing the collector of the tested system with a more efficient model?

If the parameters of both the original and replacement collector are known, one

possible solution could be the creation of a correction factor, based on the ratio of the old and new efficiencies. This correction factor would multiply the collector gain term of the ESAS parameter pair. If the new collector is more efficient, this correction factor would be greater than one, and $F_r(\tau\alpha)_n'$ would increase, reflecting the increase in efficiency. Similar correction factors could also be created for replacement heat exchangers and replacement storage tanks of equal volume but different heat loss coefficients. It is likely that the effect of reducing tank volume can not be fully described by a single correction factor, due to the effect of storage volume on stratification and temperature dynamics. Further work in this area is clearly required.

APPENDIX A

Listing of Fortran Code ESAS_PARAM

```
    PROGRAM ESAS_PARAM
**********************************************************************
* PROGRAM TO CALCULATE PARAMETER PAIRS OF ESAS BASED  *
* ON COLLECTOR AREA, TANK VOLUME, AND ASHRAE-95 SOLAR  *
* FRACTION OF ACTUAL SDHW SYSTEM.                      *
**********************************************************************
    IMPLICIT REAL (A-Z)

     OPEN(8,FILE='ESAS.OUT',STATUS='OLD')

**********************************************************************
*************INPUT COLLECTOR AREA,TANK VOLUME************
*************AND ASHRAE-95 SOLAR FRACTION*****************
**********************************************************************
    PRINT*, 'INPUT AC,VT,SF'     ! area [m2], volume [l], solar fraction

    READ*, AC,VT,SF


**********************************************************************
*************SRCC OPERATING CONDITIONS********************
**********************************************************************
    TA=22.0                                  ! Ambient temperature [°C]

    TM=22.0                                  ! Mains temperature [°C]

    TS=50.0                                  ! Set temperature [°C]

    TENV=22.0                                ! Tank environ. temperature[°C]

    HT=17022.0                               ! Total radiation per unit area
                                             ! incident on collector surface
                                             ! (Adjust if necessary) [kJ]


    CP=4.19                                  ! Specific heat [kJ/m2°C]
```

```
      MD=375.0                                  ! Total daily draw [l]

************************************************************
*******DETERMINE AVERAGE SYSTEM TEMPERATURES******
************************************************************
      TD=SF*(TS-TM)+TM                          ! Average draw temperature [°C]

      TT=TD                                     ! Average tank temperature [°C]

      A= 1 - 8.75E-4*(AC*HT/VT)                 ! Eq. 2.9
     +    + 5.28E-7*(AC*HT/VT)**2

      B=  6.47E-4*(AC*HT/VT)                    ! Eq. 2.10
     +  + 1.04E-7*(AC*HT/VT)**2

      TCIN=MAX(TD,(TS-TM)*(A*SF+B)+TM)          ! Average collector inlet temp. [°C]

************************************************************
*****************ESTIMATE TANK LOSSES*****************
************************************************************
      H=1.492                                   ! Tank height [m]

      R=(VT/1000/(3.1416*H))**0.5               ! Tank radius [m]

      UATANK=9.4876*(R**2+H*R)                  ! UA of tank  [kJ/m2hr°C]

      QLOSS=UATANK*(TT-TENV)*24                 ! Tank losses [kJ]

************************************************************
***SOLVE EQUATION 2.29 EXPLICITLY FOR FR-TAU-ALPHA***
************************************************************
      GMAX=HT/5.0                               ! Peak radiation of triangular
                                                ! approximation [kJ/hr]

      QDRAW=MD*CP*(TD-TM)                       ! Energy of draw [kJ]

      DO 500  FRUL_PR=7.2,28.8,3.6              ! ESAS collector. loss coeff.
                                                 [kJ/m2hr°C]

         A=1.0                                  ! Variable of quadratic eq.

         B=-2.0-(QLOSS+QDRAW)/((5.0)
     +     *(FRUL_PR*(TCIN-TA)*AC))             !    "      "      "      "

         C=1.0                                  !    "      "      "      "
```

```
      GTC=GMAX*(-B-(B**2-4*A*C)**0.5)  ! critical radiation level;
     +   /(2.*A)                       ! from applying quadratic [kJ/hr]
                                       ! equation.to Eq 2.27

      FRTA_PR=FRUL_PR*(TCIN-TA)/GTC    ! ESAS collector gain coeff.

      WRITE(8,400) FRUL_PR/3.6,FRTA_PR

400   FORMAT(2X,F6.1,2X,F6.4)

500  CONTINUE

     END
```

APPENDIX B

Sample SAS TRNSYS Deck

```
*****************************************
*    TRNSYS DECK FOR ONE-YEAR           *
*    SIMULATION OF ESAS                 *
*****************************************
SIMULATION 1 8760 .25
LIMITS 50 30

CONSTANTS 20
TBOIL=5000.          Boil temperature
UT=1.51              Tank loss coefficient
TSET=50.             Set temperasture
TMAINS=7.96          Mains temperature
TENV=22.             Tank environment temperature
LAT=43.13            Latitude
PANELS=1.0           Number of collector panels
AREA=1.0             Collector area
CP=4.19              Specific heat
FRTAN=0.7244         ESAS collector gain coefficient
FRUL=18.0            ESAS collector loss coefficient
B0=0.000001          Incident angle modifier constant
RHO=0.0              Ground reflectance
POWER=20000.0        Maximum power of in-line heater
MDOTC=500.0          Collector flow rate
GTEST=MDOTC / AREA   Reference value for corection of
                     collector gain and loss coefficients
                     (set such that no correction is made)
VTANK=0.3            Tank volume
HXEFF=-1.0           Heat exchanger efficiency
TUDB=1.0             Upper controller dead band temp.
TLDB=0.0             Lower controller dead band temp

UNIT 9 TYPE 9  DATA READER
PARAMETERS 10
2 1 -1 1 0 -2 1 0 10 1
(T15,F4.0,T20,F4.1)
```

```
UNIT 16 TYPE 16  RADIATION PROCESSOR
PARAMETERS 7
3  1  1  LAT  4871  0.0 -1
INPUTS 6
9,1  9,19  9,20  0,0  0,0  0,0
0.0  0.0   0.0   RHO  LAT  0.0

UNIT 1 TYPE 1  FLAT PLATE COLLECTOR
PARAMETERS 12
1  PANELS  AREA  CP  1  GTEST  FRTAN  FRUL  HXEFF  CP  1  B0
INPUTS 10
3,1    3,2  3,2  9,2   16,6  16,4  16,5  0,0  16,9  0,0
TMAINS  0.0  0.0  TENV  0.0   0.0   0.0   RHO  90.0  LAT

UNIT 3 TYPE 3  PUMP
PARAMETERS 1
MDOTC
INPUTS 3
4,1   4,2  2,1
TSET  0.0  0.0

UNIT 2 TYPE 2  PUMP CONTROLLER
PARAMETERS 3
3  TUDB  TLDB
INPUTS 3
1,1    4,1    2,1
TMAINS  TMAINS  0.0

UNIT 4 TYPE 4  SOLAR STORAGE TANK (WELL-MIXED)
PARAMETERS 6
1  VTANK  4.19  1000.  UT  -1.492
INPUTS 5
13,1   13,2  0,0    14,1  0,0
TMAINS  0.0  TMAINS  0.0  TENV
DERIVATIVES 1
TMAINS

UNIT 6 TYPE 6 IN-LINE AUXILLIARY HEATER
PARAMETERS 3
POWER  TSET  4.19
INPUTS 3
4,3    4,4  0,0
TMAINS 0.0  1
```

```
UNIT 13 TYPE 13 RELIEF VALVE
PARAMETERS 2
TBOIL 4.19
INPUTS 3
1,1    1,2   1,1
TMAINS  0.0   TMAINS

UNIT 14 TYPE 14    SRCC DRAW PROFILE
PARS 28
0,0 8,0 8,125 9,125 9,0 12,0 12,125 13,125 13,0
17,0 17,125 18,125 18,0 24,0

UNIT 28 TYPE 28  MONTHLY SIMULATION SUMMARY
PARAMETERS 35
-1   1  8760  0  2   1
-11 -4
-12 -2 2 -1 24 1 -4
-13 -4
-14 -2 2 -4
-15 -4
-16 -4
-17 -17 -3
-16  3  -3  2  -4
-18 -4
INPUTS 8
4,7  9,1  13,3  9,2  4,5  6,3  4,6  4,9
LABELS 10
DELTAE HBAR ITOT TABAR QLOSS QAUX QSOL QLOAD SOLF QU

END
-11 -4
-12 -2 2 -1 24 1 -4
-13 -4
-14 -2 2 -4
-15 -4
-16 -4
-17 -17 -3
-16  3  -3  2  -4
-18 -4
INPUTS 8
4,7  9,1  13,3  9,2  4,5  6,3  4,6  4,9
LABELS 10
DELTAE HBAR ITOT TABAR QLOSS QAUX QSOL QLOAD SOLF QU

END
```

REFERENCES

1. International Energy Agency, *Summary of National Approaches to Short-term SDHW Systems Testing*, Technical report, August (1984)

2. ASHRAE, Standard 95-1981, "Methods of Testing to Determine the Thermal Performance of Solar Domestic Hot Water Systems," *Proceedings of the 1982 ASES Passive Solar Conference*, ASES (1982)

3. Klein, S.A., *et al.,TRNSYS 12.2 User's Manual*, University of Wisconsin-Madison, Engineering Experiment Station Report 38-12 (1983)

4. Klein, S.A., "A Design Procedure for Solar Heating Systems," Ph.D. Thesis, University of Wisconsin-Madison (1976)

5. SRCC, Standard 200-82, "Test Methods and Minimum Standards for Certifying Solar Water Heating Systems," Solar Rating and Certification Corporation, Washington, D.C., April (1983)

6. Zollner, A., "A Performance Prediction Methodology for Integral Collection Storage Solar Domestic Hot Water Systems," *Journal of Solar Energy Engineering*, Volume 107, p. 265, November, (1985)

7. DSET Labs, Solar System Test Report, No. 82SYS0816-SS, Client Specified Test, DSET Laboratories, Inc., Phoenix AZ, September (1982)

8. Fowlkes Engineering, 31 Gardner Park Dr., Bozeman, MT 59715 Hourly Experimental Data, July (1984)

9. Fanney, A.H., and Klein S.A., "Comparison of Experimental and Calculated Performance of Integral Collector -Storage Solar Water Heaters," *Solar Energy*, Volume 38, No. 5, pp 303-309 (1987)

10 Fanney, A.H.,and Klein S.A., "Performance of Solar Domestic Hot Water Systems at the National Bureau of Standards -- Measurements and Predictions," *Journal of Solar Energy Engineering*, Volume 105, p. 311, August, (1983)

11. Duffie, J.A. and Mitchell, J.W., "F-Chart: Predictions and Measurements," *Journal of Solar Energy Engineering*, Vol. 105, p. 4, February, (1983)

12 Pearson, K A., "Utilizability Design Methods for Predicting the Long-Term Performance of Solar Water Heating Systems," Masters thesis, University of Wisconsin-Madison, (1981)

13 Copsey, A.B., "A Modification of the F-Chart Method for Solar Domestic Hot Water Systems with Stratified Storage," M. S. Thesis, University of Wisconsin-Madison (1984)

14 Morrison, G.L. and Braun, J. E., "System Modelling and Operation Characteristics of Thermosyphon Solar Water Heaters," *Solar Energy*, Volume 34, pp. 389-405, (1985)

15 Hottel, H.C. and Whilier, A., *Transactions of the Conference on the Use of Solar Energy, 2,* part I, 74. University of Arizona Press, (1958)

16. Liu, B.Y.H. and Jordan, R.C, "A Rational Procedure for Predicting the Long-Term Average Performance of Flat-Plate Solar-Energy Collectors," *Solar Energy*, Volume 7, p. 53, (1963)

17. Klein, S.A., "Calculation of Flat-Plate Collector Utilizability," *Solar Energy*, Volume 21, p. 393, (1978)

18. Erbs, D.G., "Estimation of the Diffuse Radiation Fraction for Hourly, Daily and Monthly-Average Global Radiation," Solar Energy, Volume 28, p.293 (1982)

19 Fanney, A.H., and Thomas, W.C., "Simulation of Thermal Performance of Solar Collector Arrays," *ASME Journal of Solar Energy Engineering*, Aug. 1981.

20. Kummer, J.P., "Thermal Performance of Three Freeze Protection Methods as Applied to a Large Solar Energy System." M.S. Thesis, University of Wisconsin-Madison, (1986)

21 Mutch, J.J., "Residential Water Heating, Fuel Consumption, Economics and Public Policy," Report R-1498-NSF, Rand Corperation, May, (1974)

22 Fanney,A.H., and Klein, S.A., "A Rating Procedure of Solar Domestic Water Heating Systems," *Journal of Solar Energy Engineering,* Vol. 105, p. 430, November, (1983)